5-2012

IDENTIFICATION AND CHARACTERIZATION OF DISTINCT POPULATIONS OF CLONOGENIC BONE MARROW STROMAL CELLS CAPABLE OF TRANSFERRING THE HEMATOPOIETIC MICROENVIRONMENT IN VIVO AND SUPPORTING LT-HSCs IN VITRO

Colby Suire

IDENTIFICATION AND CHARACTERIZATION OF DISTINCT POPULATIONS OF CLONOGENIC BONE MARROW STROMAL CELLS CAPABLE OF TRANSFERRING THE HEMATOPOIETIC MICROENVIRONMENT IN VIVO AND SUPPORTING LT-HSCs IN VITRO

By

Colby Gerard Suire, B.S.

APPROVED:

_____

Paul J. Simmons, PhD

Supervisory Professor

_____

Brian R. Davis, PhD

_____

Guillermina Lozano, PhD

_____

Karen Hirschi, PhD

_____

Mikhail G. Kolonin, PhD

_____

Dean, The Univeristy of Texas

Graduate School of Biomedical Science at Houston

IDENTIFICATION AND CHARACTERIZATION OF DISTINCT POPULATIONS OF CLONOGENIC BONE MARROW STROMAL CELLS CAPABLE OF TRANSFERRING THE HEMATOPOIETIC MICROENVIRONMENT IN VIVO AND SUPPORTING LT-HSCs IN VITRO

A

DISSERTATION

Presented to the Faculty of
The University of Texas Health
Science Center at Houston and
The University of Texas
M.D. Anderson Cancer Center Graduate
School of Biomedical Sciences in Partial
Fullfilment

of the Requirements for the Degree of

DOCTOR OF PHILOSOPHY

By

Colby Gerard Suire, B.S.

May, 2012

2012

DEDICATION

I dedicate this dissertation to my wonderful wife and best friend, Robin L. Suire and the most precious gift of my life, my son Asa Alexzander Suire for their unconditional love and support.

ACKNOWLEDGEMENTS

I wish to first and foremost offer my most sincere appreciate and thanks to my mentor Dr. Paul J. Simmons without whom the work presented in my dissertation would not have been possible. His dedication to my development as a scientist and his deep curiosity in answering complex scientific questions have served both as a source of inspiration and motivation throughout my graduate training and will continue to be a benchmark for my own scientific aspirations.

I am deeply grateful to my supervisory committee members Dr. Brian R. Davis, Dr. Karen Hirschi, Dr. Guillermina Lozano, and Dr. Mikhail G. Kolonin who have helped guide me, through there expertise and mentorship, providing invaluable insight, support and critical evaluation of the data presented in this dissertation. In particular, I would like to thank Dr. Brian R. Davis for serving as my interim supervisor in Dr. Simmons absence. He has always made himself available for discussion and advice. Additionally, I would also like to make a special acknowledgement to Dr. Guillermina Lozano who played an instrumental role in my scientific training during my first year as a graduate student in the Department of Cancer Genetics at MDACC. It was through her thorough and critical evaluation of scientific data that I first learned how to ask scientifically valid questions and the importance of mouse genetics. Additionally, she has provided excellent mentorship and support during my time of transition to Dr. Simmons lab. I thank Dr. Karen Hirschi for her support and advice in designing experiments, which were instrument for both this dissertation and the publication she has co-authored as a result of this work. I thank Dr. Mikhail G. Kolonin for

providing mice used in my dissertation as well as for always being critical and questioning my results.

I would also like to thank Dr. Rick Wetsel for serving on my advisory committee and serving as the Chair of my PhD candidacy exam. In addition, I thank Dr. David Haviland and Dr. Patrick Zweidler-McKay for also serving on my advisory and exam committees. Additionally, Dr. David Haviland was an excellent resource providing assistance of the FACS based isolation strategies I used for cell isolation and characterization. I wish to also thank Dr. Naoki Nakayama for his advice and support in my scientific training.

I wish to thank all past and present members of Dr. Simmons' lab. In particular, Dr. Nathalie Brouard whom has provided extensive assistance throughout this dissertation and has contributed significantly to my scientific development and training. I thank Dr. Jeannie Javni for her critical leadership and management of the Center for Stem Cell Research and Dr. Simmon's lab. Dr. Nadine Matthias for her assistance with some of the transplantation studies and managing the mouse colony. I especially thank Suprita Trilok, Wei Liao, Jason Williams and Kevin Cao for their assistance in maintaining a functional lab and ordering supplies and reagents. I would also like to thank Stephanie Baca for all of her assistance in administrative issues and travel accommodations. Lastly, I thank Dr. Amy Hazen and Dr. Monique Pierre for their support and training and Dr. Hazen for assistance with FACS based techniques.

On both a personal and profession note, I would like to sincerely thank Tamara Jatoba, Dr. Hussein Abbas and Dr. Yan Zhang who have not only contributed to my scientific development through the exchange of ideas and protocols during my graduate training, but more importantly for being friends and a source of constant motivation and encouragement. I also thank Dr. Ana Crane, Dr. Alexas Daquinag, Jiangang Zhao and Felipe Amaya for their assistance in developing experiments and protocols and sharing reagents and ideas. I thank Sarah Amra who provided assistance with tissue sectioning and H&E staining and Michael Starbuck performed the resin embedding, sectioning and staining of nondecalcified bone tissue, all of which are presented in this dissertation. Additionally, I wish to thank Dr. Zhengmei Mao for her assistance and training in confocal microscopy, Evan Johnson for performing the micro-CT analysis and Tuan Tran for performing microarray analysis both at the University of Texas Medical School at Houston.

I further wish to thank the entire staff of GSBS who have always provided support and assistance. In particular, Dr. Jon Wiener, Dr. Victoria Knutson and Dr. Thomas Goka for their support and advice throughout my graduate training.

Lastly and perhaps most importantly, I wish to thank my family for their continued support, encouragement and love. In particular, my wife, Robin, who continues to be a source of support, encouragement and motivation. She has demonstrated exceptional patience throughout this long and time consuming journey. Additionally, I thank my son Asa, to whom I dedicate this dissertation for his love and for always providing me with a reason to smile and enjoy life. I also

thank my parents and two brothers for their continued source of motivation and encouragement throughout my life.

IDENTIFICATION AND CHARACTERIZATION OF DISTINCT POPULATIONS OF CLONOGENIC BONE MARROW STROMAL CELLS CAPABLE OF TRANSFERRING THE HEMATOPOIETIC MICROENVIRONMENT IN VIVO AND SUPPORTING LT-HSCs IN VITRO

Publication No._____

Colby G. Suire, Ph.D.

Supervisory Professor: Paul J. Simmons, Ph.D.

Bone marrow (BM) stromal cells are ascribed two key functions, 1) stem cells for non-hematopoietic tissues (MSC) and 2) as components of the hematopoietic stem cell niche. Current approaches studying the stromal cell system in the mouse are complicated by the low yield of clonogenic progenitors (CFU-F). Given the perivascular location of MSC in BM, we developed an alternative methodology to isolate MSC from mBM. An intact 'plug' of bone marrow is expelled from bones and enzymatically disaggregated to yield a single cell suspension. The recovery of CFU-F (1917.95$\pm$199) reproducibly exceeds that obtained using the standard BM flushing technique (14.32$\pm$1.9) by at least 2 orders of magnitude ($P<0.001$; $N = 8$) with an accompanying 196-fold enrichment of CFU-F frequency.

Purified BM stromal and vascular endothelial cell populations are readily obtained by FACS. A detailed immunophenotypic analysis of lineage depleted BM identified PDGFRαβ^{POS} stromal cell subpopulations distinguished by their expression of CD105. Both subpopulations retained their original phenotype of CD105 expression in culture and demonstrate MSC properties of multi-lineage differentiation and the ability to transfer the hematopoietic microenvironment in vivo. To determine the capacity of either subpopulation to support long-term multi-lineage reconstituting HSCs, we fractionated BM stromal cells into either the Lin^{NEG}PDGFRαβ^{POS}CD105^{POS} and LIN^{NEG}PDGFRαβ^{POS}CD105$^{LOW/-}$ populations and tested their capacity to support LT-HSC by co-culturing each population with either 1 or 10 HSCs for 10 days. Following the 10 day co-culture period, both populations supported transplantable HSCs from 10 cells/well co-

cultures demonstrating high levels of donor repopulation with an average of 65±23.6% chimerism from $CD105^{POS}$ co-cultures and 49.3±19.5% chimerism from the $CD105^{NEG}$ co-cultures. However, we observed a significant difference when mice were transplanted with the progeny of a single co-cultured HSC. In these experiments, $CD105^{POS}$ co-cultures (100%) demonstrated long-term multi-lineage reconstitution, while only 4 of 8 mice (50%) from $CD105^{NEG}$ -single HSC co-cultures demonstrated long-term reconstitution, suggesting a more limited expansion of functional stem cells. Taken together, these results demonstrate that the PDGFRαβ$CD105^{POS}$ stromal cell subpopulation is distinguished by a unique capacity to support the expansion of long-term reconstituting HSCs in vitro.

TABLE OF CONTENTS

LIST OF FIGURES

LIST OF TABLES

CHAPTER 1:

OVERVIEW AND AIMS

1-1: THE HEMATOPOIETIC SYSTEM: OVERVIEW

The hematopoietic system is one of the most highly regenerative systems in mammals with approximately 10^{11} mature blood cells being replaced each day in humans [1]. Along with the inception of BM transplantations nearly 40 years ago [1], a significant amount of progress has been gained from a growing knowledge regarding the identification, localization and regulation of hematopoietic stem cells (HSC) and has, as a consequence, ushered in the development of cellular and molecular therapies for hematological disease such as leukemia. Key observations of individuals who died of hematopoietic failure following the fall out from radiation exposure after the atomic bomb explosions in Hiroshima and Nagasaki in 1945, became a paradigm to study the hematopoietic system in humans and mice. Seminal experiments in hematopoietic cell transplantation, began following the observation that morbidity due to radiation poisoning could be prevented in mice by protecting the spleen with a lead shield [2, 3] and subsequently by transplanting spleen or bone marrow cells into irradiated host [4, 5].

Currently, bone marrow transplantation remains a widely used treatment modality for many human genetic disorders, bone marrow failure and cancers [6, 7]. Traditionally whole bone marrow was used as the primary source of hematopoietic stem/progenitors (HSPCs) for donor derived blood reconstitution in patients. Additionally, the cytokine granulocyte colony-stimulating factor (G-CSF) is given either to patients or donors to mobilize HSPCs into circulation from which the cells

can then be recovered by aphaeresis and transplanted into patients. Although successful for many patients, bone marrow transplantation from these adult sources comes with both limitations and caveats. One such limitation is that adult cell sources of HSPCs from either BM or mobilized peripheral blood require a high degree of matching of the Histocompatibility complex leukocyte antigen (HLA) between donor and recipient to reduce the risk of graft versus host disease [8]. As a consequence, many patients are left without the option of an appropriately matched donor.

More recently, umbilical cord blood (UCB) units are becoming an increasingly used source of HSPCs for cellular therapy. In 1988 Dr. Elaine Gluckman and colleagues [9] performed the first successful transplantation using a cryo-preserved UCB unit. Since the first reported UCB transplant, many patients have been successfully treated with cryo-preserved UCB units for a variety of malignant and non-malignant hematological disorders [10]. UCB transplantations do not require the same stringent level of HLA matching as adult cell sources. However, a significant limitation associated with the use of UCB is the low number of HSPCs per UCB unit which results in delayed engraftment rate for neutrophils and platelets and a markedly protracted rate of lymphoid reconstitution [11]. Currently, due to the reduced HSPC number, UCB units are generally only considered sufficient for transplantation of children and progress in the application of CB in the adult setting has been significantly hampered by delayed engraftment kinetics [12, 13]. Therefore, it is the interest of many labs to overcome the limitations hampering progress in many adult stem cell fields encompassed in the rarity of the resident adult stem cell

populations and the largely inability to maintain and/or expand functional stem cells ex vivo. Consequently, there remains a pressing clinical need to develop improved strategies for ex vivo propagation of functional hematopoietic stem cells in order to be able to fully realize the therapeutic potential of UCB. Like many adult tissue stem cells, HSCs are localized to and regulated by extrinsic cues from highly specialized 'microenvironments' referred to as stem cell *'niches'* [14, 15]. Evidence from many model organisms suggests that the local microenvironment is key in regulating stem cell behavior such as self-renewal, proliferation and differentiation [14, 15]. Recent progress has seen the concept of the hematopoietic niche, first proposed by Ray Schofield, reduced to a discrete cellular entity within the bone marrow [16]. Current data suggest that hematopoietic stem cells (HSC) exist both in association with osteoblasts at the endosteal surface of bone **(Osteoblastic niche)** [17-19] and also in contiguity with the bone marrow vasculature and perivascular stromal cells **(Vascular niche)** [20-21]. Additionally, recent data suggests that the perivascular cells situated around sinusoidal endothelial cells (adventitial reticular cells) not only comprise a critical cellular component of the vascular niche, but also serve as a resident population of stromal stem/progenitor cells, also known as 'skeletal' and 'mesenchymal' stem cells (MSCs) [22-25].

These findings bring together the long standing idea that not only do two distinct lineages of adult stem cell populations exist within the same tissue, the adult BM; but they are also intimately associated with one another such that one population, the stromal stem/progenitor cells, is beginning to emerge as a key cellular constituent of the hematopoietic microenvironment with a direct role in

governing HSC behavior (26). In light of these findings, the mouse model provides an excellent experimental system to further identify and characterize the molecules governing the extrinsic regulation of HSCs with the prospect of being able to use these molecules found within the in vivo microenvironment in order to develop improved strategies for the ex vivo expansion of HSCs. When considering addressing this very interesting hypothesis, one must also bear in mind the difficulty found in studying two rare adult stem cell populations simultaneously. Although the cell surface phenotype for the purification of murine HSCs has been well defined [20], cell surface markers allowing for the isolation of purified populations of mesenchymal stromal stem/progenitor cells from mouse bone marrow is still greatly lacking [27]. Unfortunately much of what is known in the mouse regarding the stromal cell compartment is largely based on retrospective analysis of a heterogeneous population of cultured bone marrow stromal cells (BMSCs) and as such there is little reproduced data suggesting the identity and location of MSCs in vivo. Furthermore, technical limitations and the lack of adequate isolation strategies for working with bone marrow tissue, in addition to the large percentage of hematopoietic cells comprising bone marrow cellularity have hampered progress in using the mouse model.

A major outstanding question in the field of mouse MSC biology has been the identification and localization of the cells responsible for establishing the hematopoietic microenvironment in vivo and whether or not the cells studied in laboratories actually have identical counterparts in vivo. In the human BM, the in vivo

location and the ability to isolate MSCs has recently been described [22, 27], however in the mouse system there remains much more confusion.

This thesis has been centered on addressing some of these difficulties and has gained significant scientific understanding of the intricacies involved in both MSC and HSC biology. The following chapters (1) describe a robust and reproducible approach to both identify and isolate cellular components of the vascular niche **[28],** (2) provide evidence of distinct stromal stem/progenitor populations that exist in vivo within the BM and exhibit transcriptional programs that suggest different physiological roles, and (3) functional data supporting their role as hematopoietic niche cellular elements.

1-2: AIMS

The overall objective of this dissertation is to investigate the properties of defined subpopulations of mouse bone marrow stromal cells. This study is aimed at understanding the biology of the bone marrow vascular/perivascular niche and in elucidating the role of bone marrow derived stromal stem/progenitor cells in regulating hematopoietic stem cell (HSC) behavior. The specific goals are to prospectively isolate candidate populations by means of their distinct cell surface immunophenotype, to investigate the multilineage differentiation potential of each stromal cell subpopulation and to measure their ability to support the maintenance of long-term repopulating hematopoietic stem cells (HSCs) in vitro. Accordingly, a combination of in vitro and in vivo functional assays were utilized to first evaluate the stem cell properties of distinct stromal cell populations. Additionally, co-culture and in vivo long-term blood reconstitution assays were employed to investigate the ability of the bone morrow stromal progenitor populations to support and/or expand mouse LSKCD48^{-}CD150^{+} (LSKSLAM) HSCs. Given recent reports demonstrating that the vascular niche comprises both sinusoidal endothelial cells and the subendothelial perivascular cells surrounding the sinusoidal wall [20, 25], this co-culture system therefore serves as an experimental platform from which to identify novel molecules, associated with the vascular niche, involved in regulating the survival and proliferation of functional hematopoietic stem cells. Furthermore, the knowledge gained from these studies will inform the development of more effective approaches to recapitulate hematopoietic vascular niche function ex vivo resulting in improved

methodologies for the cultivation and expansion of HSCs for therapeutic benefit.

To begin addressing these objectives, it was necessary to first develop a reproducible methodology that would allow the identification of a specific immunophenotype for the prospective isolation of subpopulations of bone marrow stromal stem/progenitor cells (MSCs). Current evidence from numerous investigators has demonstrated that MSC occupy a perivascular location within a number of tissues, including the bone marrow [22, 23, 26,115, 116]. Therefore, we postulated that preservation of the vasculature would be critical to maximizing the yield MSC physically situated along the abluminal surface of blood vessels.

In the Chapter 3 of this thesis, I describe a methodology I developed based on a step-wise enzymatic disaggregation of bone marrow tissue, which led to significant findings of a complex cellular organization contained within the bone marrow stromal compartment. These initial results led us to hypothesize that the **adult mouse bone marrow contains phenotypically distinct populations of MSC, which contribute to the maintenance of HSCs associated with the BM stem cell niches and are prospectively isolatable by distinct immunophenotypes.**

In Chapter 4, I investigate the multipotency of phenotypically defined candidate stromal stem/progenitor populations. I demonstrate, for the first time, that the cells commonly referred to in the literature as '*mesenchymal stem cells*' are in fact derive from distinct, phenotypically defined subpopulations of stromal cells in mouse bone marrow. The canonical MSC properties (i.e. differentiation to bone,

adipose and cartilage tissue) of these stromal cell subpopulations were analyzed by both in vitro and in vivo assays. Furthermore, transcriptional profiling was used to gain insight into their biological roles in vivo and these data suggest that each population is enriched in a small set of genes governing specific biological functions.

In Chapter 5, I determine the ability of each population to recapitulate the functional properties of the hematopoietic microenvironment in vitro by their capacity, using co-culture assays, to maintain and/or expand long-term repopulating mouse HSCs. For these studies a CD45.1/CD45.2 congenic transplant model was utilized to investigate the potential of co-cultured mouse HSCs to provide long-term multi-lineage repopulation in lethally irradiated host. I began these studies by first utilizing the FACS-based methodology described by Kiel, et al. [20] to isolate HSC from mouse bone marrow and validating their potency in the congenic transplant model. Using this rigorous, well-validated transplant model, a quantitative assessment was conducted to determine the capacity of different stromal cell subpopulations to support the maintenance and/or numerical expansion of competitive long-term repopulating HSCs.

The studies proposed herein are unique in several important respects. First, this project for the first time demonstrates that the cells commonly referred to in the literature as '*mesenchymal stem cells*' in fact derive from distinct populations of stromal cells within mouse BM. Secondly, these studies demonstrate that the hematopoietic supportive capacity of marrow stromal cells resides in discrete subpopulations that can be prospectively isolated by phenotype and contain the functional attributes associated with MSC. These data consequently provide

important additional insights into the ongoing debate, demonstrating that ***m***arrow ***s***tromal ***c***ells (*MSC*) with HSC-supportive functions and ***m***esenchymal ***s***tem ***c***ells (*MSC*) are represented within distinct populations of bone marrow stromal cells. Furthermore, the identification of unique stromal cell subpopulations with enhanced HSC maintenance potential in vitro provide the basis for future studies directed at defining the molecular mechanisms responsible for maintaining hematopoietic stem cell function during ex vivo expansion protocols.

CHAPTER 2: INTRODUCTION

HEMATOPOIETIC STEM CELLS (HSC) : ARCHETYPAL ADULT STEM CELLS

2-1: DISCOVERY OF HEMATOPOIETIC STEM CELLS

Stem cells are classically defined by three principal characteristics; the ability to self-renew, extensive proliferative potential and the ability to differentiate into multiple lineages providing a paradigm for tissue formation and maintenance during turnover (Figure 2-1) [1]. The hematopoietic system continues to be one of the most well characterized systems used in studying mammalian adult stem cells [6]. Importantly, hematopoietic stem cells are able to undergo self-renewal for the life of an organism and subsequently provide progenitor cells responsible for replenishing the entire hematopoietic system [29]. Pioneering work by Till and McCulloch in the early 1960's led to the identification of a subset of cells within the bone marrow (BM), which upon transplantation into lethally irradiated recipients, contained properties of differentiation, multi-potentiality and self-renewal by forming macroscopic colonies in the spleen of recipient animals, from which they coined the term colony forming unit-spleen (CFU-S) [30]. Originally thought to be hematopoietic stem cells, the colonies that formed in the spleen were initiated by progenitor cells and were comprised largely of cells of the myeloid lineage such as erythrocytes, granulocytes and megakaryocytes. However, subsequent work by these authors later identified additional colonies comprised of cells from the lymphoid lineage [31].

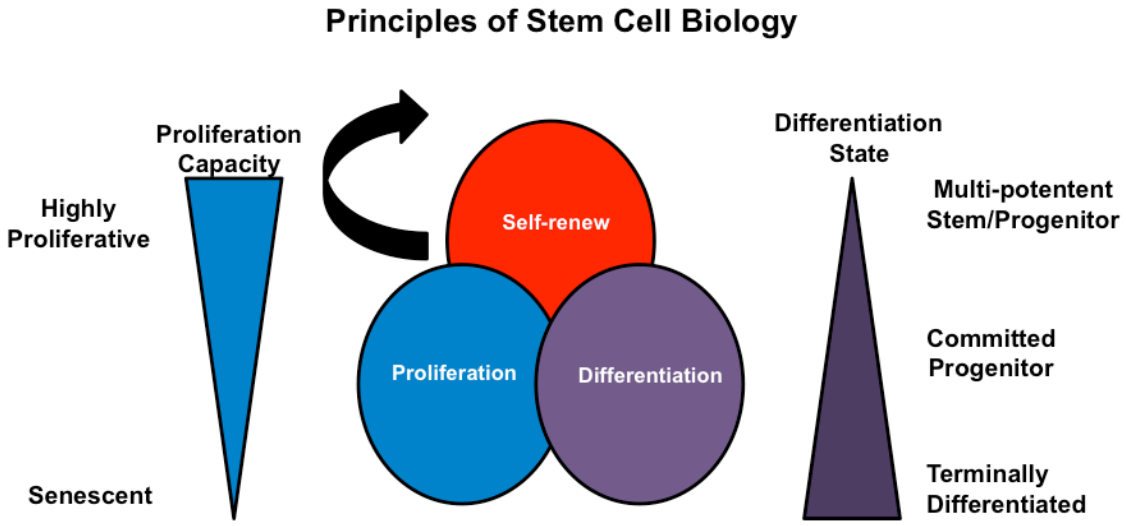

Figure 2-1: Principles of Stem Cell Biology. *Stem cells are largely quiescent cells in vivo but can be induced, during times of stress, injury or during maintenance of tissue homeostasis, to undergo self-renewal generating more stem cells in order to maintain the stem cell pool and/or to proliferate generating progenitor cells which then become mature cell types of the resident tissue.*

Additionally, a subset of these colony-forming cells could reform multi-potent CFU-S in the spleens when transplanted into secondary recipients [32]. These pioneering experiments led Till and McCulloch to propose the idea that some of the cells responsible for forming colonies of multiple hematopoietic lineages were hematopoietic stem cells, owing to the ability to undergo self-renewal and multi-potential differentiation [3]. However, although the cells responsible for forming the colonies in the spleen were of clonal origin [33], they were not derived from hematopoietic stem cells as initially thought. It was later demonstrated by work from Norman Iscove and colleagues in the 1980's that these early CFU-S cells were instead derived from oligopotent progenitors [34].

While these findings were instrumental in developing the concept of a hematopoietic stem cell that generates all mature blood cell types, it was not until the late 1980's and 1990's that populations could be isolated which were demonstrated to be enriched in HSCs. Furthermore, tools from both mouse genetics and molecular biology became available for researches to develop functional assays to quantitatively measure HSCs within distinct phenotypically defined populations [35]. Work from Dr. Irving Weissman's lab has led the field in search for cell-surface markers that allowed for the prospective isolation of populations of hematopoietic cells enriched in functional HSCs. As such, the work by his group and others have led to the development of a distinct immuno-phenotype for isolating HSCs in addition to more lineage restricted progenitor populations [20, 36-38]. It is now widely accepted that HSCs are contained within a rare population of cell within the adult bone marrow that are negative for mature hematopoietic markers (both of myeloid

and lymphoid lineages) (Lin-), but express both Sca-1 (stem cell antigen-1) [36] and c-kit [39], most commonly referred to in the literature as LSK.

Of equal importance to the ability to isolate enriched populations of HSCs was the development of functional assays to measure the frequency of HSCs within a defined population. Boyse and colleagues [40] were instrumental in developing congenic mouse strains, which would overcome the barrier of immune rejection. By generating mouse strains that differed only in one allele for the leukocyte common antigen Ly5/CD45 that is expressed on the cell surface of all hematopoietic cells, it now became possible with the use of specific monoclonal antibodies to distinguish the strain of hematopoietic cells derived from the host from that of the donor cells under in vivo transplantation assays [3]. These assays are now regarded as the gold standard for assessing HSC function and are commonly used by all labs interested in addressing fundamental questions in hematopoietic stem cell biology. More recently with the development of these powerful tools, researchers have been able to isolate single HSCs which upon transplantation into a lethally irradiated host can reconstitute the entire blood system thereby definitively demonstrating the enormous regenerative potential of HSCs. Work from Sean Morrison's lab has led to an immunophenotype using the SLAM family molecules, CD48 and CD150, that has led to the highest level of enrichment of HSCs to date, whereby 1 of every 2 cells within the LSKCD48-CD150+ population were able to provide long-term multi-lineage reconstitution of the entire hematopoietic system [20].

2-2: HEMATOPOIETIC HIERARCHY

Because HSCs are now routinely isolated and are defined by rigorous long-term reconstitution transplantation assays, significant progress has been made in not only characterizing HSCs but also in establishing a model for the differentiation of HSCs into multiple lineages. The hematopoietic system is structured such that the rare multipotent, self-renewing hematopoietic stem cells (HSCs) are located at the apex of a three-tiered hierarchy (Figure 2-2) [1, 41]. According to this model, HSCs give rise to daughter cells, some of which will remain as stem cells while others will undergo successive progression of differentiation pathways into individual blood lineages [42]. Long-term blood reconstituting HSCs (LT-HSCs) are able to self-renew for the life of the organism and also give rise to short-term reconstituting HSCs (ST-HSCs), which are able to maintain self-renewing properties for approximately 8 weeks upon transplantation into lethally irradiated recipients [43]. Although ST-HSCs have a limited self-renewal capacity, they have extensive proliferative potential and are able to serve as a supply source for various lineage restricted progenitor populations [38]. The IL-17 receptor positive population gives rise to the common lymphoid progenitors (CLP) producing mature cells committed to lymphoid fates. B cells, T cells, natural killer (NK) cells and dendritic cells are all descendents of the CLP progenitor population. The common myeloid progenitor (CMP) population gives rise to lineage restricted progenitor cells of both the myeloid

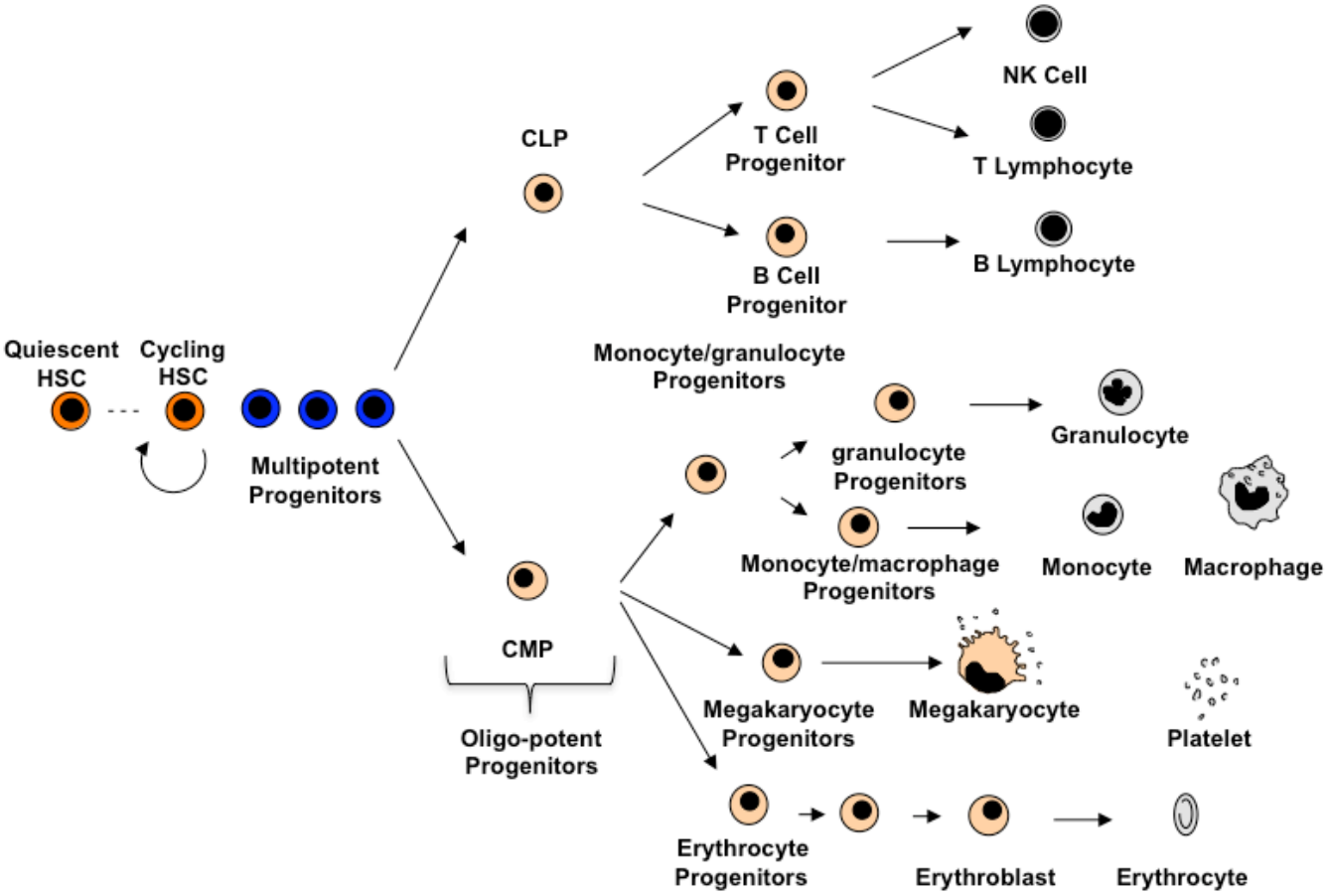

Figure 2-2: Schematic Illustration of the Hematopoietic Developmental Hierarchy. *Self-renewing hematopoietic stem cells reside at the top of a tiered hierarchy giving rise to multipotent progenitor daughter cells. The multipotent progenitor cells then give rise to oligo-potent progenitors of either the common myeloid progenitors (CMP) or common lymphoid progenitors. These oligo-potent progenitors give rise to a number of lineage restricted intermediate progenitors which in turn differentiate into the mature effector cells of the hematopoietic system. (Image generated by Nathalie Brouard, PhD)*

and erythroid lineages. Mature granulocyte and macrophage effector cells are derived from the granulocyte-macrophage progenitor (GMP) population and mature megakaryocytes and erythroid cells are generated from the megakaryocyte-erythroid progenitor (MEP) fraction of lineage restricted progenitor cells [3].

The hierarchical organization of hematopoiesis is long established and well validated and as a consequence, is often cited as a paradigm for the organization of stem and progenitors in other constitutively renewing tissues. Within the defined layers of the hierarchy, the entire hematopoietic system is maintained in a tightly coordinated manner in which self-renewal versus differentiation programs are balanced based on the prevailing need of the organism (i.e. under normal steady state homeostasis or under stress conditions such as occur during infection) without depleting the critical source of HSCs. There are several well-defined intrinsic regulators, such as lineage specific transcription factors, that play critical roles in maintaining the organizational structure of hematopoiesis. However, this balanced effort is also coordinated by external regulation from distinct micro-environmental cues, which form critical cellular and extra-cellular components in regulating self-renewal in addition to lineage specific differentiation pathways [44].

2-3: ONTOGENY OF HEMATOPOIESIS

Ontogeny of the hematopoietic system is established in two waves throughout embryo development. Interestingly, HSC development is marked by temporally regulated changes in anatomical location [45, 46], whereby at each stage HSCs are exposed to qualitatively different microenvironments endowing specific functions (Figure 2-3). The mammalian yolk sac is the first site for the emergence of hematopoiesis, termed primitive hematopoiesis. Here the primary focus is placed on the generation of erythrocytes to facilitate tissue oxygenation of the rapidly growing mouse embryo at 7-7.5 dpc [41, 47]. Experimental evidence from Goldie et al. demonstrated that at a clonal level, a population of specialized endothelial cells isolated from mouse E8.25 yolk sack were able to generate hematopoietic progenitor cells [48].

Following the formation of primitive hematopoiesis within the yolk sac, Godin and colleagues defined the para-aortic splanchnopleur region as the site of emergence of definitive pluripotent HSCs in mice at 10.5 dpc, [49, 50]. The para-aortic splanchnopleur region further differentiates into the aorta-gonad-mesonephros region (AGM). Some of the most convincing evidence, supporting the role of the AMG as the site of emergence of definitive HSCs, was demonstrated by in vivo long-term multi-lineage repopulation provided by intra-embryonic hematopoietic precursors in lethally irradiated adult recipients [51]. These precursors were able to give rise to lymphoid and myeloid lineages eight months after transplantation. More recently, strong experimental evidence has demonstrated that specialized embryonic

endothelial cells within the AGM, termed hemogenic endothelium, actually serve as the source for de novo generation of definitive hematopoiesis [52].

Following the emergence of definitive hematopoiesis in the AGM, the fetal liver becomes the primary site of hematopoiesis at E11.0 dpc. From E11.0 to E15.5, HSCs in the fetal liver are actively in the cell cycle and undergo rapid expansion followed by a decline prior to colonizing other hematopoietic organs such as the spleen and bone marrow where HSCs are found to be largely quiescent [38]. Studies by Christensen et al., demonstrated that long-term repopulating HSCs are found in circulation throughout fetal development and begin to colonize the fetal bone marrow at E17.5 after the onset of bone and vasculature development [53]. Throughout murine adult life the bone marrow remains the primary site of hematopoiesis during steady state conditions, however 100-400 LT-HSCs may be found in circulation at any one time [54].

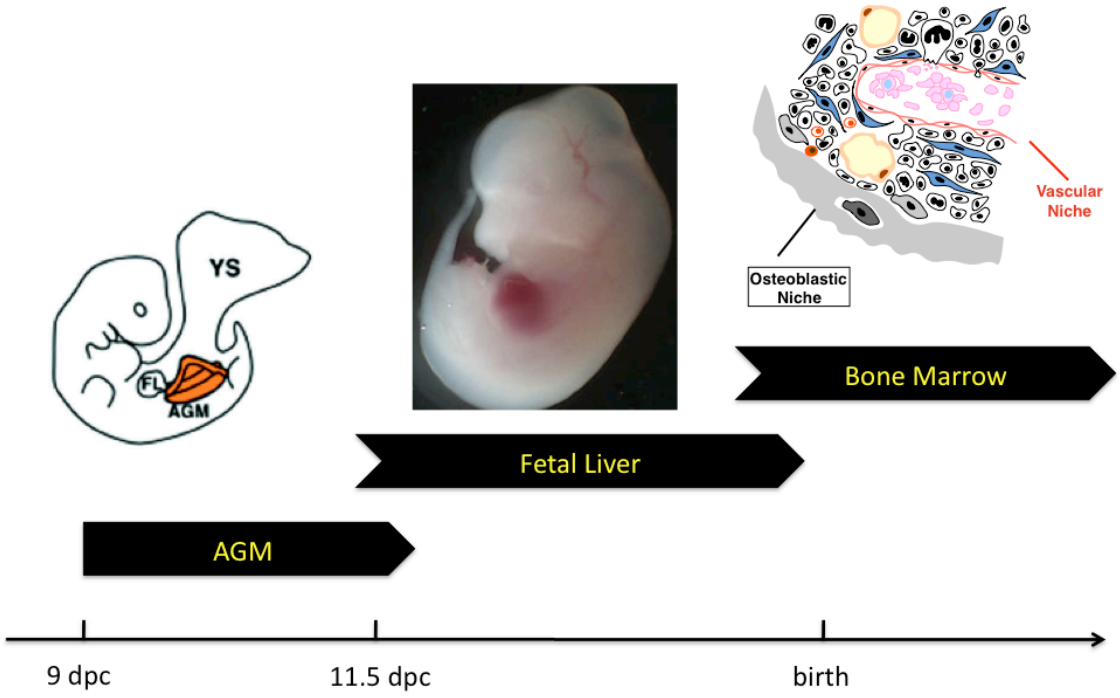

Figure 2-3: Hematopoietic Ontogeny in the mouse. *Hematopoietic stem cells first arise from specific endothelial cells within the AMG region of the developing embryo at around 9 DPC. Following the generation of definitive hematopoiesis in the AGM, HSCs are know to migrate to fetal liver were they undergo a massive expansion in vivo. Prior to birth and following the process of endochondral ossification of long bones, hematopoiesis moves to the bone marrow where it is to remain under normal homeostatic conditions. (Image generated by Nathalie Brouard, PhD)*

2-4: THE HEMATOPOIETIC MICROENVIRONMENT

The hematopoietic microenvironment (HM) is classically thought of as a mileau of cells (hematopoietic and non-hematopoietic stroma), extra-cellular matrix proteins and growth factors associated with the ECM (Figure 2-4) [55, 56]. The term stroma is derived from Greek and essentially refers to the physical entity (bed) upon which somethings lays. In hematopoiesis, the stroma is considered the substrate or scaffold unpon which hematopoiesis occurs [85]. The progressive identification of the hematopoietic microenvironment dates to the early 1960s, where initial studies noted that in lethally irradiated animals that were reconstituted by transfusion with BM cells, hematopoietic colonies develop only in the BM and spleen [30]. Furthermore when high doses of radiation were given to destroy the stromal elements of the BM a resulting permanent state of aplasia followed. And hence, a sequential regeneration of the marrow stromal cells preceded resumption of hematopoiesis in the bone marrow [57, 58]. However, some of the most convincing evidence of the role of the microenvironment came from using genetic mouse models. Mice with mutant recessive alleles in either the *Sl/Sl*^{d} and *W/W*^{V} loci gave rise to macrocytic anemia. Interestingly, bone marrow cells from *Sl/Sl*^{d} mice were able to rescue lethally irradiated wild-type littermates and *W/W*^{V} mice [59]. These studies conclude that the defect in *Sl/Sl*^{d} mice was expressed phenotypically as a failure of the HM. It is now understood that the ***W*** locus encodes the c-Kit pro-oncogene and the Steel locus encodes for its ligand, stem cell factor.

Later studies by Dexter and colleagues in the mid 1970s resulted in the establishment of a culture system that maintained primitive mouse hematopoietic progenitor cells in vitro [60, 61]. From these observations the authors conclude that the maintenance of hematopoiesis in vitro was dependent on an adherent layer of marrow derived cells whose composition reflected the phenotypic diversity of the stromal elements in the BM in vivo [61]. The historical importance of these findings allowed Ray Schofield to formulate his niche hypothesis in which he states that,

> *"the stem cell is seen in association with other cells which determine its behavior. It becomes essentially a fixed tissue cell. Its maturation is prevented and as a result its continued proliferation as a stem cell is assured. Its progeny, unless they can occupy a similar stem cell 'niche', acquire a high probability of differentiation"* [16].

Since the inception of the regulatory role of the BM stroma governing hematopoietic stem and progenitor cell behavior, there has been an increasing interest to identify cells and molecules responsible for orchestrating HSC quiescence, self-renewal, differentiation and proliferation. Two primary approaches have been applied to the discovery of such regulatory molecules; one approach has been through the use of mouse genetics and the other has been to use in vitro assays of either long-term marrow cultures or suspension cultures as an experimental tool to identify both cellular and molecular constituents that control HSC behavior. Several factors have been identified to have a genetic requirement and include stem cell factor (SCF), Thrombopoeitin (TPO), CXCL12 (SDF-1), osteopontin, and angiopoietin (Ang-1) [15, 62]. As such, most investigators in search

of additional regulatory mechanisms controlling HSC expansion in vitro have used several combinations of these factors in soluble form. However although essential in vivo, combinations of these molecules are unable to support either the maintenance or expansion of purified HSCs in vitro. Additional efforts have traditionally been to use adherent stromal cells from hematopoietic tissues as a means to identify cells with the ability to support and expand transplantable HSCs in vitro. In this regard, the adult bone marrow has been met with little success, however work from Ihor Lemischka's lab in the late 1990's was able to identify a fetal liver stromal line with the ability to support the maintenance of HSCs [63]. Although significant advances have been made in the pursuit to identify HSC governing molecules, there was previously a lack of evidence regarding the in vivo identification of the specific cells responsible for these molecules as well as a continued difficulty in isolating such cells. However, recently significant progress has been made and has begun to elucidate a more precise location of hematopoietic niches and the regulatory networks involved in governing HSC behavior.

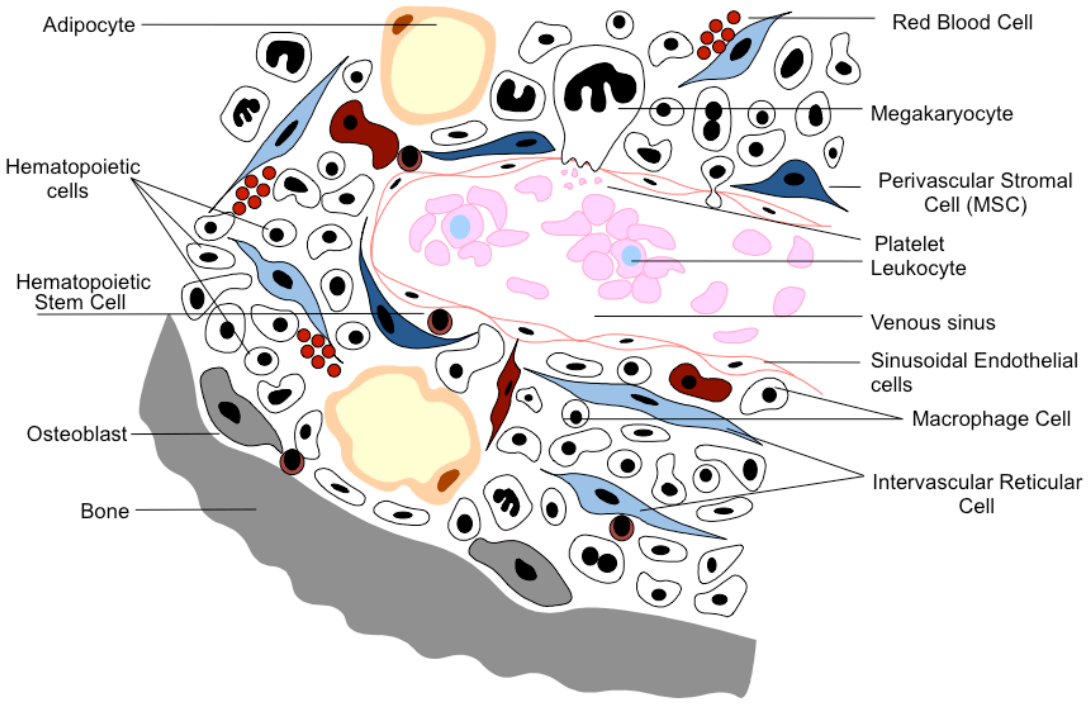

Figure 2-4: Schematic representation of hematopoietic microenvironment (HME). *The bone marrow HME is comprised of a diverse group of non-hematopoietic stromal cells, including adventitial reticular cells, stromal progenitor cells (CFU-F), endothelial cells, osteoblast and adipocytes and hematopoietic macrophage cells. These cell types generate both critical extracellular matrix and soluble regulatory molecules governing hematopoietic cell biology. (Modified from image generated by Nathalie Brouard, PhD)*

2-5: IDENTIFICATION OF THE HEMATOPOIETIC STEM CELL NICHE

Due to the difficulty of studying bone tissue in situ and limitations in technology, it was not until several years later that a more exact location and cellular composition of the hematopoietic bone marrow microenvironment began to be identified [17-26]. Current data suggest that pre-osteoblast cells lining the endosteal region serve a functional niche referred to as the endosteal niche, while HSCs have also been found residing adjacent to the sinusoidal endothelial and perivascular stromal stem/progenitor cells.

THE ENDOSTEAL NICHE

Early reports suggested that the endosteal zone of the bone marrow is highly enriched in cells which form multi-lineage colonies in the spleens of irradiated mice making it a candidate location of the hematopoietic niche [64]. A subsequent study by Nilsson et al. provided additional evidence in support of an endosteal niche, when labeled HSCs were transplanted and shown to localize to the endosteal region of the bone marrow [65]. Additionally, in vitro co-culture studies showed osteoblasts support hematopoietic progenitors [66]. However, a more exact role of osteoblast as a component of the endosteal niche was later highlighted by two seminal reports. Using two different genetic models both groups demonstrated that an increase in osteoblast cells lining the endosteum was followed by a concomitant increase HSC frequency within the bone marrow [18, 19]. Since these initial reports, many functional studies have now identified both positive and negative regulators generated by osteoblasts at the endosteal region, including osteopontin [67, 68],

angiopoietin-1 [69], thrombopoietin [70, 71] and SDF-1 (CXCL-12) [72]. Several studies support the role of adhesion molecules such as Jagged-1 and N-cadherin in establishing direct cell contact between HSCs and cells lining the endosteal surface [18, 19]. It was proposed that these adhesion molecules where important in maintaining proper HSC functioning in vivo, however conditional deletion of Jagged-1 in bone marrow cells suggests it is not necessary for HSC maintenance in vivo [73]. Furthermore, Sean Morrison's group has recently shown that N-cadherin is not expressed on LT-HSCs [74] and the conditional deletion of N-cadherin in HSCs has no effect on bone marrow cellularity or the frequency of HSCs [75], suggesting that N-cadherin is not necessary for maintaining HSCs in vivo. Although the exact molecular mechanisms underlying the support of HSC by osteoblastic cells remain to be fully elucidated, there remains significant evidence supporting the role of the niche in regulating HSC quiescence and maintenance [17, 76].

The Vascular Niche

Throughout ontogeny the sites of hematopoiesis change and interestingly, data suggest that in each of these developmental stages HSCs share close interactions with endothelial cells [77]. More recent evidence supports the hypothesis that embryonic endothelium give rise to multilineage hematopoietic cells, termed hemogenic endothelium [48, 51, 52, 78]. It is important to note that hematopoiesis occurs prior to the development of bone during embryogenesis, which suggests that HSCs are maintained primarily in vascular or perivascular microenvironments early during ontogeny as well as in areas of extra-medullary hematopoiesis such as the spleen [78]. Work by Shahin Rafii's group has led to the

concept of a proliferative zone surrounding the vascular microenvironment. This notion is supported by in vitro and in vivo studies that suggest that adult bone marrow endothelial cells promote the proliferation and differentiation of hematopoietic progenitors [79] and support the expansion of HSCs in vitro [80].

In 2005, the Morrison lab identified the close association of highly enriched LSKCD48-CD150^{+} HSCs with sinusoidal endothelial cells of the bone marrow suggesting the presence of a vascular niche for regulating HSCs [20]. Recent reports using CXCL12-GFP knockin [21, 24] and Nestin-GFP transgenic [23] mouse models have demonstrated that perivascular reticular cells were critical for maintaining the HSC pool in vivo (Figure 2-5) [23, 24] and selective ablation of these cells leads to a 50% reduction of phenotypically identified HSCs. However, it is not clear from these studies if there is an actual decrease in functional HSCs. These data support previous reports in human BM, which demonstrated that CD146+ subendothelial adventitial reticular cells function as both osteoprogenitor cells (MSC) and HSC niche constituents [22]. Furthermore, the existence of a vascular/perivascular niche is supported by the observation that HSCs are rapidly mobilized into circulation following cytokine treatment [81] and that the regeneration of sinusoidal endothelial cells following myeloablation treatment is necessary for hematopoietic reconstitution to occur [82].

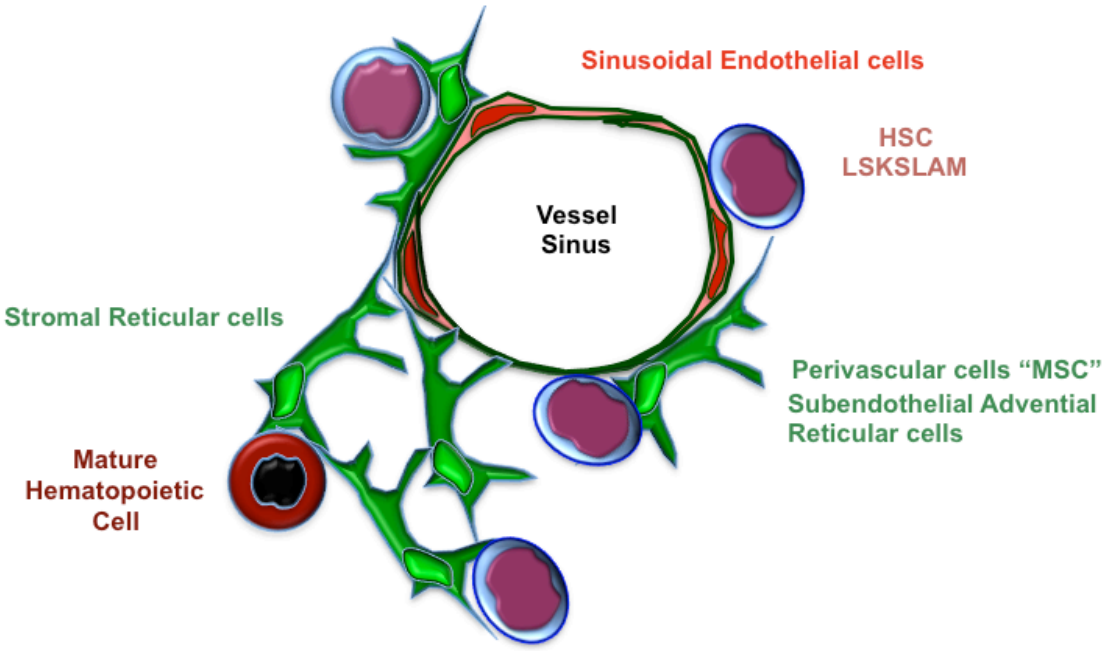

Figure 2-5: Schematic representation of the vascular niche in adult mouse bone marrow. *HSCs are localized directly adjacent to endothelial sinusoids and are often in direct contact with the cellular processes of adventitial reticular cells situated along the abluminal surface of vessel sinuses. Additional stromal cells within the inter-sinusoidal spaces make up a complex stromal reticulum providing a scaffold for HSC and mature hematopoietic cell migration throughout the bone marrow.*

2-7: UNRESOLVED QUESTIONS

To date the exact location, cellular constituents and molecules involved in regulating hematopoietic stem cells remains a highly contentious and active area of research. It remains to be determined if two distinct niches exist and if so do they have different functional roles in regulating HSCs. Recently there has been an emergence of data using specialized imagining techniques which show the endosteal zone as being highly vascularized [83, 84]. These findings demonstrate that the vascular niche containing perivascular stromal cells would lie in close proximity to the proposed endosteal niche and raise an important question of whether or not distinct niches exist. It is possible that HSCs are found next to endothelial and perivascular cells during times of migration in and out of circulation as well as during homeostasis [15, 25] while only a very minor portion actually reside along the endosteal surface. However, in light of recent advances in imaging it is unlikely that HSCs located along the endosteal surface are completely removed from any potential interaction, be it physical or from soluble molecules, with vascular and perivascular cells. Data from our own studies presented in this dissertation and elsewhere have demonstrated that the vascular/stromal system is a vast and complex network which encompasses the entire bone marrow diameter from one endosteal surface of a femur to the other, and continues along the full length of a femur from the hypertrophic cartilaginous zone at the growth plate up to the trabecular region of the femoral head.

Although the use of genetic mouse models previously mentioned have proved useful in identifying perivascular stromal cells that provide critical support for maintaining HSC behavior, there is little evidence of specific immunophenotypes for these candidate cell populations which can be used for prospective identification and isolation. In particular, these mouse models are not commercially available which further hinders progress in the field by limiting the labs, which can reproduce and validate these reports. Within the following chapters, I provide evidence of distinct immunophenotypes, which allow prospective isolation of candidate cell populations, both stromal and vascular, and data that supports the hypothesis that perivascular stromal stem/progenitor cells are the major cellular constituents of functionally critical hematopoietic regulatory molecules.

CHAPTER 3:

ISOLATION OF THE STROMAL-VASCULAR FRACTION FROM ADULT MURINE BONE MARROW [28]

3-1: PREFACE

In this chapter, I describe a methodology I developed based on a step-wise enzymatic disaggregation of bone marrow tissue, which led not only to a significant improvement in the yield of clonogenic stromal cell progenitors (CFU-F) but also revealed a previously unappreciated complexity in the composition and organization of cells that comprise the bone marrow stromal compartment **[28].** The initial findings presented within this chapter led us to further **hypothesize that the adult mouse bone marrow contains phenotypically distinct populations of MSC, which contribute to the maintenance of HSC niches and are prospectively isolatable by distinct immunophenotypes.**

3-2: THE NON-HEMATOPOIETIC STEM CELL COMPONENT OF THE BONE MARROW: MARROW STROMAL STEM CELLS (MSC)

The post-natal bone marrow of adult mammals is comprised of both hematopoietic and non-hematopoietic cellular elements, each of which is supported by a specific stem cell population, HSC and mesenchymal stem cells (MSC), respectively. Thus, not only does the bone marrow harbor two distinct populations of stem cells, but recent data also suggest that these two stem cells physically co-localize within the marrow, an interaction that is functionally required for the maintenance of HSC. The anatomical structure of the bone marrow tissue is made up of highly branched vascular network consisting of arteries, arterioles and large dilated sinusoids and a heterogeneous stromal cell reticulum of perivascular and inter-sinusoidal cells, whereby the multitude of hematopoietic lineages reside [55, 56].

The BM stroma encompasses a heterogeneous group of cell types found between the inner endosteal surfaces of bones and the outer surface of blood vessels including non-hematopoietic adipocytes, perivascular reticular cells and osteoblast [26]. Existing within the marrow stromal elements is a rare population of multi-potent stem/progenitor cells historically referred to as “stromal” stem cells. More recently, the term “skeletal” or “mesenchymal” stem cells (MSC) [85, 86, 87-91] (Figure 2-6) has been extensively used to describe these cells in the literature. The multi-lineage differentiation capacity of MSC and their corresponding regenerative potential along with a unique ability to suppress T cell proliferation, has

engendered a considerable amount of interest in the potential application of these cells in a range of cellular therapies.

Circumstantial evidence demonstrating the existence of a non-hemtopoietic adult stem/progenitor cell within the BM stromal compartment can be found in early studies by Crosby and colleagues. Following physical or irradiation damage, the BM stromal tissue was found to undergo a process of complete regeneration [57, 58]. Additional studies demonstrated the osteogenic potential of bone marrow stromal cells, which were able to generate histologically proven bone ossicles complete with a surrounding layer of cortical bone and a cavity filled with active hematopoietic marrow supporting stromal cells and adipocytes following transplantation of boneless fragments of BM to an ectopic site [26, 92]. Subsequently in a series of pioneering studies, Friedenstein and colleagues provided a direct demonstration of stromal stem/progenitor cells by characterizing a population of clonogenic adherent cells derived from the BM of rodents, which resembled fibroblasts in morphology and nature leading to the term, colony forming unit-fibroblast (CFU-F) [86, 91, 93]. Since these initial observations, there has been a considerable interest in identifying the source of stromal clonogenic precursors in nearly all mammalian tissues examined. A defining feature of marrow CFU-F is the heterogeneity frequently observed regarding colony size, an indication of proliferative differences in the founding CFU-F progeny, and the differentiation potential of individual colonies [86, 88, 120]. Following these observations mentioned above, Owen and colleagues hypothesized that in the adult BM a stromal cell hierarchy exists, which is constituted of a rare ‘pluri-potent stromal stem cell’ that through the processes of self-renewal and

differentiation gave rise to the entire non-hematopoietic stromal system (86).

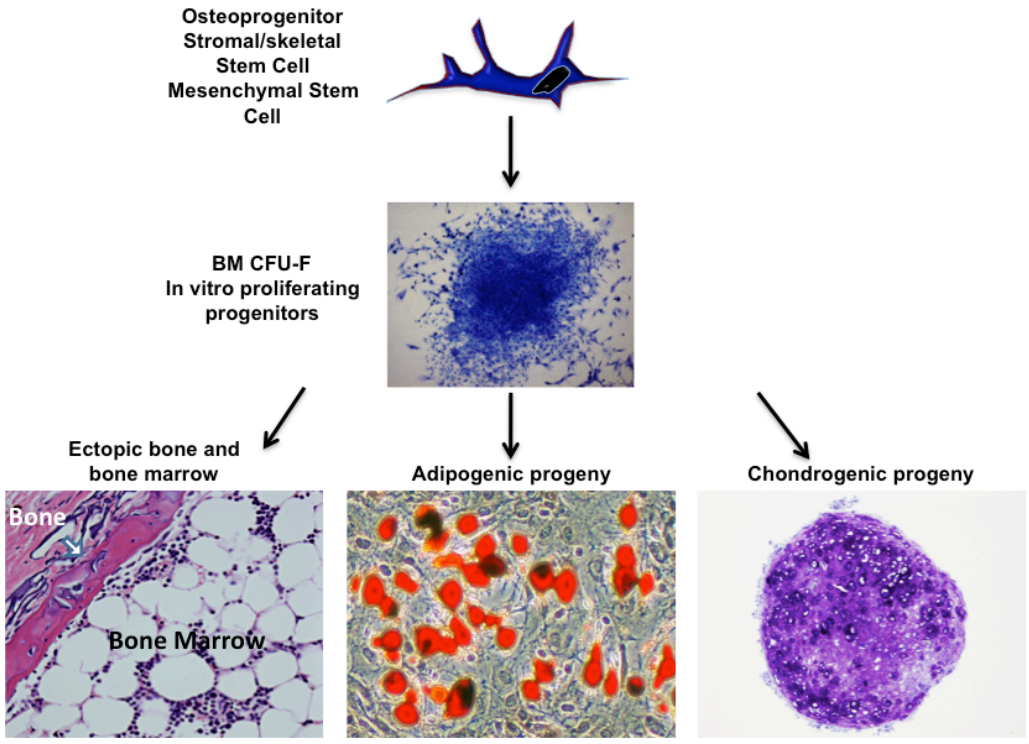

Figure 3-1: Schematic diagram of bone marrow stromal stem cells development potential. *A rare population of stromal stem cells gives rise to highly proliferative clonogenic progeny in vitro (CFU-F). CFU-F can undergo multi-lineage differentiation into osteogenic, adipogenic and hematopoietic supporting stroma lineages in vivo and generate adipogenic and chondrogenic progeny in vitro.*

The apparent multilineage differentiation potential of bone marrow stromal tissue was first illustrated by the seminal studies of Tavassoli and Crosby [92]. In these experiments, transplantation of bone-free pieces of bone marrow tissue to ectopic sites generated histologically proven bone ossicles complete with a surrounding layer of cortical bone and a cavity filled with active hematopoietic marrow supporting stromal cells and adipocytes. These studies were the first to reveal the intrinsic osteogenic potential of BM and invoked the existence within the marrow of a population(s) of cells with the differentiation potential to generate bone and the other stromal tissues of BM.

Subsequently, early pioneering work by Friedenstein and colleagues described a population of plastic-adherent, clonogenic progenitors, which, based on the fibroblastic morphology of their progeny in the colonies, he termed colony-forming unit-fibroblast (CFU-F) [93]. Additional studies by Friedenstein and colleagues further substantiated Tavassoli and Crosby's initial findings by demonstrating the in vivo multilineage differentiation capacity of CFU-F [88, 94]. What was most striking about these studies was that hematopoiesis was maintained within these ossicles only after bone was formed and vascular endothelial cells of host origin had invaded the ectopic ossicles, demonstrating a sequence of events that mimic the developmental events of bone and bone marrow formation [95]. Currently, it is hypothesized that a portion of the founding cells that give rise to CFU-F are derived from the subendothelial adventitial reticular cells (Westen-Bainton cells). Interestingly, this subendothelial region of the marrow sinusoids is not only the location of the HSC vascular niche, but is also proposed to comprise the stromal

stem cell compartment as well. In support of their role as a stromal stem/progenitor cell in vivo, work from Bianco and colleagues lab demonstrated that some of the adventitial reticular cells generate mature marrow adipocytes while others give rise to the more heterogeneous population of bone marrow stromal cells [96].

These studies along with the pioneering work of Dexter and colleagues, previously mentioned, have provided key insights into the nature and biology of establishing and maintaining the hematopoietic microenvironment, highlighting the key role of the non-hematopoietic stromal stem cells in these processes and an invaluable resource in allowing Ray Schofield to formulate the ‘niche hypothesis’. Within the hematopoietic stem cell niche field, the stromal stem/progenitor population is beginning to emerge as the key player in coordinating endogenous tissue turnover and in establishing and maintaining the hematopoietic microenvironment.

Although originally identified in mice, many labs have subsequently isolated BMSCs, some of which contain stem/progenitor activity (MSC), from human, rat, rhesus monkeys, dog, and pig based on there inherent ability to attach to tissue culture plastic, undergo limited ex vivo expansion and are able to differentiate into osteogenic, adipogenic and chrondrogenic progeny in vitro and in vivo (Figure 3-1) [70-101].

However it is important to note that the majority of progress regarding the in vivo localization and immunophenotype for prospective isolation of MSC has been made using human BM samples, with few publications focusing specifically on MSC derived from mouse BM. This is largely due to the difficulty in isolating

homogeneous populations of murine BM-derived MSC, a problem exacerbated by the extreme rarity of CFU-F in murine bone marrow, which furthermore varies with the mouse strain tested. The reported incidence of CFU-F in C57BL/6 mice, the strain used for the majority of studies reported in this thesis, is in the range 0.3 - 2/1,000,000 nucleated bone marrow cells [97, 102, 106]. An additional issue is the persistence of hematopoietic cells (principally macrophages) that contaminate MSC cultures derived from mouse BM even after prolonged culture [102-106]. Although repeated passage of mouse stromal cell cultures has been reported to reduce the incidence of contaminating hematopoietic cells, a significant drawback of this strategy is the likelihood of proliferative exhaustion of the low numbers of initiating CFU-F progenitor cells and conversely, the potentiation of spontaneous transformation of cells following long term culture [107].

Although most data support the low incidence of CFU-F in mouse BM, there are studies in which significantly higher CFU-F frequencies have been reported ranging from 35-115/1,000,000) BM cells. This higher colony-forming efficiency is dependent on the addition of irradiated guinea pig stromal feeder layers [108]. Although the use of feeder cells has only been reported by a single lab, it nevertheless illustrates an important point that optimal conditions for initiating colony growth from mouse BM CFU-F have yet to be defined. Additional increases in CFU-F numbers have been reported following protocols, which involve mechanical dissociation, and trypsin digestion of the remaining bone marrow clumps as describe by Freidenstein and colleagues [109].

Taken together, the low numbers of CFU-F obtained by routine methodologies, the persistent contamination by hematopoietic cells, the fact that the majority of mouse BMSC data is based on retrospective analysis of cultured cells, and the lack of suitable markers of prospective isolation of a purified mBMSC population, has significantly hindered progress in the mBMSC field, impairing the ability to address fundamental questions regarding MSC biology through the use of genetic mouse models but also the development and preclinical testing of proposed therapeutic applications of MSC in the mouse.

While the majority of labs seeking to understand the nature and biology of mouse BMSCs use the standard method of flushing BM from long bones, some labs have attempted to improve the purity of BMSC cultures by additional methodologies including positive or negative selection and low plating densities [102-106, 109-111] while other labs have been successful in isolated a sub-population of bone derived progenitor cells by crushing and digesting compact bone [112-114]. However, these protocols have not significantly improved the yield of clonogenic progenitors and as a result have not been standardized nor widely adopted.

We, therefore, sought to develop an alternative strategy for the isolation of murine BMSC, which would provide a platform to maximally increase the stromal cell yield and allow populations of BMSCs to be prospectively isolated from freshly prepared tissue. In developing this methodology, we considered two key points regarding the structure of the BM stromal-vascular system and the localization of candidate populations. First, histological studies demonstrate that the BM hematopoietic microenvironment is organized as a complex network of stroma

including fibroblastic reticular cells and highly branched vascular arterial and dilated venous sinuses (references). Second, experimental evidence has demonstrated a perivascular location of MSC in many adult tissues, including the BM [22, 115].

Early ultra-structural studies of rat BM stroma by Leon Weiss [55] demonstrated that the reticular cells expand throughout the BM and form a three-dimensional reticulum of long cytoplasmic processes that make up the majority of the marrow parenchyma amongst which hematopoietic cells exist and interact. Interestingly, some of the marrow cells, which make up the parenchyma are mature macrophages of hematopoietic origin, while others initially characterized by membrane bound alkaline phosphatase (ALP) activity are fibroblastic in nature and are of mesenchymal origin. The ALP positive reticular cells are located within the intraparenchyma and perivascular along the sinus walls and are often referred to throughout the literature as Westen-Bainton cells as previously mentioned [116].

Taking both points into consideration along with the delicate nature of the BM structure, we initially hypothesized that the low frequencies of CFU-F reported by others is a consequence of the rigorous flushing and trituration of the bone marrow cavity used to prepare single cell suspensions and that the subsequent destruction of the marrow vasculature would lead to a diminution in the potential recovery of stromal stem/progenitor cells localized to perivascular regions along the abluminal surface of the marrow vessels. In light of our hypothesis, we developed a reproducible methodology to isolated BMSCs based upon the initial preservation of the marrow vasculature by first removing an intact plug of BM from the central cavity of long bones. Single cell suspensions are then prepared by sequential enzymatic

digestion of BM plugs, which simultaneously yields both stromal reticular and vascular endothelial cellular components of the BM. Interestingly, this novel methodology has facilitated the identification and direct isolation of phenotypically and anatomically discrete subpopulations of BMSCs. In the following chapters, I characterize, through well-validated in vivo and in vitro assays, distinct populations of clonogenic BMSCs that function as both “mesenchymal” stem/progenitor cells (Chapter 4) and as hematopoietic stem cell niche constituents (Chapter 5).

3-3: RESULTS

REMOVAL OF INACT BONE MARROW 'PLUG' MAINTAINS THE STRUCTURAL INTEGRITY OF THE MARROW VASCULTURE

Our initial hypothesis was that the mechanical destruction of the marrow vasculature ultimately destroys the stromal progenitor cells intimately associated with the vascular walls. To test this hypothesis, we developed an alternative procedure based on the removal of intact '*plugs*' of BM from murine long bones by gentle flushing of the bones with media (Fig 3-2A). This methodology leads to the removal of the central bone marrow tissue and leaves behind a thin layer of cells associated with the endosteum region (Fig 3-2 B&C). The marrow 'plugs' were then subjected to a detailed histological analysis of the plugs either embedded in resin or subjected to whole mount staining. As revealed in Figure 3-2 B, D & E, the marrow vascular structure remains well preserved, with both arterioles and sinusoids conserved, and is comparable to BM in situ. Furthermore, whole mount staining of BM plugs, using a combination of the endothelial cell-reactive antibodies MECA32 and VE-Cadherin, demonstrated a complex vascular network that spans the width of a femur (Fig 3-2 E). Having confirmed the presence of an intact vascular structure, we next sought to obtain a single cell suspension from which we could begin to characterize the various elements of the non-hematopoietic stromal-vascular fraction.

Figure 3-2: BM plug isolation and histological assessment of intact vascular structures in BM plugs. *(A) Representative images of denuded bones, removal of metaphysis and isolated intact bone marrow plug. (B-D) Resin embedded sections of BM plugs (B&D) and remaining bone tissue (mid-diaphysis) (C) following removal of marrow plug were sectioned as 5μm thick longitudinal sections and stained with H&E demonstrates intact vascular structures. (E) Whole mount image of BM plug stained with a combination of the endothelial cell-reactive antibodies MECA32 and VE-Cadherin reveals a well-organized vascular reticulum throughout the marrow. BM plugs were stained with DRAQ5 to provide a nuclear counterstain and then immersed in prolong gold anti-fade mounting medium (Molecular Probes). After applying a glass coverslip and sealing with nail hardener, specimens were inverted and allowed to cure overnight in the dark at RT prior to confocal imaging. Images were collected using 63x oil immersion objective of a Leica TCS SP5 confocal microscope and processed with the Leica LAS AF lite software. Z-stacked images were collected in 0.2 μm slices at depths of 15-25 μm with a pinhole of 1 (x63).* (This research was originally published in *Blood* Online. Suire C, Brouard N, Hirschi K, Simmons PJ. Isolation of the Stromal-Vascular Fraction of Mouse Bone Marrow Markedly Enhances the Yield of Clonogenic Stromal Progenitors. *Blood*. Prepublished January 18, 2012; DOI 10.1182/blood-2011-08-372334.)

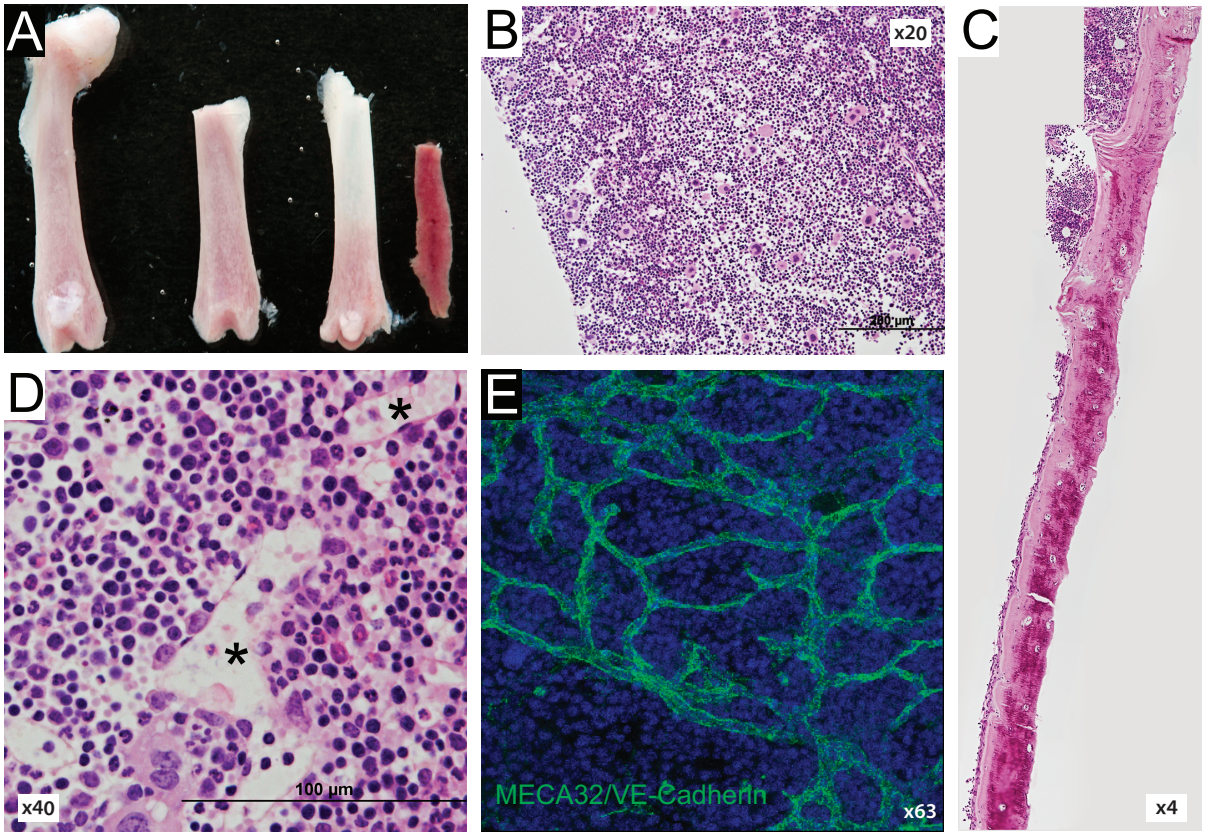
A
B
x20
200 µm
C
D
*
*
x40
100 µm
E
MECA32/VE-Cadherin
x63
x4

We then experimentally determined that three sequential digestions, each of which was 15 minutes in duration at 37 degrees C (Figure 3-3), with a combination of collagenase type I and dispase enzymes was sufficient to recover all cells as a single cell suspension and leaving behind only an acelluar matrix. This point is further illustrated in Fig 3-4 A, which demonstrates that the total number of nucleated cells recovered from each digestion as compared to the nucleated cell recovery from the standard method of rigorously flushing BM is not significantly different.

SEQUENTIAL ENZYMATIC DISAGGREGATION OF BM PLUGS MARKEDLY ENHANCES THE RECOVERY OF CFU-F

After having determined that three sequential enzymatic digestions was sufficient to obtain a single cell suspension, we then conducted a series of preliminary experiments to compare the frequency of CFU-F in sequentially digested BM (DBM) from each fraction to that obtained by the standard flushing method. As demonstrated in Figure 3-4 B, each fraction of DBM contained a significantly higher colony forming efficiency (CFE) than in the flushed BM samples, with a higher CFE within each successive fraction of DBM. Interestingly, the colony forming efficiency of CFU-F was on a range of 25 – 40 fold higher from each of the three fractions than the CFE obtained from an equivalent number of nucleated cells from flushed marrow samples. Furthermore, these date demonstrate that CFU-F progenitors revealed

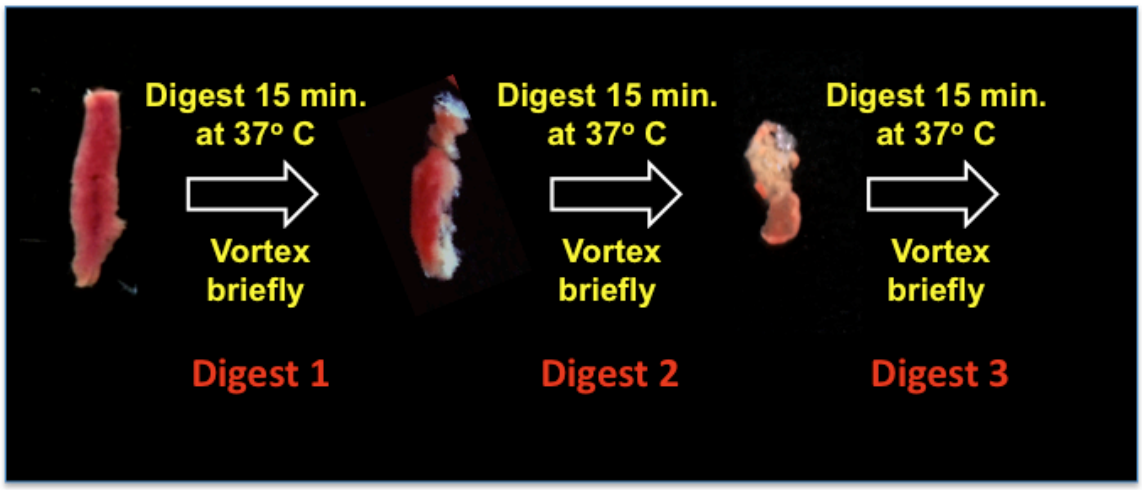

Figure 3-3: Schematic diagram of enzymatic disaggregation of bone marrow plugs. *Intact plugs of BM are gently expelled from the central cavity of long bones and transferred to an enzymatic solution of collagenase type I and neutral dispase and incubated in a water bath at 37° C for three sequential rounds at 15 minutes each. Following each successive round of digestion, the tissue becomes smaller, more disorganized and pale. Following the third incubation period only an acellular matrix remains.*

that each fraction of DBM contained significantly more CFU-F than that obtained from flushed BM, leading to a potential recovery of 3066 CFU-F per femur/tibia pair to approximately 80 CFU-F recovered from flushed BM, with approximately 62% of CFU-F being isolated following the first digestion, 31.4% of CFU-F isolated following the second digestion and 6.9% of CFU-F isolated following the final digestion (Fig. 3-4 C).

Additionally, we conducted a series of experiments comparing the frequency of CFU-F obtained by pooling the three fractions together as a more representative sample of the stromal progenitor population as a whole within BM. Data from these experiments demonstrated a 196.4 fold increase in the frequency of CFU-F in the pooled DBM with approximately $1/10^4$ mononuclear cell forming a colony, as compared to that in flushed BM (Fig 3-4 D). These observations correspond to a 113.95-fold enhancement in the CFU-F recovered by this newly developed technique and optimized growth conditions at 5% O_2 (Fig 3-4 E). In parallel, we also tested the effects of oxygen concentration of CFU-F formation. To do this, single cell suspensions of pooled DBM and flushed BM samples were plated in growth media at either 20% oxygen, normoxia (n=4) or at 5% oxygen, low oxygen (n=8). The CFE of DBM under low oxygen tension (5%) was nearly 30-fold higher than the CFE of DBM at normal oxygen tension (20%) (Fig 3-5), signifying perhaps a more physiologically relevant environment in vitro and a growth requirement in vivo.

Figure 3-4: Evaluation of clonogenic stromal progenitor cells (CFU-F) recovered from sequential enzymatic disaggregation of bone marrow plugs. *(A) Average mononucleated cell yields obtained from either standard flushing methods or from each successive digestion (n=4). (B) Incidence of CFU-F obtained from either standard flushing technique (5x10^6 mononuclear cells/well) or from each fraction of digested marrow plugs (2.5x10^5 mononuclear cells/well) plated in triplicate. (C) Recovery of CFU-F from flushed BM and each fraction of DBM calculated per femur-tibia pair. (D) Incidence of CFU-F obtained from flushed BM versus the pool of DBM fractions (1-3) (n=8). (E) Recovery of CFU-F from flushed BM and the pool of DBM fractions (1-3) calculated per femur-tibia pair. Only colonies containing >50 stromal cells are scored. CFU-F data are presented both as incidence of clonogenic cells (CFU-F/1x10^6 mononuclear cells) and as the total number of CFU-F recovered from a given number of bones (CFU-F per total nucleated cells). Data are represented as mean ± SD. Statistical analysis of CFU-F incidence was performed with SigmaStat version 3.5 and significance was assigned to p<0.05.*

(This research was originally published in *Blood* Online. Suire C, Brouard N, Hirschi K, Simmons PJ. Isolation of the Stromal-Vascular Fraction of Mouse Bone Marrow Markedly Enhances the Yield of Clonogenic Stromal Progenitors. *Blood*. Prepublished January 18, 2012; DOI 10.1182/blood-2011-08-372334.)

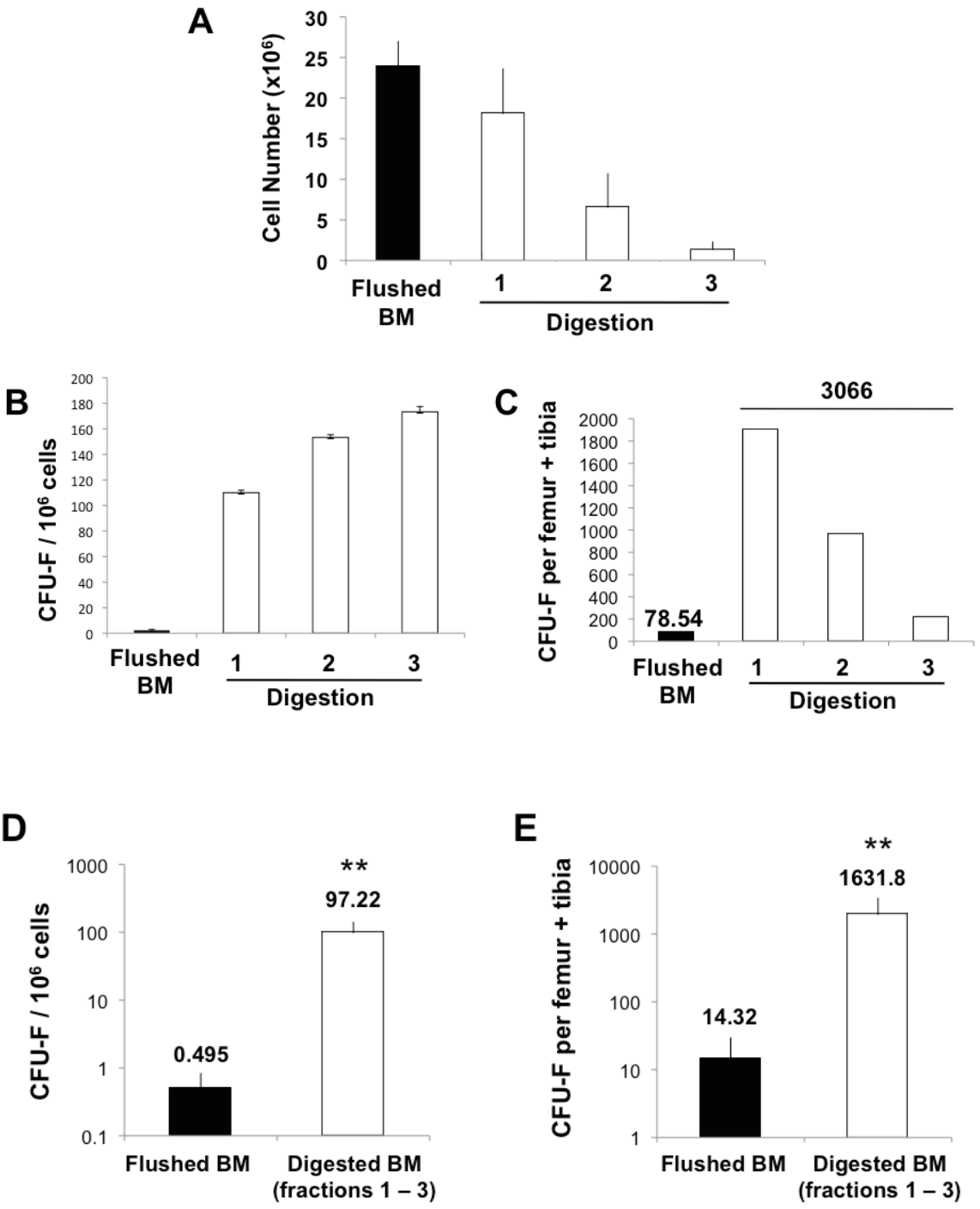
A
Cell Number (x10^6)
30
25
20
15
10
5
0
Flushed BM
1
2
3
Digestion
B
CFU-F / 10^6 cells
200
180
160
140
120
100
80
60
40
20
0
Flushed BM
1
2
3
Digestion
C
CFU-F per femur + tibia
3066
2000
1800
1600
1400
1200
1000
800
600
400
200
0
78.54
Flushed BM
1
2
3
Digestion
D
CFU-F / 10^6 cells
1000
100
10
1
0.1
**
97.22
0.495
Flushed BM
Digested BM (fractions 1 – 3)
E
CFU-F per femur + tibia
10000
1000
100
10
1
**
1631.8
14.32
Flushed BM
Digested BM (fractions 1 – 3)

Although the increase in DBM CFU-F frequency observed in these experiments exceeded the CFU-F frequency obtained from flushed BM samples by at least 2 orders of magnitude, we sought to determine the CFU-F frequency obtained from DBM samples more quantitatively by limit dilution analysis (LDA). To do this, single cell suspensions prepared from DBM were plated at a range of dilutions in 24 replicates (n=3). From these analyses, we observed the frequency of CFU-F in pooled DBM samples to be 1/2635 BM mononuclear cells (Fig 3-6), which corresponds to a recovery of 9087.7$\pm$2996 CFU-F per femur/tibia pair with a noted incidence approximately 634-fold higher than that recovered from the same amount of tissue prepared by flushing BM. Taken together, our data demonstrates that this newly developed methodology yields significantly more CFU-F as measured by both the incidence and recovery as compared to that obtained by standard flushing of BM samples and represents significance advancement in the study of BM stromal stem/progenitor cells.

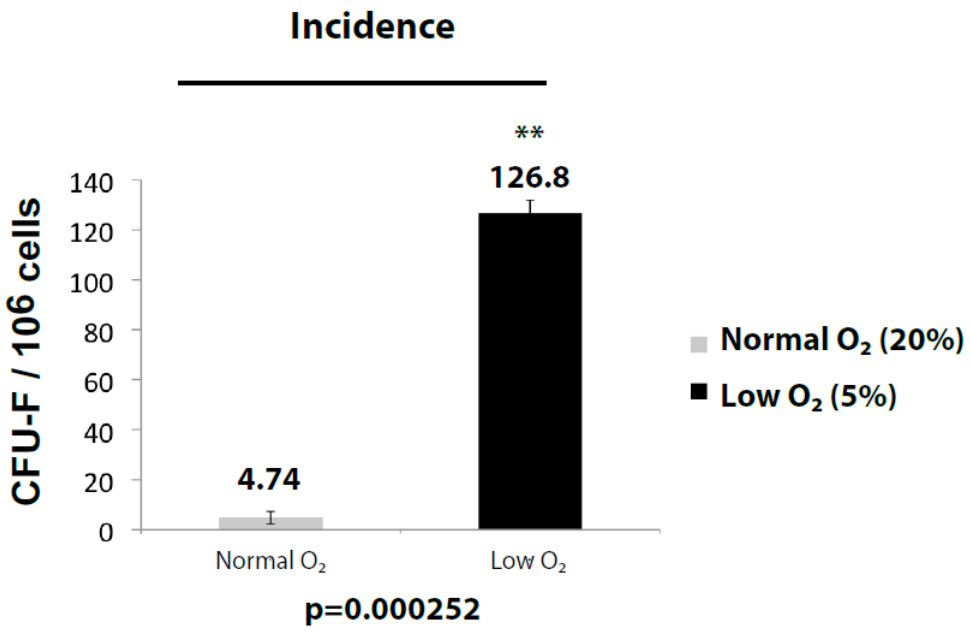

Figure 3-5: Effect of oxygen tension on CFU-F. *Whole bone marrow from sequential enzymatically disaggregated BM plugs was plated in triplicate at 20% oxygen (5x10^5 cells/well) or 5% oxygen (2x10^5 cells/well) for 14 days. Colonies were stained with 0.1% Toluidine Blue.*

(This research was originally published in *Blood* Online. Suire C, Brouard N, Hirschi K, Simmons PJ. Isolation of the Stromal-Vascular Fraction of Mouse Bone Marrow Markedly Enhances the Yield of Clonogenic Stromal Progenitors. *Blood*. Prepublished January 18, 2012; DOI 10.1182/blood-2011-08-372334.)

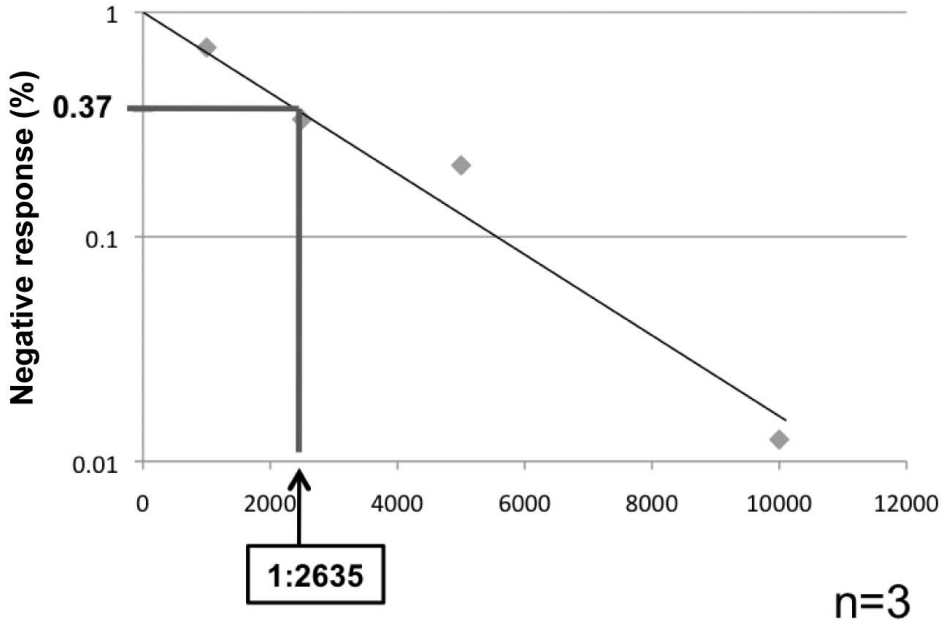

Figure 3-6: Limit Dilution Analysis of Bone Marrow CFU-F. *CFU-F incidence was quantified by limit dilution analysis (LDA). Limit dilution assays were performed by plating bone marrow mononuclear cells at various cell doses (500, 1,000, 2,500, 5,000 and 10,000 cells/well in 24 well plates) with 24 replicates per dilution. Data are from 3 independent experiments were scored and negative wells enumerated from each plate at each dilution. Data was analyzed with L-calc software (Stem Cell Technologies, Vancouver, BC) and plotted as a negative linear relationship to identify the frequency of colony forming cells.*

(This research was originally published in *Blood* Online. Suire C, Brouard N, Hirschi K, Simmons PJ. Isolation of the Stromal-Vascular Fraction of Mouse Bone Marrow Markedly Enhances the Yield of Clonogenic Stromal Progenitors. *Blood*. Prepublished January 18, 2012; DOI 10.1182/blood-2011-08-372334.)

PRIMARY MOUSE BONE MARROW CULTURES DERIVED FROM ENZYMATICALLY DISSOCIATED BM PLUGS CONTAIN THE MARROW STROMAL-VASCULAR FRACTION

In our initial experiments, we observed that when BM cell suspensions, prepared by enzymatic disaggregation, were plated at non-clonal densities of 1x10^^{6} mononuclear cells/cm^2 the cultures became 100% confluent by 5-7 days. From this observation, we next attempted to characterize the immunophenotype of these primary cultures by testing a number of antibodies directed to extra-cellular molecules by immunocytochemistry and multi-parameter flow cytometry. We reasoned that, because the vascular structure was initially intact within BM plugs (Fig 3-2 B, D&E), these cultures would contain endothelial populations as well as heterogeneous stromal cell populations. Taking into consideration the fact that stromal cells and vascular endothelial cells have different in vitro growth requirements and differential adhesive capabilities to adhere to tissues culture plastic, we conducted a series of experiments to optimize the growth for each respective cell type.

For these experiments, DBM was plated at non-clonal cell density (1x10^6 nucleated cells/cm^2) in either αMEM basal media supplemented with 20% fetal bovine serum on tissue culture plastic or in endothelial basal growth medium supplemented with a combination of endothelial growth factors (EGM2-MV) on fibronectin coated tissue culture plates in order to optimize the growth of stromal and endothelial cell constituents. Following a period of 5-7 days at 5% oxygen in either growth condition, primary (P_0) cultures were first stained in situ with antibodies to

Figure 3-7: Immunostaining of P_0 cultures and isolation and characterization of BM vascular endothelial cells. *(A i-vi) In situ staining of P_0 cultures plated on fibronectin coated chamber slides (LabTek, Nunc, Rochester, NY), cultured in EGM-2MV for 5-7 days. Vascular endothelial cells were identified by staining with a combination of VE-Cadherin-Alexa 488 and MECA32-Alexa 488 antibodies and stromal cells were stained with rat anti-mouse PDGFRα/β (purified) antibodies and revealed with donkey anti-rat Cy3 and counterstained with DAPI. IgG2a and IgG1 isotypes were used for controls (A iv-v). (B) Gating strategy for FACS purification of vascular endothelial cells from P_0 cultures plated on fibronectin coated 10cm^2 dishes at 1x10^^{6} mononuclear cells/cm^2 and cultured in EGM-2MV for 5-7 days and stained as described in methods. (C) Phase contrast images of Lin^{NEG}CD105^{BRIGHT}PDGFRαβ^{NEG} cells at passage 3 and functional analysis of DiAcetylated-LDL uptake. (D) In situ staining of Lin^{NEG}CD105^{BRIGHT}PDGFRαβ^{NEG} cells at passage 3 for endothelial markers including VEGFR2 (Di.), VE-Cadherin (Dii), CD31 and eNOS (Diii), MECA32 (Div), CD105 (Dv) and isotype controls (Dvi-vii). Nuclei were counterstained DAPI. Imaging was performed on an inverted fluorescence microscope (Olympus BX51) at both x10 and x40 original magnification and captured with an Olympus DP71 camera.*

(This research was originally published in *Blood* Online. Suire C, Brouard N, Hirschi K, Simmons PJ. Isolation of the Stromal-Vascular Fraction of Mouse Bone Marrow Markedly Enhances the Yield of Clonogenic Stromal Progenitors. *Blood*. Prepublished January 18, 2012; DOI 10.1182/blood-2011-08-372334.)

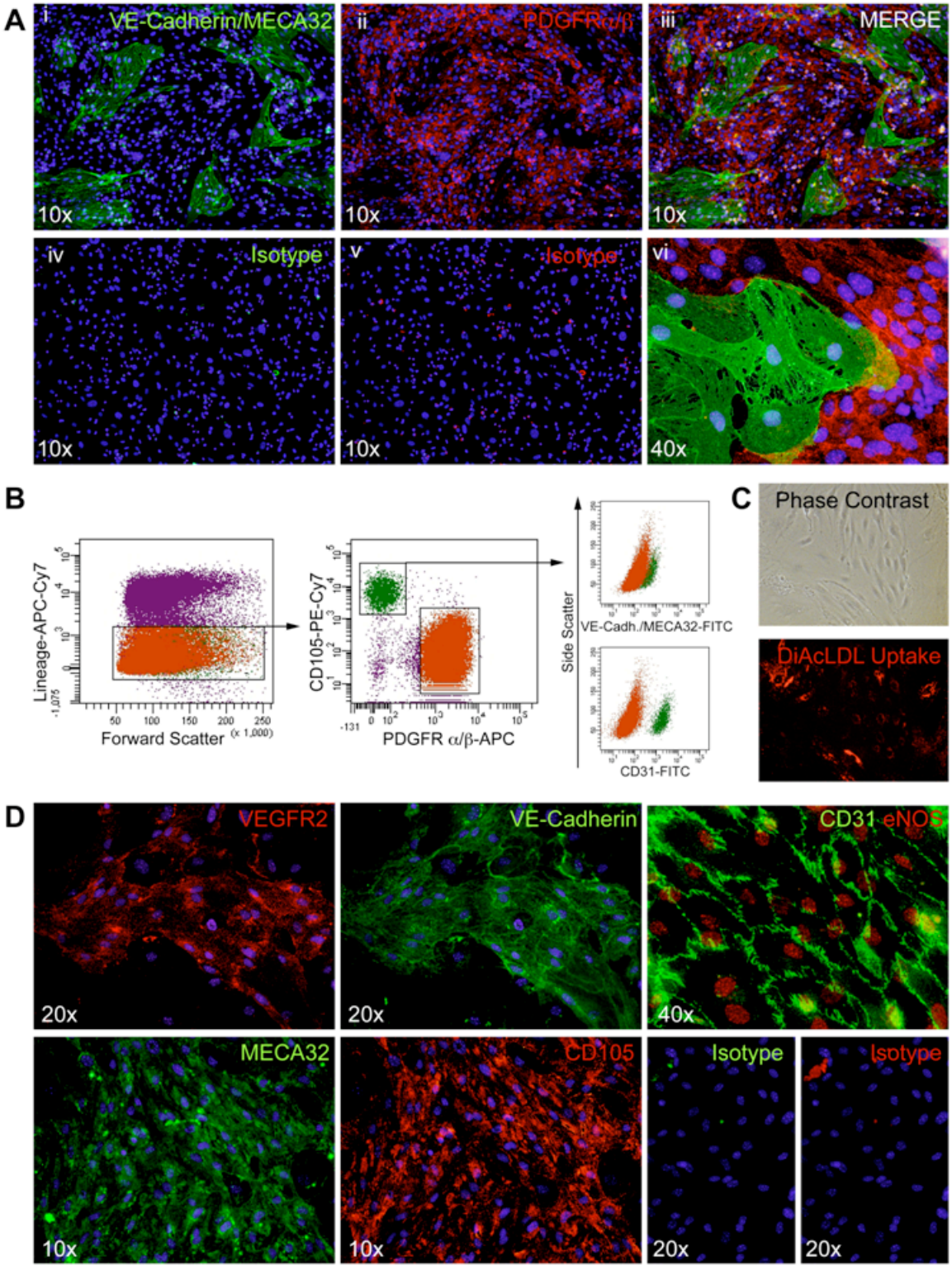
A
i
VE-Cadherin/MECA32
ii
PDGFRα/β
iii
MERGE
10x
10x
10x
iv
Isotype
v
Isotype
vi
10x
10x
40x
B
Lineage-APC-Cy7
Forward Scatter (x 1,000)
CD105-PE-Cy7
PDGFR α/β-APC
Side Scatter
VE-Cadh./MECA32-FITC
CD31-FITC
C
Phase Contrast
DiAcLDL Uptake
D
VEGFR2
VE-Cadherin
CD31 eNOS
20x
20x
40x
MECA32
CD105
Isotype
Isotype
10x
10x
20x
20x

both PDGF receptors, α and β, for stromal cell identification and with a combination of endothelial specific antibodies to VE-Cadherin, MECA32 and CD31. As shown in Figure 3-7A (i-vi), we observed discrete staining of clusters of endothelial cells surrounded by a monolayer of PDGFR$\alpha\beta^{POS}$ stromal cells. Interestingly, the size of endothelial clusters was substantially larger under the more endothelial permissive growth conditions of fibronectin coating and EGM-MV growth media (data not shown). When P_0 cultures were established from flushed BM cell preparations and grown under identical conditions, we failed to identify any CD31/VE-Cadherin/MECA32+ endothelial cells in keeping with our initial hypothesis and were able to only identify rare colonies (CFU-F) of PDGFR$\alpha\beta^{POS}$ stromal cells (data not shown).

We next used multi-parameter flow cytometric analysis, in order to both quantify the incidence of stromal and vascular endothelial cells as well as assess the feasibility of being able to isolate both populations from primary (P_0) cultures. By flow cytometric analysis, we demonstrated that 51.38$\pm$16.4% (n=5) of the adherent population was negative for hematopoietic lineage markers (LIN^{NEG}) while 64.68%$\pm$15.4% of the LIN^{NEG} cells demonstrated staining for PDGFRα and PDGFRβ, identifying them as stromal cells. Interestingly, the Lin^{NEG}PDGFR$\alpha\beta^{POS}$ population exhibited distinct subpopulations when used in combination with the cell surface marker CD105 (endoglin). These two populations were represented at nearly equal frequencies with 45.2$\pm$2.7% of the cells expressing CD105 (CD105POS) and 43.5+3.6% demonstrated low/negative expression for CD105 ($CD105^{NEG}$).

An additional 15.66%±10.6% of the LIN^{NEG} cells contained phenotypic properties of vascular endothelial cells with high levels of CD105 expression and uniformly expressed CD31, with modest levels of VE-Cadherin and MECA32 staining, while lacking expression of both PDGFRα and PDGFRβ (Figure 3-7B). While the majority of hematopoietic lineage negative cells within primary cultures of DBM consisted of stromal and vascular endothelial cells, the remaining 20% of cells appeared to be erythroid precursors based on morphology and the expression of CD71 and were unable to attach to tissue culture plastic (data not shown).

Once having identified an immunophenotype consistent with known endothelial cell markers, we used Fluorescence Activated Cell Sorting (FACS) to isolate the $Lin^{NEG}PDGFR\alpha\beta^{NEG}CD105^{bright}$ cells from P_0 cultures. Upon isolation, the cells adhered to fibronectin coated tissue culture plates, displayed characteristic cobblestone morphology (Figure 3-7C) and were able to undergo limited serial passaging in EGM2-MV media. At passage 3, the $Lin^{NEG}PDGFR\alpha\beta^{NEG}CD105^{bright}$ population demonstrated uniform uptake of DiI-Ac-LDL (Figure 3-7C) and continued to express all endothelial markers tested including VEGFR2, CD31, eNOS, CD105, MECA32 and VE-Cadherin (Figure 3-7D). Additionally, whole mount staining of BM plugs revealed an identical immunophenotype as the vascular endothelial cells in primary cultures identified as $Lin^{NEG}PDGFR\alpha\beta^{NEG}CD105^{Bright}CD144^{POS}MECA32^{POS}$ (Figure 3-8) and this phenotype can be used in the isolation of endothelial cells from single cell suspensions based on a lack of hematopoietic lineage cell surface markers, high expression of CD105 and intermediate levels of VE-Cadherin and MECA32 and lacking expression of PDGFRαβ (Figure 3-8 B).

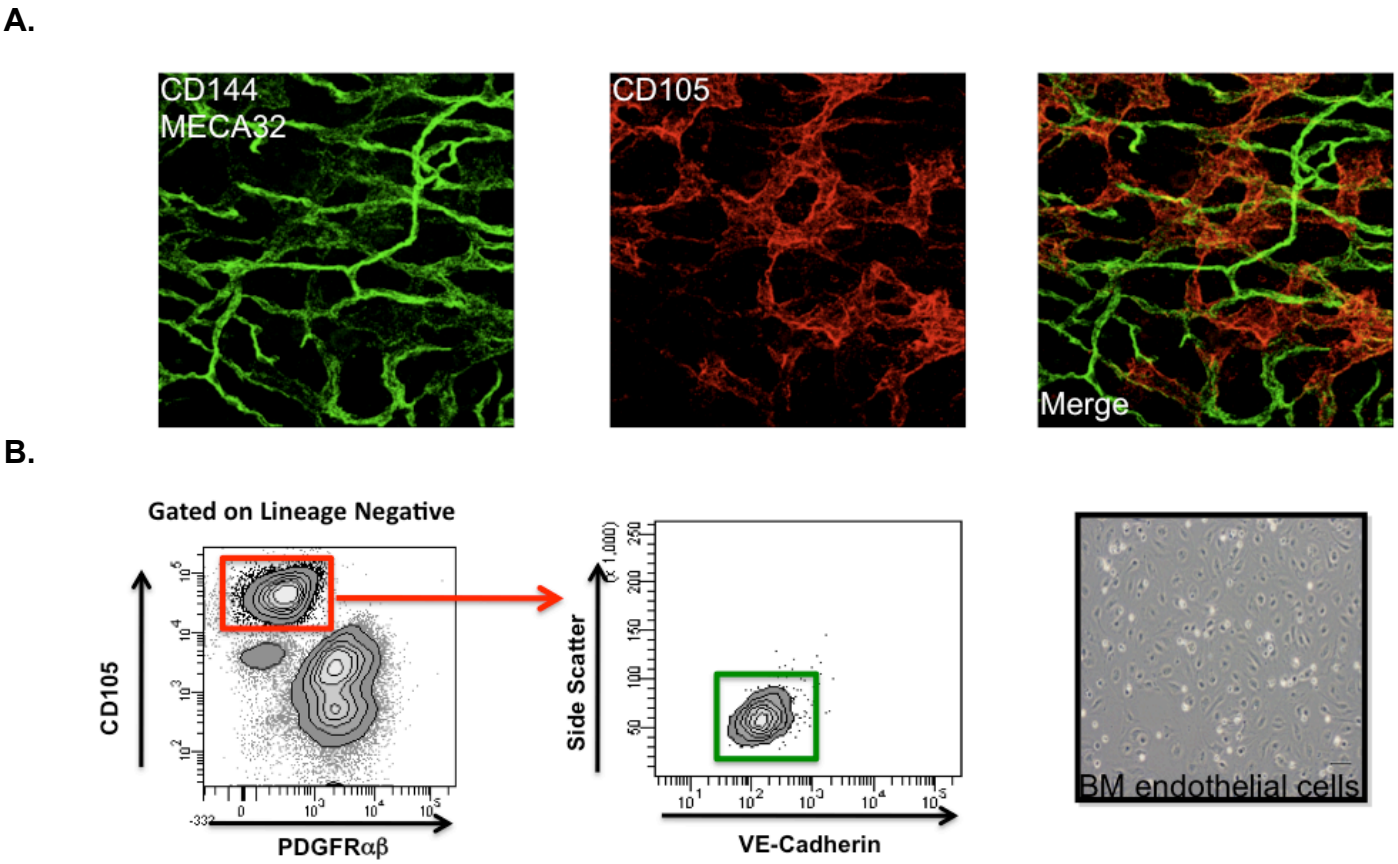

Figure 3-8: Bone marrow vasculature differentially expresses CD105. *The expression of endothelial cell surface markers in vivo was determined by whole mount staining and flow cytometry. (A) BM plugs were removed, fixed and stained as a whole mounts with antibodies to VE-Cadherin, MECA32 and CD105. High powered confocal imaging revealed distinct staining patterns for arteriole and sinusoidal vessels. Smaller vessels express high levels of VE-Cadherin and MECA32 and lower levels of CD105 cell surface expression. Larger dilated sinusoid vessels demonstrate high levels of CD105 staining and low levels of VE-Cadherin and MECA32 staining. (B) Prospective isolation of BM endothelial cells from DBM single cell suspensions and phase contrast image of isolated cells demonstrating cobblestone morphology.*

LIN^{NEG} PDGFR$\alpha\beta^{NEG}$ CELLS EXHIBIT THE PHENOTYPIC AND FUNCTIONAL PROPERTIES OF BMSCs

In parallel to using FACS to isolate the endothelial fraction from P_0 DBM cultures, we also isolated the stromal cell population as a whole based on the Lin^{NEG}PDGFRαβ^{POS} phenotype (Figure 3-9A). Upon isolation and serial passaging in αMEM media supplemented with 20% FBS, the Lin^{NEG}PDGFRαβ^{POS} population exhibited a typical polygonal stromal morphology (Fig 3-9 Bi) and demonstrated homogeneous expression for both chains of the PDGF receptors, α and β, consistent with the original phenotype used for their isolation (Fig 3-9 Bii). Additionally, we used a panel of cell surface markers routinely used by many other labs to characterize, retrospectively, the adherent population of stromal cells from mouse BM by flow cytometric analysis. Consistent with the current literature, the Lin^{NEG}PDGFRαβ^{POS} population demonstrated expression of CD29, CD51, CD73, CD105, CD146 and Sca-1 (Figure 3-9C). However, we did observe considerable differences in the level of heterogeneity of cell surface phenotypes from cells obtained by the current enzymatic disaggregation protocol (Figure 3-9D) as compared to cells obtained by standard method of flushing BM (Figure 3-9C) analyzed following identical number of passages. Additionally, the Lin^{NEG}PDGFRαβ^{POS} population isolated from DBM demonstrated a substantially greater degree of heterogeneity in the cell surface immuno-phenotypes for CD90, Sca-1 and CD105 (Figure 3-9 B&D), which likely represents a more accurate reflection of the level of stromal cell heterogeneity seen in vivo.

Figure 3-9: Isolation and phenotypic analysis of long-term cultured $Lin^{NEG}PDGFR\alpha\beta^{POS}$ bone marrow stromal cells. *(Ai-ii) Representative gating strategy of viable cells for FACS isolation of $Lin^{NEG}PDGFR\alpha\beta^{POS}$ cells from P_0 cultures. (Aii-iii) Phase contrast image and PDGFRβ immunostaining at passage 3. (B) FACS analysis of MSC markers in cultures of passage 3 $Lin^{NEG}PDGFR\alpha\beta^{POS}$ cells (n=3). FACS analysis demonstrating phenotypic differences between flushed BM (C) and DBM cells (D). FACS data was collected on BD LSR II and post-acquisition analysis was performed with BD FACS Diva 6.1.3. Data are represented as mean $\pm$ SD.*

(This research was originally published in *Blood* Online. Suire C, Brouard N, Hirschi K, Simmons PJ. Isolation of the Stromal-Vascular Fraction of Mouse Bone Marrow Markedly Enhances the Yield of Clonogenic Stromal Progenitors. *Blood*. Prepublished January 18, 2012; DOI 10.1182/blood-2011-08-372334.)

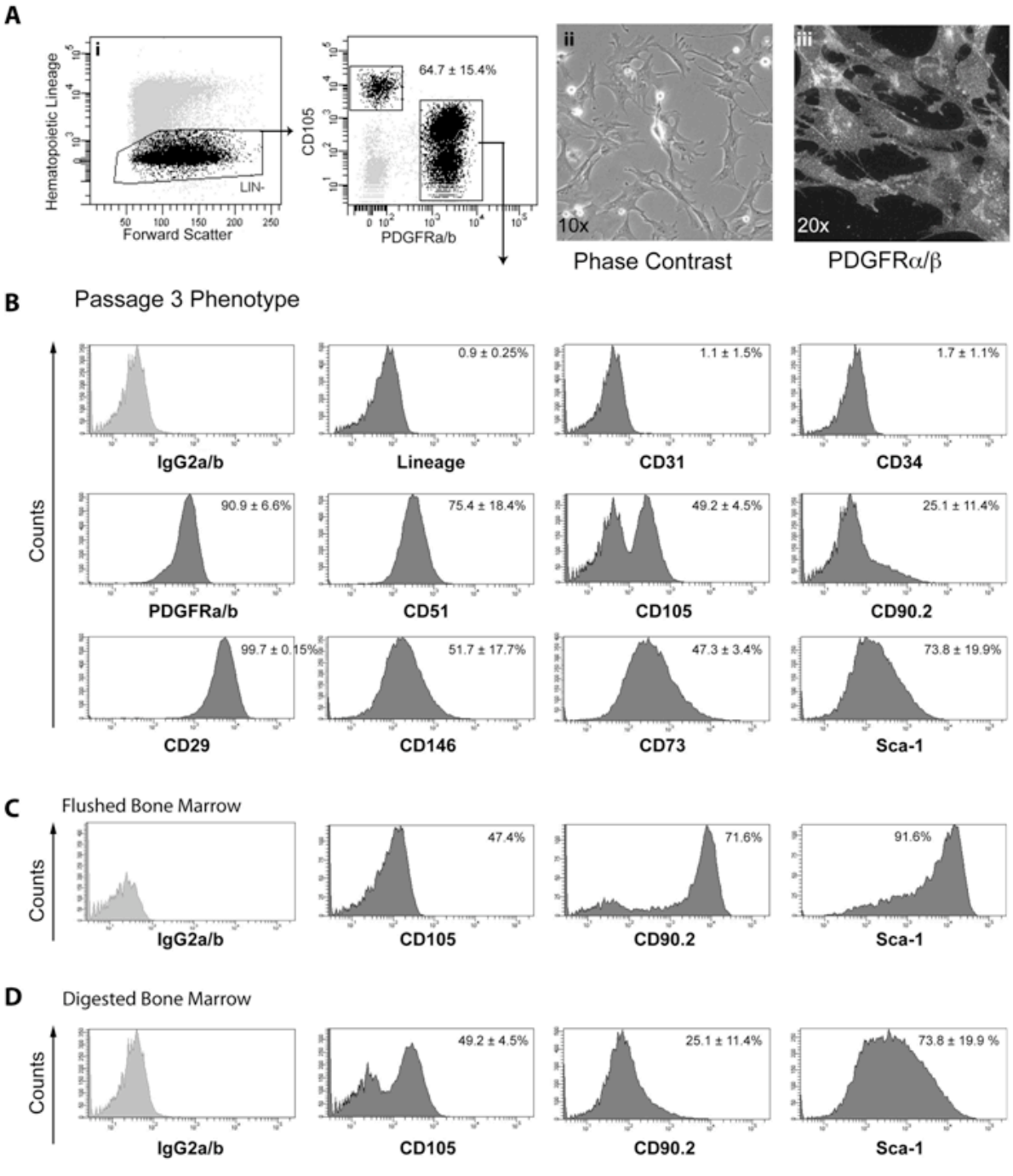
A
i
Hematopoietic Lineage
LIN-
Forward Scatter
CD105
64.7 ± 15.4%
PDGFRa/b
ii
10x
Phase Contrast
iii
20x
PDGFRα/β
B
Passage 3 Phenotype
Counts
IgG2a/b
0.9 ± 0.25%
Lineage
1.1 ± 1.5%
CD31
1.7 ± 1.1%
CD34
90.9 ± 6.6%
PDGFRa/b
75.4 ± 18.4%
CD51
49.2 ± 4.5%
CD105
25.1 ± 11.4%
CD90.2
99.7 ± 0.15%
CD29
51.7 ± 17.7%
CD146
47.3 ± 3.4%
CD73
73.8 ± 19.9%
Sca-1
C
Flushed Bone Marrow
Counts
IgG2a/b
47.4%
CD105
71.6%
CD90.2
91.6%
Sca-1
D
Digested Bone Marrow
Counts
IgG2a/b
49.2 ± 4.5%
CD105
25.1 ± 11.4%
CD90.2
73.8 ± 19.9 %
Sca-1

As noted previously, a subpopulation of multipotent stem/progenitor cells exists within the non-hematopoietic bone marrow stromal cell reticulum [85-91] of adult mice. These multipotent stem/progenitor cells are hypothesized to be the founder source for all CFU-F activity and have been shown to contain multi-lineage differentiation potential by forming histologically proven bone, mature adipocytes, hematopoietic supportive stroma and cartilage by rigorous in vivo transplantation assays [91]. We, therefore, sought to evaluate the differentiation potential of the $Lin^{NEG}PDGFR\alpha\beta^{POS}$ population obtained as described above. $Lin^{NEG}PDGFR\alpha\beta^{POS}$ cells isolated from C57Bl/6mice were collected at passage 3, loaded onto osteogenic scaffolds (GelFoam®) and allowed to attach for 1-2 days at 37°C at 5% oxygen. Additionally, empty scaffolds treated identically were used as controls. The scaffolds were then implanted subcutaneously into immune-deficient (NOD-SCID) mice by blunt dissection along the dorsal surface.

At 12 weeks post implant, animals were sacrificed, some of which were subjected to microCT imaging and scaffolds were recovered for histological analysis. In all scaffolds containing cells (n=8), we observed an outer layer of mineralized bone tissue surrounding an inner core of bone marrow comprised of donor derived adipocytes and hematopoietic supporting stroma and host derived hematopoiesis and blood vessels (Figure 3-10 Aii–iv), whereas control scaffolds (n=6) contained only fibrous connective tissue (Figures 3-10 Ai).

Figure 3-10: Multi-lineage differentiation capacity of $Lin^{NEG}PDGFR\alpha\beta^{POS}$ BMSCs. *(Ai-iv) Histology of subcutaneous transplants of either empty scaffolds (Ai) or $Lin^{NEG}PDGFR\alpha\beta^{POS}$ MSC (Aii-iv). Gelfoam scaffolds loaded with $Lin^{NEG}PDGFR\alpha\beta^{POS}$ MSC were either decalcified and embedded in paraffin for H&E staining (Aii-iii) or non-decalcified and embedded in methylmethacrylate resin for Von Kossa staining (Aiv). (B) 3D pellet cultures of $Lin^{NEG}PDGFR\alpha\beta^{POS}$ MSC embedded in paraffin and stained with Toluidine Blue (0.1% w/v) (Bi), Alcian blue (Bii), collagen type II (Biv) and mouse IgG1 isotype (Biii). (C) Oil red O staining of $Lin^{NEG}PDGFR\alpha\beta^{POS}$ MSC following adipogenic differentiation for 14 days.*

(This research was originally published in *Blood* Online. Suire C, Brouard N, Hirschi K, Simmons PJ. Isolation of the Stromal-Vascular Fraction of Mouse Bone Marrow Markedly Enhances the Yield of Clonogenic Stromal Progenitors. *Blood*. Prepublished January 18, 2012; DOI 10.1182/blood-2011-08-372334.)

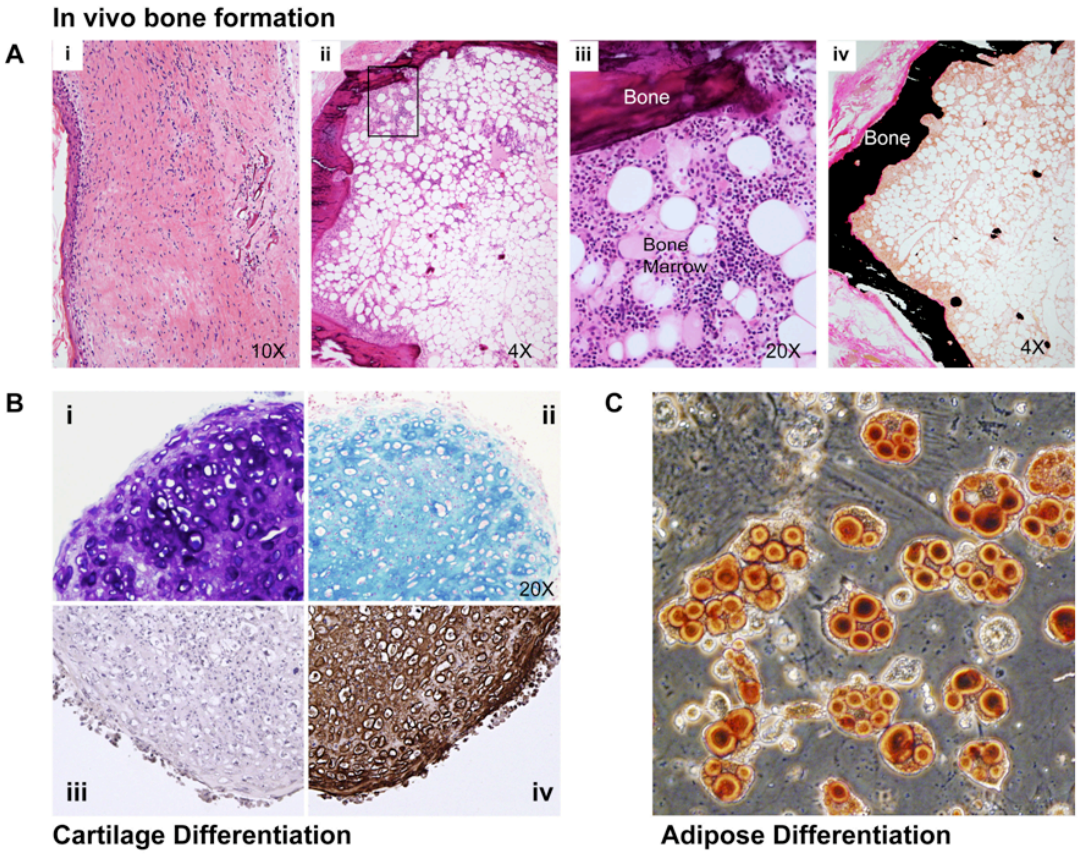
In vivo bone formation
A
i
10X
ii
4X
iii
Bone
Bone Marrow
20X
iv
Bone
4X
B
i
ii
20X
iii
iv
Cartilage Differentiation
C
Adipose Differentiation

Complementary in vitro differentiation assays were also used to validate the differentiation potential, whereby the $Lin^{NEG}PDGFR\alpha\beta^{POS}$ cells demonstrated robust chondrogenic activity under standard micromass pellet culture conditions as evidenced by collagen type II expression and the deposition of a sulphated proteoglycan-rich ECM revealed by staining with Toluidine Blue and Alcian Blue (Figure 3-10 Bi-iv). In vitro adipogenic differentiation, following exposure to PPARγ agonists, was also observed in which $Lin^{NEG}PDGFR\alpha\beta^{POS}$ cells generated prominent lipid containing vacuoles revealed by Oil Red O staining (Figure 3-10 C).

PROSPECTIVE ISOLATION OF STROMAL PROGENITOR CELLS FROM FRESHLY PREPARED ENZYMATICALLY DISAGGREGATED BONE MARROW

Collectively, the novel methodology described here demonstrates a robust reproducible approach as a means to isolate a phenotypically defined BMSC population as a whole, some of which maintain functional properties of marrow stromal stem/progenitors cells. We next sought to examine the utility of this methodology to isolate an identical population within freshly prepared DBM single cell suspensions given that the above data were obtained from $Lin^{NEG}PDGFR\alpha\beta^{POS}$ cells following a brief period of in vitro culture. Single cell suspensions from enzymatically disaggregated BM, prepared as previously described, were analyzed by flow cytometric analysis as either whole BM (WBM) or following the removal of hematopoietic lineage cells using Dynalbeads (Invitrogen). Noticeably, we observed a discrete population of $Lin^{NEG}PDGFR\alpha/\beta^{POS}$ cells within WBM from C57Bl/6 and BALB/c mice (Figure 3-11A), representing $0.087\pm0.014\%$ and $0.84\pm0.64\%$, (n=3)

respectively. When DBM samples were subjected to immunomagnetic bead depletion of the hematopoietic lineage positive cells, the frequency of the $Lin^{NEG}PDGFR\alpha/\beta^{POS}$ population increased to 51.5% in C57Bl/6 mice and 89% in BALB/c mice (Figure 3-11B). Upon prospective isolation, the $Lin^{NEG}PDGFR\alpha/\beta^{POS}$ population contained the all CFU-F activity and demonstrated colony-forming efficiencies (CFE) of 0.475% and 2.95% from C57Bl/6 and BALB/c DBM (Figure 3-11C), respectively. Interestingly in samples prepared by digesting BM from C57Bl/6 and BALB/c mice, we also observed the presence of the $PDGFR\alpha/\beta^{NEG}CD105^{brght}$ endothelial cell population in WBM, which was completely absent in samples prepared by flushing BM (Figure 3-11A). Taken together, these data support our hypothesis that the flushing of BM leads to a destruction of the marrow vasculature and a diminution of stromal stem/progenitor cells physically associated with vasculature surface.

Figure 3-11: Prospective isolation of $Lin^{NEG}PDGFR\alpha\beta^{POS}$ clonogenic progenitors from DBM. *(A) Gating strategy (left panel) and FACS analysis of whole bone marrow from C57Bl/6 and BALB/c mice demonstrating the frequency of $Lin^{NEG}PDGFR\alpha\beta^{POS}$ bone marrow stromal cells obtained from either standard flushing or sequential enzymatic disaggregation of BM plugs. (B) Gating strategy (left panel) for prospective isolation of $Lin^{NEG}PDGFR\alpha\beta^{POS}$ population from C57Bl/6 and BALB/c inbred mouse strains. (C & D) Incidence of CFU-F from prospective isolation of $Lin^{NEG}PDGFR\alpha\beta^{POS}$ BM stromal cells from C57Bl/6 and BALB/c mice. (Colonies $\geq$ 50 stromal cells; Clusters represent 10-49 stromal cells).*

(This research was originally published in *Blood* Online. Suire C, Brouard N, Hirschi K, Simmons PJ. Isolation of the Stromal-Vascular Fraction of Mouse Bone Marrow Markedly Enhances the Yield of Clonogenic Stromal Progenitors. *Blood*. Prepublished January 18, 2012; DOI 10.1182/blood-2011-08-372334.)

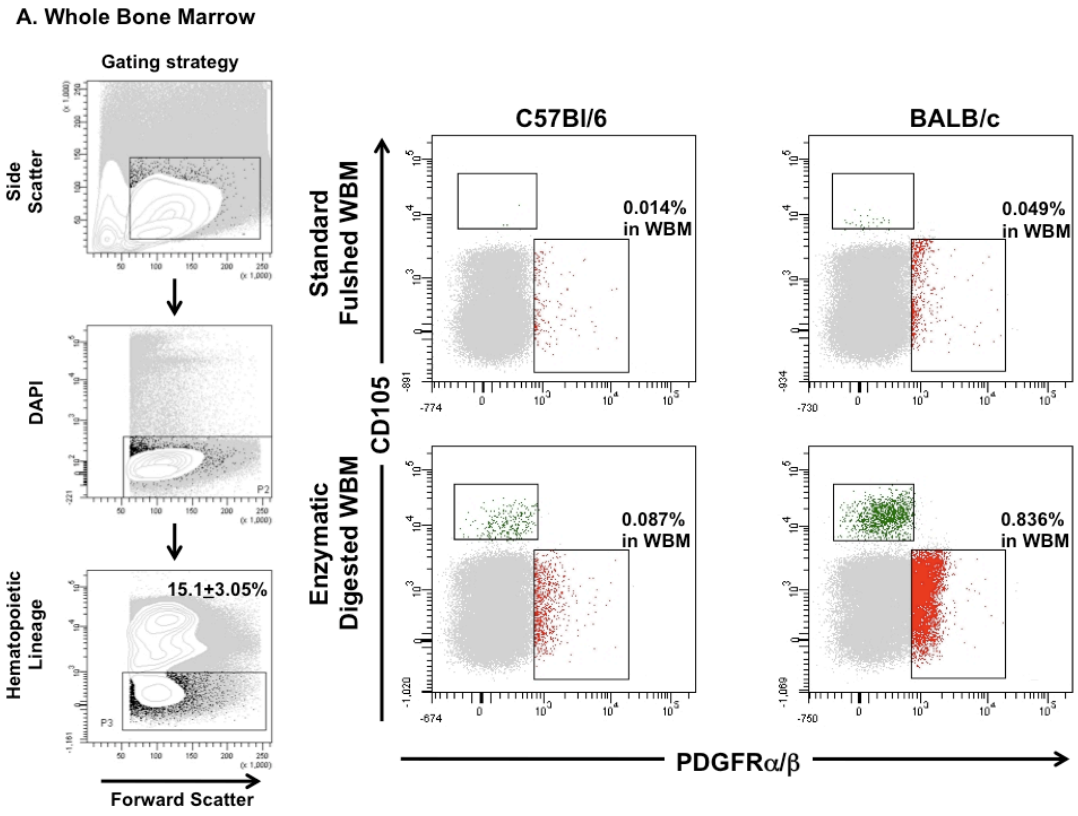
A. Whole Bone Marrow
Gating strategy
Side Scatter
DAPI
Hematopoietic Lineage
15.1±3.05%
Forward Scatter
C57Bl/6
BALB/c
Standard Fulshed WBM
Enzymatic Digested WBM
CD105
0.014% in WBM
0.049% in WBM
0.087% in WBM
0.836% in WBM
PDGFRα/β

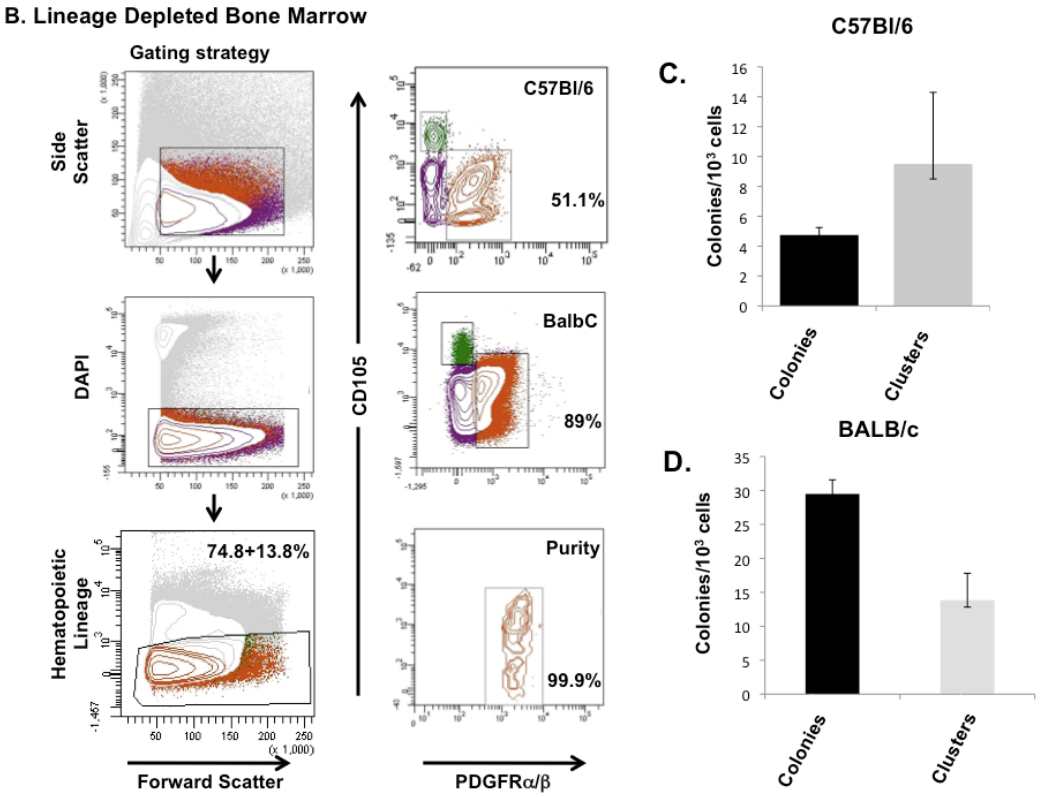
B. Lineage Depleted Bone Marrow
Gating strategy
Side Scatter
DAPI
Hematopoietic Lineage
74.8+13.8%
Forward Scatter
CD105
C57Bl/6
51.1%
BalbC
89%
Purity
99.9%
PDGFRα/β
C.
C57Bl/6
Colonies/10³ cells
Colonies
Clusters
D.
BALB/c
Colonies/10³ cells
Colonies
Clusters

ASSESSMENT OF THE IN VIVO LOCALIZATION OF BONE MARROW STROMAL CELL RETICULUM

Once having determined the distinct immunophenotype for clonogenic stromal progenitor cells and vascular endothelial cells, we next sought to determine the anatomical localization of each population within freshly prepared plugs of BM using whole mount staining. To do this, we chose a combination of cell surface markers that where useful for identifying respective cell populations in primary cultures of DBM by either immunocytochemistry or flow cytometry. We used a novel whole mount staining methodology with a panel of antibodies directed against known endothelial cell surface markers including the combination of VE-Cadherin/MECA32 and CD105. Interestingly, we observed a distinct pattern of staining that revealed a complex vascular network, spanning the entire cross-sectional distance of BM plugs removed from C57Bl/6 femurs and consisted of arterioles, smaller capillaries and larger dilated sinusoidal vessels (Figure 3-8A), with sinusoidal endothelial cells demonstrating the highest staining intensity to CD105.

Additional whole mount samples prepared with the combination of PDGFRα and PDGFRβ antibodies as pan-stromal cell markers and VE-Cadherin and MECA32 antibodies for vascular endothelial staining demonstrated a complex stromal cell reticulum of PDGFRα/β^{POS} cells with long cytoplasmic extensions spanning across the hematopoietic space and interacting with VE-Cadherin/MECA32 reactive vasculature (Figure 3-12) and hematopoietic lineage positive cells (Figure 3-13), while a subset of PDGFRα/β^{POS} cells were localized to perivascular regions of VE-Cadherin/MECA32^{POS} arterioles (Figure 12) and CD105

reactive sinusoids (Figure 3-14) as well as within inter-sinusoidal regions. This staining pattern, therefore, is useful for identifying the precise localization of subpopulations of both stromal and endothelial cells and is consistent with our multi-parameter flow cytometric analysis used to prospectively isolate the stromal vascular fraction of mouse BM.

Figure 3-12: PDGFRαβ^{POS} stromal cells are localized to perivascular and inter-sinusoidal regions in vivo. *Whole mount staining of BM plugs. Vascular endothelial cells were identified with VE-Cadherin-Alexa 488 and MECA32-Alexa 488 antibodies (I, upper left) and stromal cells were identified with PDGFRα/β antibodies and revealed with donkey anti-rat Cy3 (ii, lower left). Nuclei were counter stained with DRAQ5. Z-stack merged image (iii, upper right) and single step merged image (iv, lower right) identifying perivascular (asterisk) and intersinusoidal (arrow) localization. Images were collected using a 63x oil immersion objective on zoom factor of 3 with a Leica TCS SP5 confocal microscope and processed with the Leica LAS AF lite software. Z-stacked images were collected in 0.2 μm slices at depths of 15-25 μm with a pinhole of 1.*

(This research was originally published in *Blood* Online. Suire C, Brouard N, Hirschi K, Simmons PJ. Isolation of the Stromal-Vascular Fraction of Mouse Bone Marrow Markedly Enhances the Yield of Clonogenic Stromal Progenitors. *Blood*. Prepublished January 18, 2012; DOI 10.1182/blood-2011-08-372334.)

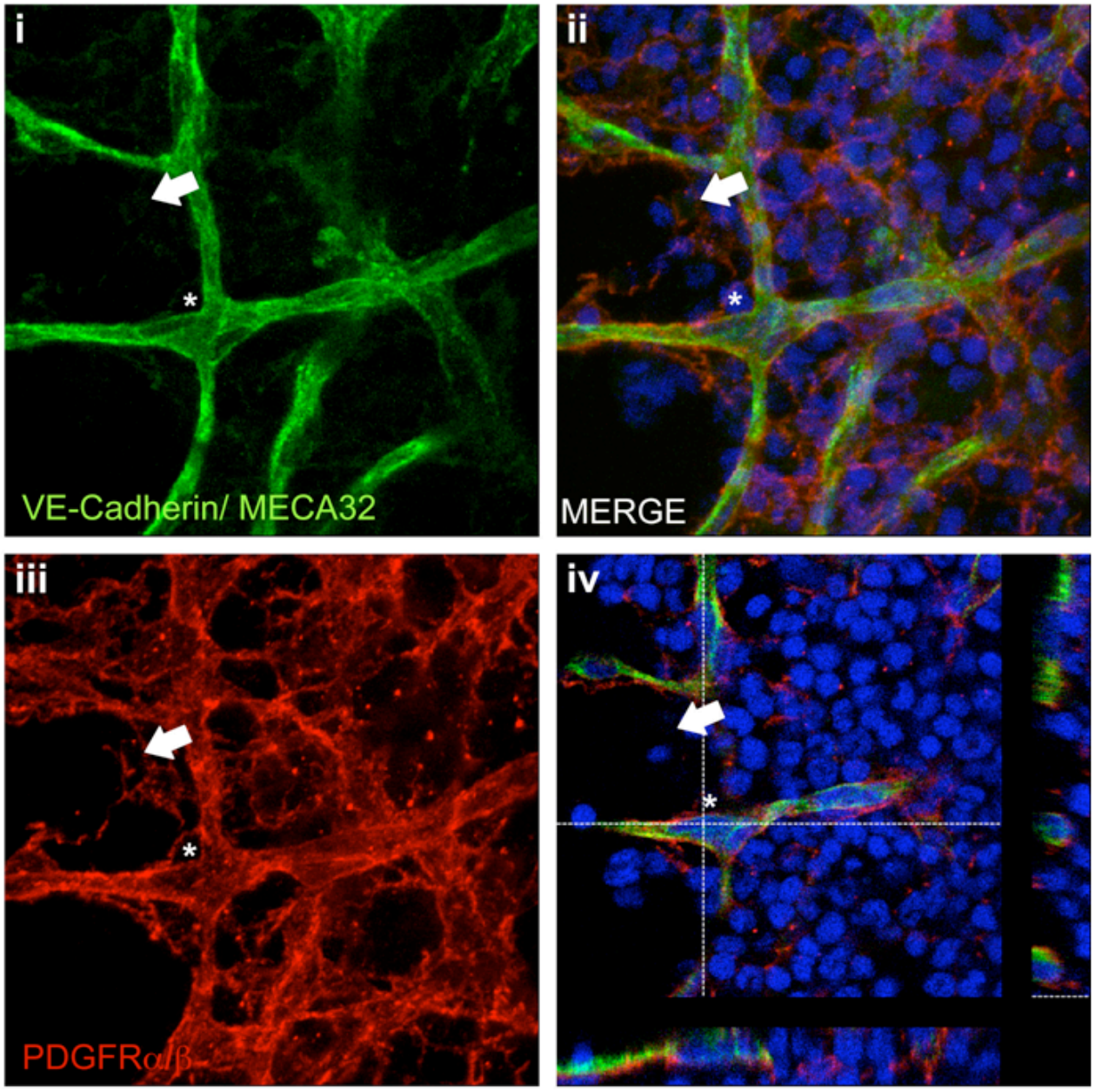
i
VE-Cadherin/ MECA32
ii
MERGE
iii
PDGFRα/β
iv

Figure 3-13: PDGFRαβ^{POS} stromal cells create a complex stromal scaffolding of cellular processes interacting with hematopoietic cells throughout extra-vascular space in vivo. *Whole mount staining of BM plugs. Vascular endothelial cells were identified with VE-Cadherin-Alexa 488 and MECA32-Alexa 488 antibodies (i, upper left) and stromal cells were identified with PDGFRα/β antibodies and revealed with donkey anti-rat Cy3 (ii, upper right). Hematopoietic lineage positive cells (iii, lower left) were identified with the lineage marker panel (see methods table 1) conjugated to biotin and revealed with streptavidin-Alexa 594. Single step slice of Z-stacked merged image (iv, lower right). Images were collected using a 63x oil immersion objective with a Leica TCS SP5 confocal microscope and processed with the Leica LAS AF lite software. Z-stacked images were collected in 0.2 μm slices at depths of 15-25 μm with a pinhole of 1.*

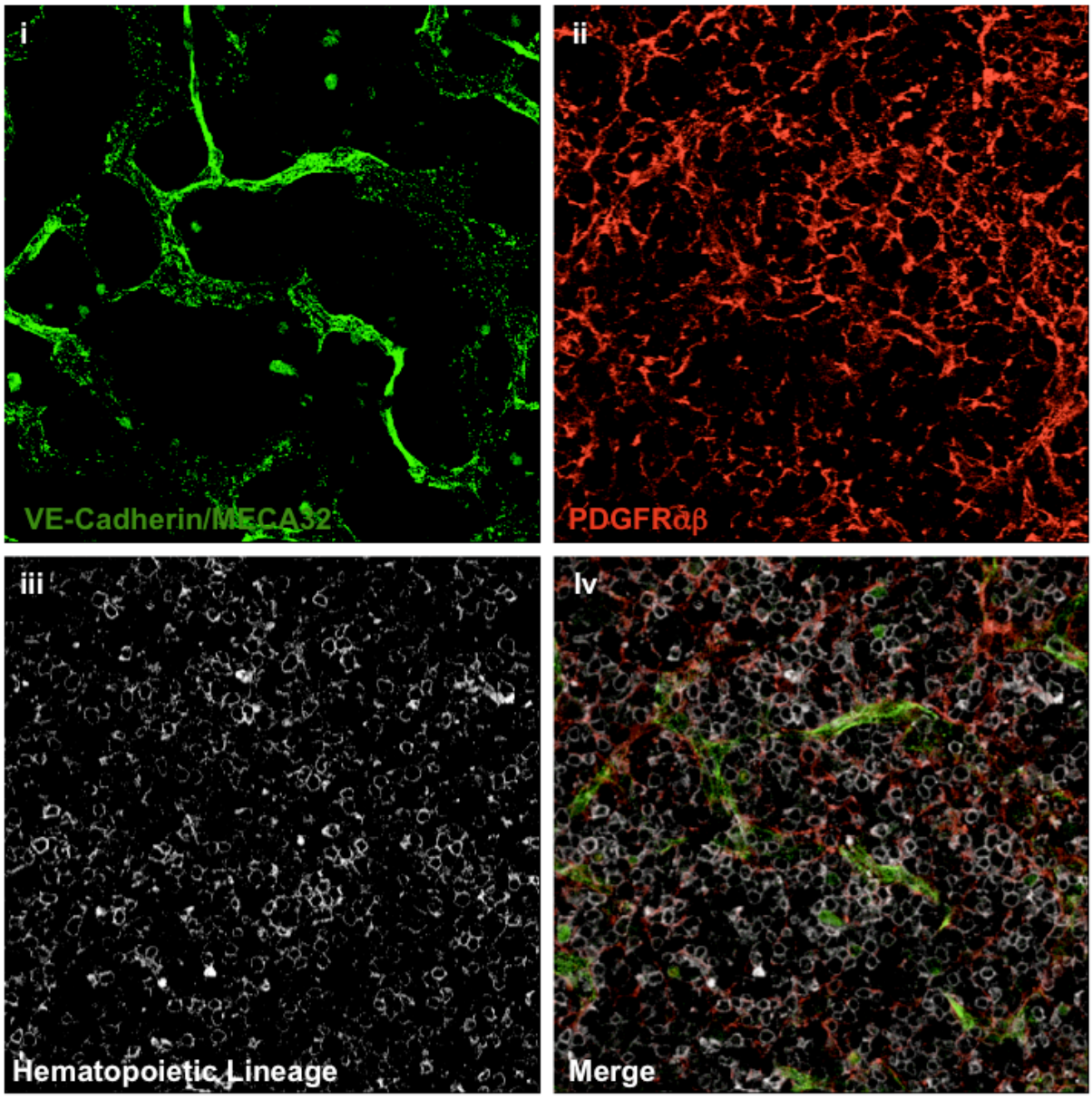
i
VE-Cadherin/MECA32
ii
PDGFRαβ
iii
Hematopoietic Lineage
Iv
Merge

Figure 3-14: Subendothelial adventitial reticular cells adjacent to sinusoid vessels are PDGFRαβ^{POS} stromal cells. *Whole mount staining of BM plugs. Sinusoidal endothelial cells were identified with CD105 antibody (i, upper left) and stromal cells were identified with PDGFRα/β antibodies and revealed with donkey anti-rat Cy3 (ii, upper right). Nuclei were counter stained with DRAQ5 (iii, lower left). Single step slice of Z-stacked merged image (iv, lower right). Images were collected using a 63x oil immersion objective on zoom factor of 2 with a Leica TCS SP5 confocal microscope and processed with the Leica LAS AF lite software. Z-stacked images were collected in 0.2 μm slices at depths of 15-25 μm with a pinhole of 1. Arrow-head indicates sinusoidal perivascular PDGFRα/β stromal cell.*

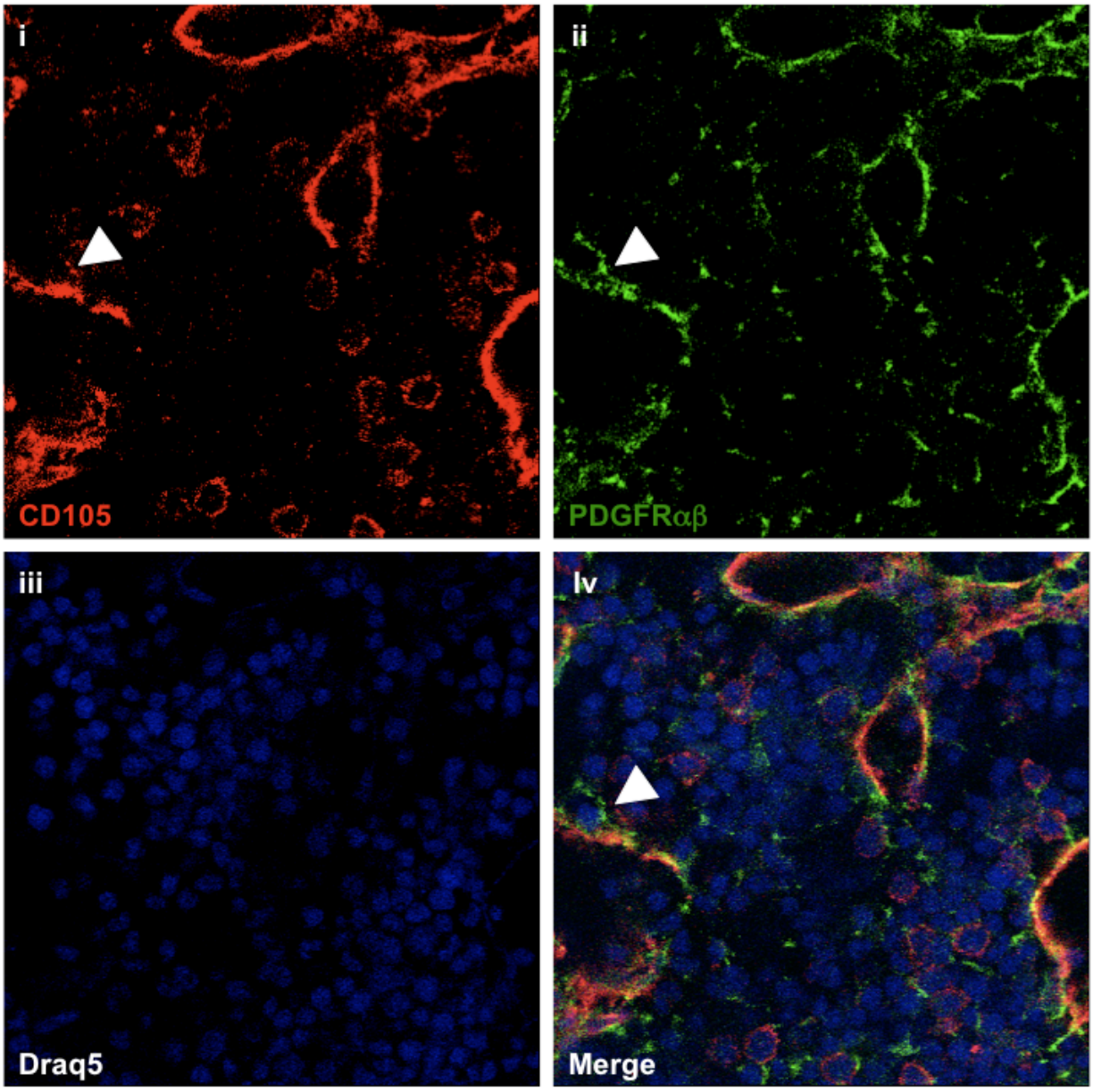
i
CD105
ii
PDGFRαβ
iii
Draq5
Iv
Merge

3-4: SUMMARY

Taken together, these data represent a simple and robust methodology that allows the simultaneous identification and isolation of both the stromal and vascular cellular components of mouse BM with a yield of CFU-F that far exceeds that reported in any previous study. Purified BM stromal cell populations devoid of hematopoietic contamination are readily obtained by prospective isolation and demonstrate robust multilineage differentiation into bone, adipose and chondrogenic progeny using standard in vitro bioassays and in vivo transplant models.

Furthermore, by developing a novel whole mount staining methodology, we are able to obtain a detailed three-dimensional organization of the stromal-vascular reticulum. This methodology demonstrates the complexity of the stromal system within the bone marrow and localizes a subpopulation of stromal cells to perivascular niches while the remaining stromal cells are found to be dispersed throughout the marrow parenchyma and contain long cytoplasmic extensions which all appear to contact parts of the vascular structure providing the basis for a cellular scaffolding for hematopoietic adhesion and migration throughout the BM. By identifying the respective location and a cell surface phenotype leading to the prospective isolations of clonogenic progenitors (CFU-F), these studies will greatly enhance experimental strategies designed to analyze not only MSC identity and function in vivo, but also the function of the vascular hematopoietic stem cell niche.

CHAPTER 4:

ISOLATION AND FUNCTIONAL CHARACTERIZATION OF DISTINCT POPULATIONS OF STROMAL PROGENITOR CELLS

4-1: PREFACE

In the following chapter, I investigate the identity and nature of the cells in mouse BM that give rise to cultures of stromal cells most commonly referred to as mesenchymal stem cells (MSC). I demonstrate, for the first time, that the cells commonly referred to in the literature as '*mesenchymal stem cells*' are in fact derived from phenotypically and anatomically distinct ***subpopulations*** of stromal cells in mouse bone marrow not from a single population of stromal progenitors as implied by the vast majority of studies published to this point in time.

Much of the field of MSC biology is based on the characterization of culture expanded stromal cells using panels of antibodies directed at cell surface markers identified based on their abundant and homogenous expression on these cells. One such marker is CD105 (endoglin). In the previous chapter, I demonstrated using the improved methodology for isolation of CFU-F from DBM, that following in vitro passage up to passage 3 the stromal cells exhibited bimodal expression of CD105 with distinct $CD105^{POS}$ and $CD105^{NEG}$ subpopulations. This was in marked contrast to cultures established using the standard BM flushing technique, which exhibited homogeneous CD105 expression in accord with previous reports in the literature. We postulate that this discrepancy is due largely to differences in the methodologies employed by investigators to obtain single BM cell suspensions. Specifically, that flushing of BM results in both quantitative and qualitative reductions in the yield of stromal progenitors cells and hence does not permit isolation of a stromal cell population that reflects the phenotypic diversity present in the intact mouse BM.

In this chapter, I provide evidence that both $CD105^{POS}$ and $CD105^{NEG}$ subpopulations contain clonogenic stem/progenitor cell activity and both exhibit the functional properties of MSC as demonstrated by differentiation to bone, adipose and cartilage tissue using both in vitro and in vivo assays. Finally, transcriptional profiling was performed on the two subpopulations immediately following their isolation from the DBM to gain insight into their biological roles in vivo. Analysis of these data demonstrate that the $Lin^{NEG}PDGFR\alpha\beta^{POS}CD105^{POS}$ population contains an over-represented list of genes involved in angiogenesis, blood vessel morphogenesis and blood vessel development consistent with the role of pericytes. However, The $CD105^{NEG}$ population contains a list of over-represented genes involved in biomineralization, ossification and skeletal development suggesting this population contains cells more committed to the osteoblast lineage and may serve as a source of direct progenitors for bone formation.

4-2: INTRODUCTION

In adult mammals, the bone marrow is the place of residence of two phenotypically and functionally distinct adult stem cell populations. The first of these are the hematopoietic stem cell (HSC), perhaps the most extensively studied and best characterized populations of adult or tissue stem cells in all of vertebrate physiology. The second stem cell population in the BM are non-hematopoietic multipotent stromal stem/progenitor cells originally identified through the pioneering studies of Friedenstein and colleagues who first described the multilineage differentiation properties (bone, cartilage and adipose tissue) of these BM-derived stem cells through rigorous in vivo transplantation assays [88]. By comparison with HSC, the non-hematopoietic stromal stem cells are a far less well-understood population of tissue stem cells. In part this is due to a lack of consistency in the terms used to describe such cells in the literature such as “osteogenic,” “stromal” and “skeletal” stem cells. However, the term mesenchymal stem cell (MSC), coined by Arnold Caplan’s lab in the early 1990’s, has more recently been ascribed to these cells and is the term most commonly referred to in current literature [117].

The multi-lineage differentiation potential originally identified by the seminal transplantation studies of boneless fragments of marrow conducted by Tavassoli and Crosby [92] in the late 1960’s, provided key founding evidence for what would subsequently emerge as the field of marrow stromal progenitor biology. Shortly thereafter in the 1970’s, Friedenstein and colleagues described a population of plastic-adherent, clonogenic stromal progenitors, after which he coined the term

colony-forming unit-fibroblast (CFU-F) [93], that were responsible for the formation of ectopic bone and transferring the hematopoietic microenvironment in vivo. It was proven that this process recapitulates the developmental origin of bone and bone marrow formation established by cells of mesenchymal lineage during endochondral ossification [118] and hence the term ‘stromal stem cell’ was born.

Taken together, these data demonstrate that a rare population of bone marrow stromal cells are both clonogenic in nature and contain the capacity to generate the diversity of cells found within the adult bone-bone marrow tissue. Furthermore, in humans it has been demonstrated, at a clonal level, that a single cell responsible for generating a CFU-F can be expanded in culture and go on to generate bone, fat and hematopoietic supporting stroma in vivo [119]. CFU-F derived colonies exhibit considerable morphological, phenotypic and functional heterogeneity as demonstrated both in vitro and in vivo [86]. The most striking evidence emerged from the seminal experiments of Friedenstein and colleagues who transplanted single colonies derived from mouse BM ectopically beneath the renal capsule in mice. They found that a minor proportion of colonies (approximately 15%) exhibited the capacity to generate a complete bone marrow organ beneath the renal capsule, comprising a bony ossicle, adipose tissue and a typical marrow stromal reticulum supporting the associated hematopoietic tissue (the latter derived from the host mouse) and hence appeared to exhibit a multipotent differentiation potential. In contrast, the majority of colonies either failed to generate any ectopic tissue, generated bone tissue only or a fibroblastic connective tissue sometimes containing adipose cells. Based on these data a hierarchy of stromal cell

differentiation has been proposed [86] in which a multipotent self-renewing stromal stem cell at the apex of this hierarchy gives rise to more committed progenitors with reduced proliferative potential whose differentiation potential is restricted to one of the stromal cell lineages of the BM, bone, fat or cartilage (see Figure 3-1). Although, these data provide evidence that stromal stem cells are clonogenic and multipotent, it also highlighted a key fact that just as in the hierarchy described for hematopoietic stem and progenitor cells, clonogenicity per se does not equate to stem cell potential.

Historically, it has been suggested that a single population of multipotent stromal progenitors within adult murine bone marrow is responsible for all CFU-F activity and subsequently are the cells that are able to undergo multi-lineage differentiation. Initial observations by Westen and Bainton, suggested that subendothelial adventitial reticular cells expressing membrane bound alkaline phosphatase [116] were candidate founder cells for CFU-F and subsequent data in humans demonstrated that these cells generate adipocytes and osteoblasts in vivo [120]. Additional studies with human bone marrow identified an immunoglobulin superfamily adhesion molecule, Muc18/MelCAM/CD146 as a cell surface marker of the population of subendothelial BMSCs. When BM cells exhibiting high levels of CD146 were isolated by FACS all measurable CFU-F activity was restricted to the CD146+ fraction and these cells demonstrated the ability to generate ectopic bone and transfer the hematopoietic microenvironment in vivo. Interestingly, these authors also provided evidence that only the BMSCs and not bone derived cells, were able to transfer the hematopoietic microenvironment suggesting that BMSCs contain a

more primitive stem cell population [22]. Together, these data point to the subendothelial adventitial reticular cell as the likely in vivo MSC candidate. However, such experiments have not yet been performed in adult mice and data based largely on retrospective analysis of culture-expanded MSC is limited by the unproven and highly unlikely assumption that the pattern of gene expression of the multiply passaged progeny of MSC in vitro accurately reflects that of the founder stromal progenitor cell in-situ in the BM. Consequently, data based on analysis of the phenotypic properties of MSC in vitro cannot necessarily be relied upon to accurately predict a cell surface phenotype that will allow unequivocal identification and localization of the in vivo counterpart within the bone marrow tissue.

Recent data using transgenic reporter strains has begun to shed some light on a candidate subpopulation of stromal stem/progenitor cells in vivo. The chemokine stromal derived factor 1 (SDF-1/CXCL12) as implied by the name, is abundantly expressed by bone marrow stromal cells and plays a key physiological role as a chemoattractant for hematopoietic stem/progenitor cells by virtue of their expression of the counter-receptor for SDF-1, CXCR4. Using a CXCL12-GFP knockin model Omatsu et al. [24] demonstrated that GFP^+ cells in the BM with their long cytoplasmic process and anatomical distribution both in association with the BM vasculature and in the intersinusoidal spaces exhibit features consistent with their identity as reticular cells. The authors further demonstrated that the GFP^+ cells express alkaline phosphatase in vitro and are able to differentiate into osteoblastic progeny and give rise to adipocytes in vivo following 5-FU treatment [24]. Recent work from Frenette and colleagues, using a transgenic mouse model in which GFP

expression is under the control of the neural-specific regulatory elements of the nestin gene (Nes-GFP$^+$), demonstrated that GFP$^+$ cells in the BM were localized exclusively to perivascular regions [23]. In addition, GFP$^+$ cells isolated from the bone marrow by FACS contained all measurable CFU-F activity and exhibited MSC activity as demonstrated by standard in vitro differentiation assays and by in vivo ectopic transplantation experiments. Consistent with the physiological role of Nestin expressing cells as MSC, when these authors performed lineage-tracing studies using a nestin-cre/Rosa LacZ mouse model, they identified some contribution to cartilage and bone in the developing mouse embryo. However, because not all of the developing bone appeared to be derived from the Nestin expressing cells, it suggests that there may be additional stromal stem/progenitor populations that also contribute to the developing bone and may also serve as an alternative source of resident stem/progenitor populations. Collectively, these two studies shed important light on the identity of stromal progenitors and in addition, are consistent with the notion that multiple stromal stem/progenitor populations may exist within adult murine bone marrow [25].

During bone development, mammals undergo a process of endochondral ossification where mesenchymal condensation generates hypertrophic cartilage, which is surrounded by osteoblast progenitors responsible for generating a bony collar [85, 118]. Following the formation of the outer bone periosteum, vascular invasion occurs bringing along perivascular cells, which then seed the newly formed marrow cavity.

This developmental process has recently been very eloquently demonstrated by Kronenberg and colleagues using transgenic mouse models. Using two different mouse models to perform lineage tracing studies, these authors provide evidence that Osterix expressing precursors give rise to the bone marrow stromal cells, osteoblasts and pericytes in the developing bone marrow stroma, while more mature Collagen type I expressing osteoblasts were confined to the perichondrial regions and never moved into the developing marrow cavity [121]. These data illustrate at a cellular level that at least some of the adult BMSCs are originally derived from osteoblast precursors in the developing bone-bone marrow organ. However, it is not clear from these studies if ***all*** of the adult bone marrow MSC and CFU-F are derived from the Osterix expressing precursor cells. It therefore remains possible that additional population(s) of cells with the functional properties of MSC remain to be identified in post-natal adult mouse BM which may differ in their developmental origins and/or may represent a distinct source of perivascular cells that colonize the adventitial surface of blood vessels at the time of the initial wave of vasculature invasion.

One potential source of such cells is suggested by the elegant lineage tracing studies of Nishikawa and colleagues whose data suggest that some of the stromal cell compartment is actually developmentally derived from the neural crest [122]. Again using lineage-tracing studies, these authors demonstrate with the use of a neural crest specific promoter driving expression in a temporal manner of Cre recombinase, P0-Cre/Rosa-EGFP, that some of the perivascular cells in adult BM are $EGFP^{+}$. P0 is a neural crest specific gene active during the wave of neural crest

migration and is not expressed in WT adult BM. Collectively, these two sets of data offer an intriguing hypothesis suggesting that BMSCs are derived from at least two distinct developmental origins.

Despite these recent important advances, the field of mouse BMSC biology is still beset by many uncertainties with regards to the defining characteristics of MSC in vivo. Furthermore although often cited, the existence of a hierarchy within the adult BMSC system within mouse BM remains largely hypothetical and has not been validated rigorously by retroviral gene marking and transplantation studies that have proved so powerful in defining the multilineage differentiation potential of HSC. Nor has it been possible to dissect, phenotypically by prospective isolation of distinct subsets, the cellular constituents of this supposed stromal stem-progenitor cell hierarchy as again has been achieved in very great detail in the hematopoietic system [reviewed in 3].

In the previous chapter, a novel methodology that greatly increases the yield of clonogenic stromal stem/progenitor cells was described that simultaneously allows for the prospective isolation of the stromal/vascular fraction from murine bone marrow. By means of this methodology we have identified ***subpopulations*** of stromal cells based on their distinct immunophenotypes, which have not been previously reported and whose physiological roles consequently remain unknown. The studies described in the following chapter have begun to resolve the identity and function of these distinct populations of stromal stem/progenitor cells. Here, I describe the isolation and characterization of distinct populations of clonogenic BMSCs with stem/progenitor properties by fractionating the $Lin^{NEG}PDGFR\alpha/\beta^{POS}$ population using

of the TGF-β family co-receptor, endoglin (CD105). Through various lines of investigation using both in vitro bioassays and in vivo transplantation studies, I demonstrate that the $Lin^{NEG}PDGFR\alpha/\beta^{POS}CD105^{POS}$ and $Lin^{NEG}PDGFR\alpha/\beta^{POS}CD105^{NEG}$ populations each contain independent clonogenic progenitors with the ability to generate ectopic bone and bone marrow. By means of transcriptional profiling of the prospectively isolated populations, evidence is provided consistent both with distinct anatomical localization in vivo and of potentially different biological functions. Such data form the basis of future experimental approaches to define putative stromal cell hierarchies in the mouse BM stromal cell system.

4-3: RESULTS

Distinct populations of bone marrow stromal cells initiate both long-term stromal cell cultures and generate all CFU-F activity

We have previously identified a composite phenotype for the BM stromal cell population as a whole in fresh marrow based on the lack of hematopoietic lineage markers and expression of both the alpha and beta chains of the PDGF receptors ($Lin^{NEG}PDGFR\alpha/\beta^{POS}$) [28], which interestingly exhibited a bimodal expression for CD105. We next sought to determine if stromal cell clonogenic activity could be further enriched for based on CD105 (endoglin) expression as suggested by most retrospective analysis in the reported literature. Within both primary cultures and in freshly prepared DBM samples, we identified a $Lin^{NEG}PDGFR\alpha\beta^{POS}CD105^{POS}$ (referred to throughout as $CD105^{POS}$) and a $Lin^{NEG}PDGFR\alpha\beta^{POS}CD105^{LOW/NEG}$ ($CD105^{NEG}$) population. We therefore asked the question whether or not these two populations exhibit different functional properties.

Primary cultures of BMSCs were obtained from enzymatically disaggregated BM plugs and plated at either nonclonal (1x10^6 cells/cm^2) or at clonal densities (1x10^4 cell/cm^2). In both cases, flow cytometric analysis demonstrated that clonal and non-clonal cultures exhibited a bi-modal expression for CD105 within the $LIN^{NEG}PDGFR\alpha\beta^{POS}$ stromal cell population at nearly equal frequencies (Figure 4-1A i-ii), with no significant difference in the percentage of each population. At nonclonal

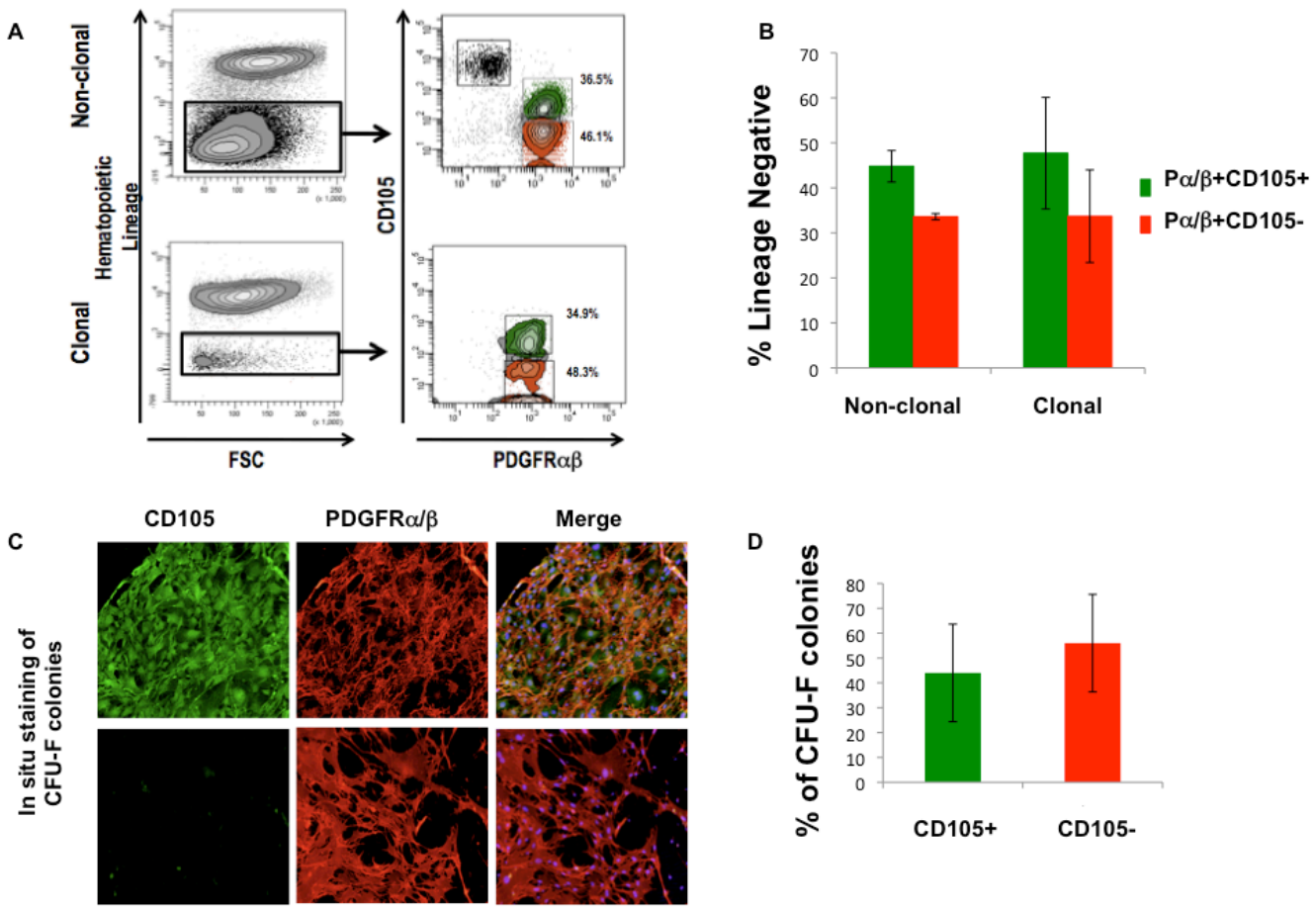

Figure 4-1: PDGFRαβ^{POS}CD105^{POS} and CD105^{NEG} cells initiate whole bone marrow CFU-F cultures. *(A) Representative flow cytometric analysis of primary cultures of DBM plated at non-clonal and at clonal densities demonstrates equal frequency of each population within the hematopoietic lineage negative cells. (B) Quantification of flow cytometric analysis for CD105^{POS} and CD105^{NEG} populations. (C) Representative in situ immunocytochemical staining of individual CFU-F colonies demonstrates homogeneous expression for CD105 within individual CFU-F. (D) Quantification of CFU-F in situ staining from 3 independent donors plated in triplicate. A total of 12 colonies were scored per donor. Data represent mean ± S.D.*

density, the $CD105^{POS}$ fraction represents (45.2± 2.65%) of the $Lin^{NEG}PDGFR\alpha\beta^{POS}$ population and the $CD105^{NEG}$ fraction represents (43.5± 3.6%) of the population by flow cytometric analysis (Figure 4-1A i). Interestingly, when BM mononuclear cells were plated at clonal density, the $CD105^{POS}$ and $CD105^{NEG}$ populations were represented at nearly equal frequencies within the $LIN^{NEG}PDGFR\alpha\beta^{POS}$ population, 48.2± 15.03% and 40.0± 12.5% respectively. In addition, in situ staining of primary cultures of DBM derived CFU-F revealed that single colonies were either all reactive or all negative for CD105 (Figure 4-1C), demonstrating that both $CD105^{POS}$ (44±19.6%) and $CD105^{NEG}$ (56±19.7%) cells initiate CFU-F colonies from whole bone marrow (Figure 4-1 A-D), with no significant difference in the number of colonies generated.

Next, we sought to determine the frequency of CFU-F generated within each population from freshly prepared DBM samples. By flow cytometric analysis, the $CD105^{POS}$ population represented significantly more of the $Lin^{NEG}PDGFR\alpha\beta^{POS}$ fraction with averages of 44.3% and 63.9%, in C57Bl/6 and BALB/c mice, respectively while the $CD105^{NEG}$ population represented 23.7% and 16.7% in the same two strains (Figure 4-2 B). As shown in Figure 4-2 C, both the $CD105^{POS}$ and $CD105^{LOW/-}$ populations generate CFU-F, when prospectively isolated, however the $CD105^{POS}$ population contained significantly more CFU-F per 1000 cells plated in C57Bl/6 mice suggesting that this population is more enriched in CFU-F activity (Figure 4-2C). However, the difference in the number of CFU-F formed from each prospectively isolated population was not statistically different in BALB/c mice

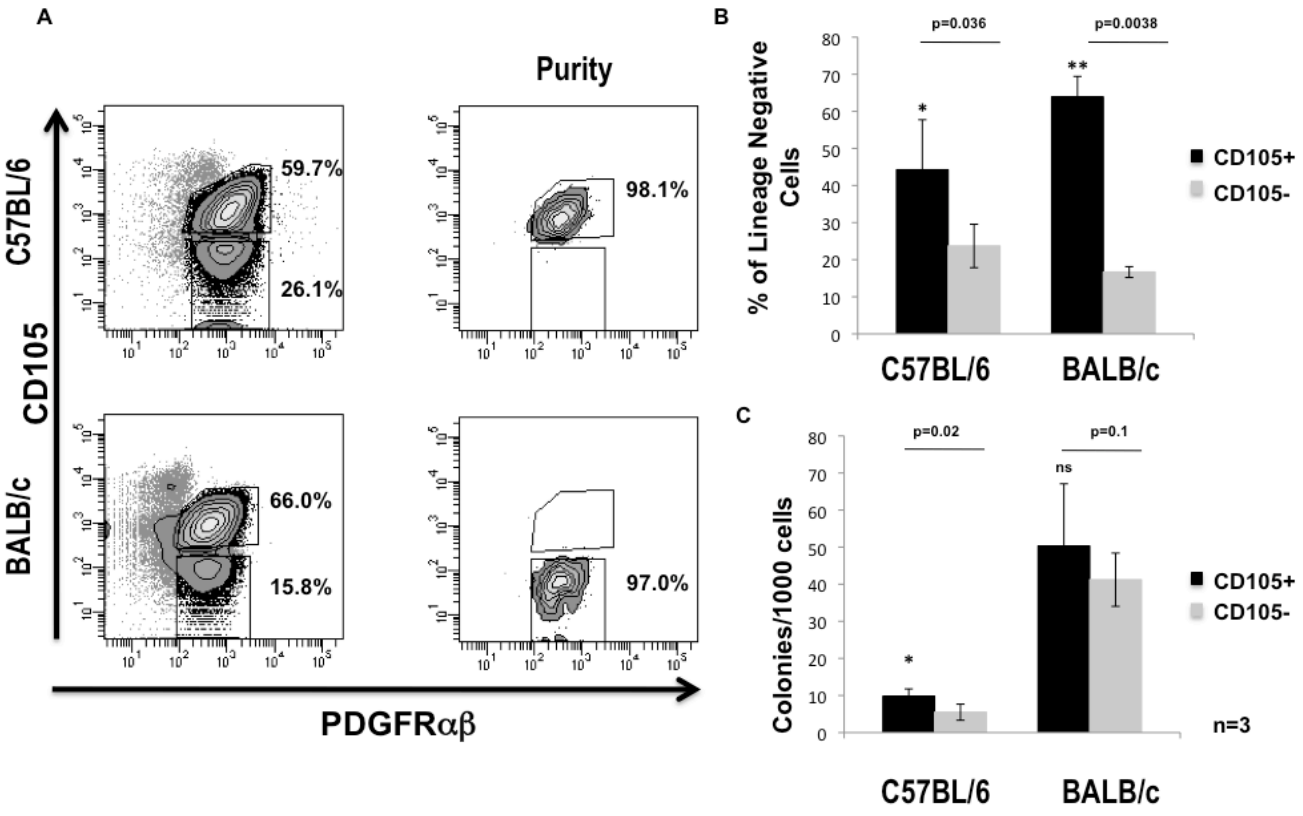

Figure 4-2. Lin^{NEG}PDGFRαβ^{POS}CD105^{POS} and CD105^{NEG} populations prospectively isolated from digested BM plugs are highly enriched in CFU-F activity. *(A) Prospective isolation of CD105^{POS} and CD105^{NEG} populations from enzymatically prepared BM plugs in C57Bl/6 and BALB/c mice. (B) Quantification of the percentage of viable cells gated through hematopoietic lineage negative population. (C) Number of CFU-F colonies generated from sorted populations in C57Bl/6 and BALB/c mice.*

highlighting a difference in the two strains of mice. Interestingly, this purification strategy for CFU-F isolation yields a 50-100 fold increase in the CFU-F obtained as compared to unfractionated whole BM samples. And while the percentage of the $CD105^{POS}$ population in vivo represents at least 50% more of the total $Lin^{NEG}PDGFR\alpha/\beta$ population (Figure 4-2 A&B), this observation suggests that it is more heterogeneous in terms of clonogenic activity and potentially function. Taken together, these data demonstrate that phenotypically distinct subpopulations of clonogenic stromal progenitor cells exist within mouse BM in vivo and equally contribute to the generation of CFU-F in culture.

Having previously noted that the bimodal expression of $CD105^{POS}$ and $CD105^{NEG}$ exists within total BM cultures up to passage 3 (Figure 3-9 B&D), we next wanted to determine if this bimodal expression would persist long term in culture over multiple additional serial passages or would change over time. To perform these experiments, DBM was plated in culture at non-clonal dilutions and multi-parameter flow cytometric analysis was conducted following serial passaging at P0, P3, P6 and P9. We observed a significant and progressive increase in the percentage of $CD105^{POS}$ cells in the cultures after passage 3 and by passage 9, the entire $LIN^{NEG}PDGFR\alpha\beta^{POS}$ fraction homogenously expressed CD105 (Figure 4-3 A&B).

This data suggests one of three possible scenarios; 1) a hierarchy exists whereby the $CD105^{NEG}$ cells represent a more primitive population that give rise to $CD105^{POS}$ cells more representative of a committed progenitor (Figure 4-4A); scenario 2) $CD105^{POS}$ cells have a greater proliferative capacity in vitro and

eventually overtake cultures following serial passaging (Figure 4-4B); or scenario 3) all stromal cells begin to express CD105 following extended culture periods representing an in vitro artifact (Figure 4-4C). To begin addressing each possible scenario, DBM single cell suspensions were fractionated by FACS into $CD105^{POS}$ and $CD105^{NEG}$ populations, and analyzed for their expression of CD105 by flow cytometric analysis following serial passaging. Up to passage 6, we were unable to detect any level of inter-conversion between these two immunophenotypes (Figure 4-5) suggesting that distinct subpopulations within the bone marrow stromal compartment can initiate and maintain long-term marrow cultures, ruling out the likelihood of scenarios 1 and 3, and suggesting that $CD105^{POS}$ cells contain a greater proliferative capacity in vitro and eventually overtake cultures of unfractionated WBM. In support of this, the $CD105^{NEG}$ population failed to proliferate beyond passage 6, at which time the majority of cells became large flattened bi-nucleated cells that stop dividing while at the same passage history, the $CD105^{POS}$population continued to proliferate at least to passage 9.

Figure 4-3. DBM cultures demonstrate homogeneous for CD105 expression following ex vivo expansion. (*A) Representative FACS plots of whole bone marrow cultures prepared from enzymatic disaggregation of BM plugs. Gating is set according to isotype controls (B) Quantification of flow cytometric analysis demonstrating an increase in frequency of hematopoietic lineage negative cells and $CD105^{POS}$ cells concomitant to a complete loss of the $CD105^{NEG}$ population. Data are represented as the mean $\pm$ Std. Dev. n=3. Statistical analysis was performed with student t-test and significance assigned to $p<0.05$ (*), and $p<0.0001$ (**).*

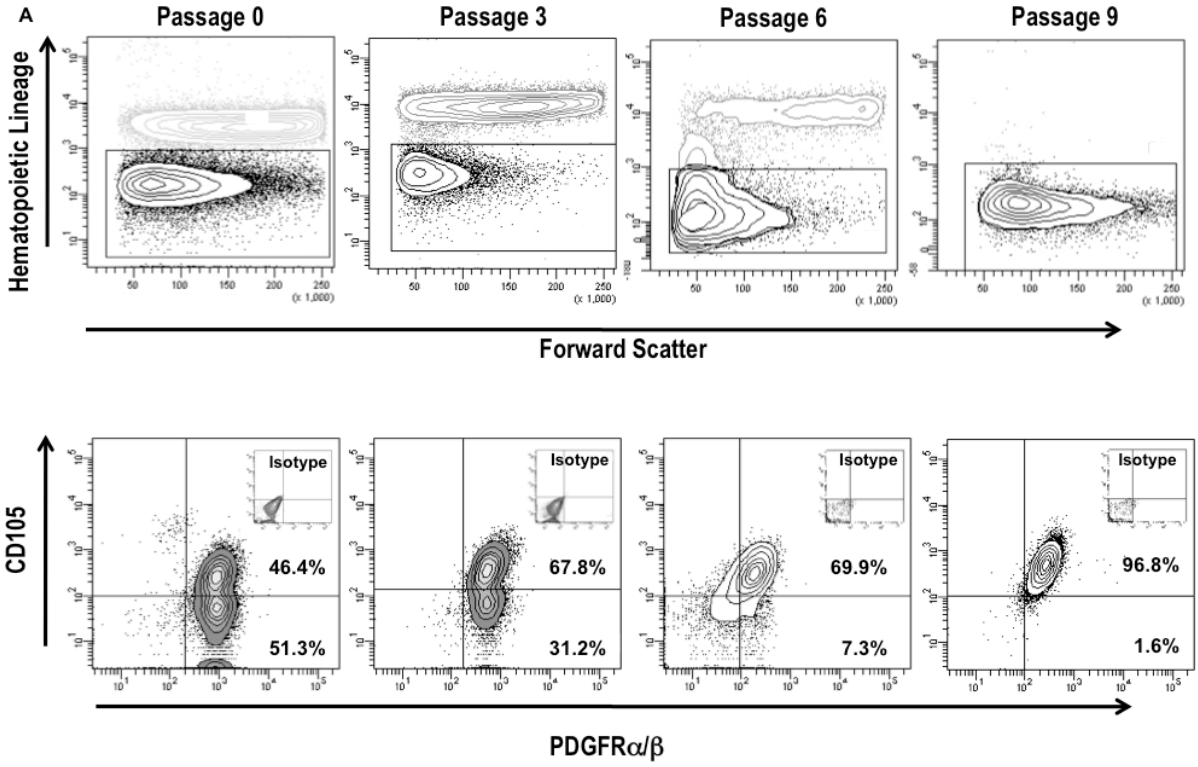
A
Passage 0
Passage 3
Passage 6
Passage 9
Hematopoietic Lineage
Forward Scatter
CD105
PDGFRα/β
Isotype
46.4%
51.3%
67.8%
31.2%
69.9%
7.3%
96.8%
1.6%

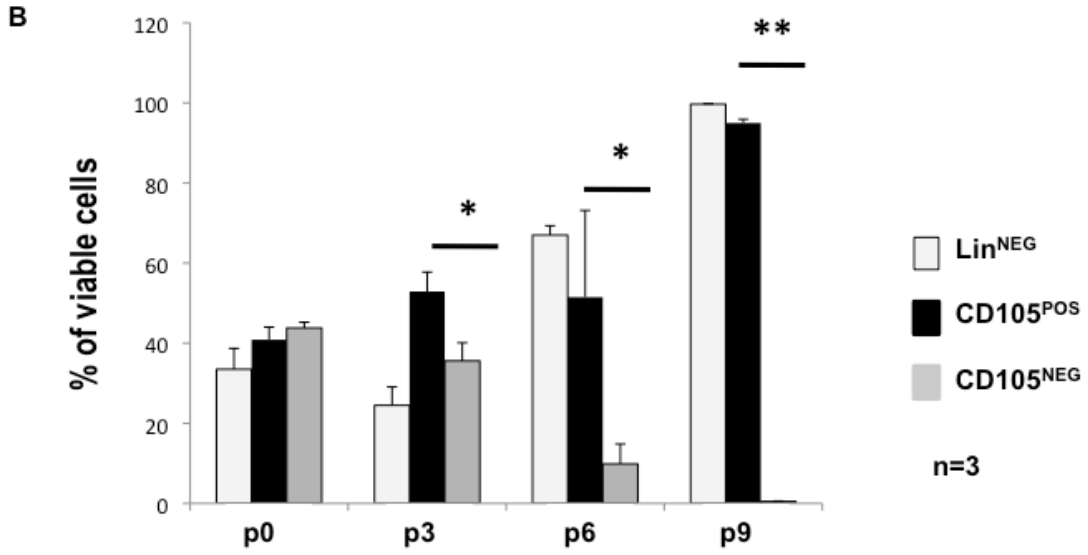
B
% of viable cells
120
100
80
60
40
20
0
p0
p3
p6
p9
*
*
**
Lin^NEG
CD105^POS
CD105^NEG
n=3

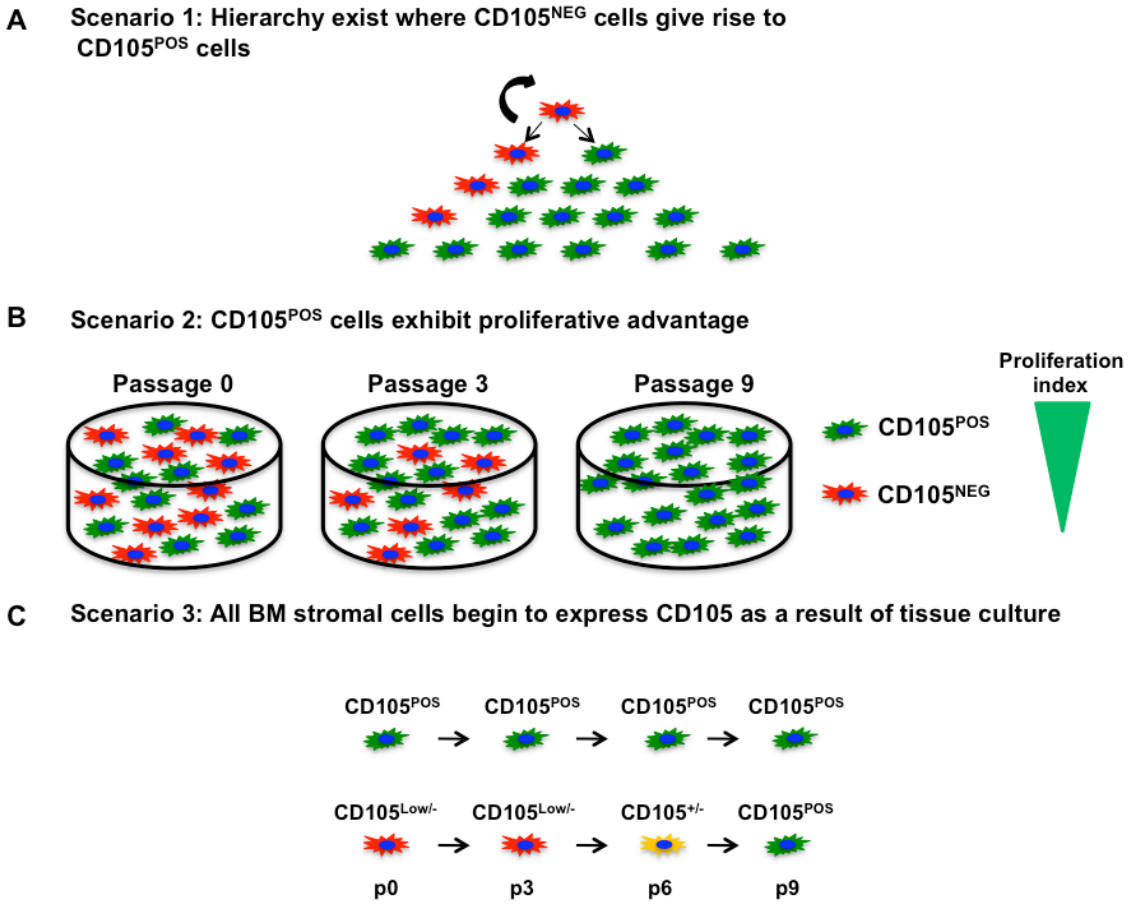

Figure 4-4: Schematic diagram of possible explanations leading to homogeneous CD105 expression following extended culture. *(A) Scenario 1: existence of a stem/progenitor hierarchy with CD105^{NEG} population representing a more primitive stem/progenitors with limited self-renewal capabilities which undergo asymmetric divisions giving rise to more committed CD105^{POS} progenitors. (B) Scenario 2: CD105^{POS} cells demonstrate a greater proliferative capacity and over-take cultures following extended passage history. (C) Scenario 3: All BMSCs begin to express CD105 following increasing passage history.*

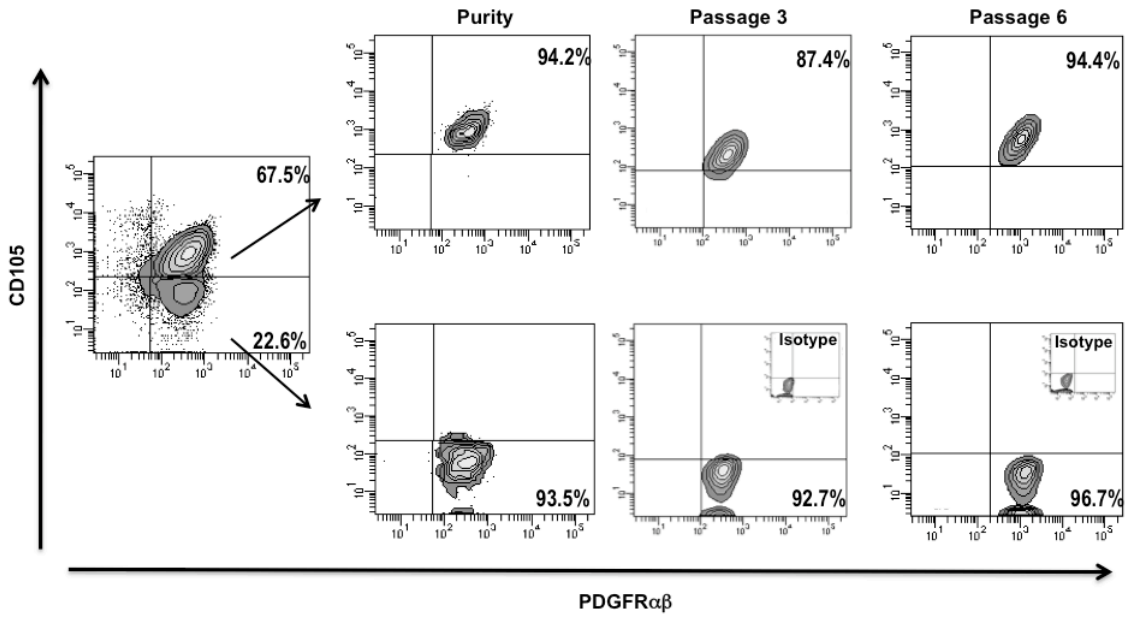

Figure 4-5: Lin^{NEG}PDGFRαβ^{POS}CD105^{POS} and CD105^{NEG} cells fractionated from freshly prepared BM samples maintain their original CD105^{POS} or CD105^{NEG} phenotype in culture. *Flow cytometric analysis demonstrating maintenance of the input phenotype with respect to CD105 expression following serial in vitro passage of mouse DBM derived BMSC.*

A subpopulation of prospectively isolated $Lin^{NEG}PDGFR\alpha/\beta CD105^{POS}$ cells co-express mature pericyte and subendothelial adventitial reticular cell markers in vivo

Although all CFU-F are contained within the $CD105^{POS}$ and $CD105^{NEG}$ fractions, not all cells expressing either of these markers are able to form CFU-F suggesting that each population remains heterogeneous in regards to clonogenic activity. To further assess the level of heterogeneity within each population, we prospectively isolated $Lin^{NEG}PDGFR\alpha/\beta$ population as a whole by FACS and cells were used to prepare cytospins and dual labeled for CD105 in pair-wise combination with a panel of pericyte/mural cell markers, including NG2, alkaline phosphatase (ALP) and α smooth muscle actin (αSMA). Accordingly, the $CD105^{POS}$ and $CD105^{NEG}$ populations were represented at nearly equal frequencies by cytospin, 57.9% and 41.6%, respectively, as that determined by flow cytometric analysis validating the use of this approach (Figure 4-6B). 100% of the cells exhibited staining with antibody to PDGFRβ, as expected, confirming the purity of the sorted cell population (Figure 4-6 A v&vi, & B). The percentage of $CD105^{POS}$ cells exhibiting co-staining for these additional pericyte/mural cell markers is represented in Figure 4-6B. Approximately 18% and 28%, respectively, of $CD105^{POS}$ cells expressed αSMA and NG2, suggesting that a minor subpopulation of cells within this phenotype are smooth muscle/perivascular cells. Conversely, all of the cells that expressed either αSMA (A vii-ix), NG2 (A x-xii) or ALP (A xiii-xv) were also positive for CD105 (white arrows), demonstrating that cells exhibiting expression of the well

documented pericyte markers αSMA and NG2 are restricted to the $Lin^{NEG}PDGFR\alpha/\beta CD105^{POS}$ subpopulation.

Figure 4-6: Prospectively isolated Lin^{NEG}PDGFR$\alpha\beta^{POS}$CD105^{POS} cells co-express pericyte/mural cell markers in vivo. *(A i-xvi) Representative images of Immunohistochemistry staining of prospectively isolated PDGFRα/β^{POS} cells with a combination of cell surface markers to CD105, PDGFRβ, αSMA, NG2 and Alkaline Phosphatase or isotype controls. PDFGRβ was used as a positive control demonstrating 100% of sorted cells expressing PDFGRβ (A v-vi). A subpopulation of CD105^{POS} cells (white arrows) express αSMA (A vii-ix), NG2 (A x-xii) and ALP (A xiii-xv). Isotype controls: Rb-IgG, Ms-IgG and Gt-IgG isotype controls (A i-iii). Nuclei were counterstained with DAPI in prolong Gold anti-fade mounting media. Images were captured on am Olympus 70x epifluorescent microscope with an Olympus camera under identical exposure time at 40x magnification. White arrows indicate double positive cells for CD105 and αSMA, NG2 and ALP. Yellow arrowheads indicate CD105^{NEG} cells lacking expression for any additional markers tested. (B) Quantification of cells expressing each marker from 3-5 fields of view per slide. Data represent mean $\pm$ Std. dev. (C & D) Flow cytometric analysis of transgenic mouse strains demonstrating expression of αSMA (C) and NG2 (D) within the CD105^{POS} population. (E) Whole mount staining of WT BM plugs demonstrating a perivascular localization of PDGFRα/β^{POS}NG2^{POS} cells along smaller arteriole vessels consistent with mature pericyte function in vivo. Images were captured using a 63x oil immersion objective of a Leica TCS SP5 confocal microscope and processed with the Leica LAS AF lite software. Z-stacked images were collected in 0.2 μm slices at depths of 15-25 μm with a pinhole of 1 (x63).*

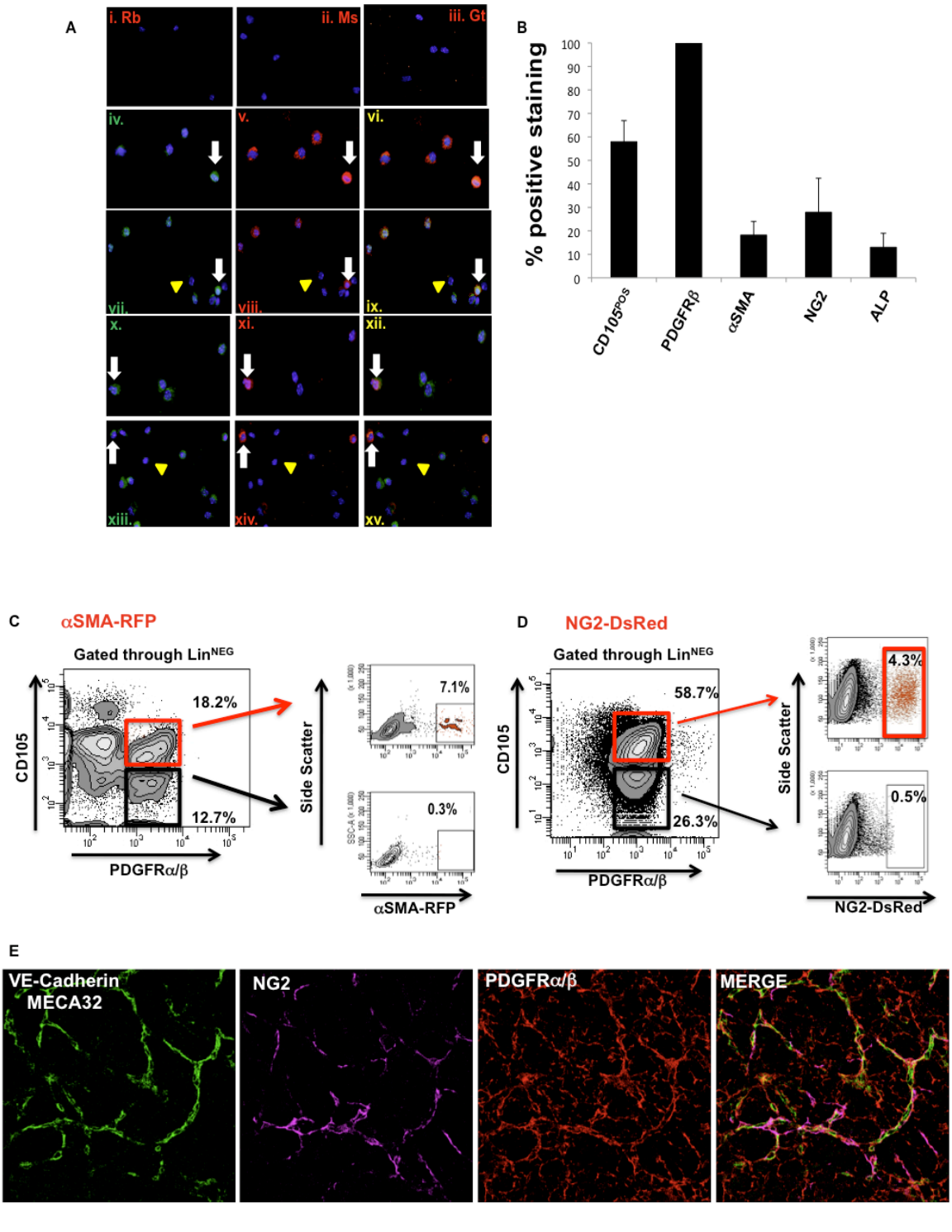
A
i. Rb
ii. Ms
iii. Gt
iv.
v.
vi.
vii.
viii.
ix.
x.
xi.
xii.
xiii.
xiv.
xv.
B
% positive staining
100
90
80
70
60
50
40
30
20
10
0
CD105POS
PDGFRβ
αSMA
NG2
ALP
C
αSMA-RFP
Gated through LinNEG
18.2%
12.7%
CD105
PDGFRα/β
Side Scatter
7.1%
0.3%
αSMA-RFP
D
NG2-DsRed
Gated through LinNEG
58.7%
26.3%
CD105
PDGFRα/β
Side Scatter
4.3%
0.5%
NG2-DsRed
E
VE-Cadherin
MECA32
NG2
PDGFRα/β
MERGE

We next validated these results by flow cytometric analysis of two different transgenic mouse models, the first in which the αSMA promoter drives expression of RFP (αSMA-RFP; generously supplied by Dr Frank Marini, MD Anderson Cancer Center, Houston, TX) and the second strain in which the NG2 promoter drives expression of DsRed (Tg(Cspg4-DsRed.T1)1Akik/J [124]) (Figure 4-6 C&D). From each strain BM plugs were isolated and subjected to sequential enzymatic disaggregation as previously described to yield a suspension of DBM which was then analyzed for either RFP or DsRed expression (as appropriate) in combination with the Lineage panel, PDGFRα/β and CD105.

This approach confirmed the immunocytochemistry data demonstrating that all of the αSMA-RFP and NG2-DsRed expressing cells fell within the $CD105^{POS}$ fraction, representing 7.1% and 4.2%, respectively (Figure 4-6 C&D). Additionally, whole mount staining of BM plugs was performed to determine the in situ localization of NG2 positive cells within the BM. From this staining, we observed that the $PDGFR\alpha/\beta^{POS}CD105^{POS}NG2^{POS}$ cells were localized to smaller blood vessels which were reactive for both VE-Cadherin and MECA32 antibodies (Figure 4-6 E), a finding consistent with the known localization of pericytes [125]. Importantly, the $PDGFRa/b^{POS}CD105^{POS}NG2^{POS}$ population was also assayed for its content of CFU-F and exhibited a CFE of 0.4% (4 colonies/1000 cells plated). Interestingly from the same mice, the $Lin^{NEG}PDGFRa/b^{POS}CD105^{POS}NG2^{NEG}$ population contained a colony forming efficiency of approximately 1.2%. Taken together these data demonstrate that differential expression of CD105 allows the resolution of the stromal progenitor population of mouse BM into subpopulations that differ in their

phenotype and anatomical location within the BM and implies that they may be hierarchically related.

$Lin^{NEG}PDGFR\alpha/\beta CD105^{POS}$ and $CD105^{LOW/-}$ populations exhibit multi-lineage differentiation in vitro and generate ectopic bone tissue with associated hematopoietic bone marrow in vivo

We next, assessed the differentiation potential of the each population through a series of in vitro and in vivo differentiation assays. For these experiments, DBM from freshly prepared BM was fractionated based on $Lin^{NEG}PDGFR\alpha/\beta^{POS}CD105^{POS}$ and $CD105^{LOW/-}$ phenotypes by FACS and expanded to passage 3. At passage 3 or 4, each population was first subjected to in vitro multi-lineage differentiation assays. To assess differentiation along the osteogenic lineage, cultures were plated in basal medium for 2-3 days and followed by exposure to the standard osteogenic differentiation culture conditions (ascorbic acid, dexamethasone and inorganic phosphate; see Materials & Methods) for 14 days. At day 14, cultures were fixed and histochemical staining performed to reveal alkaline phosphatase activity as a marker of osteoblastic differentiation in combination with calcium-phosphate mineralized deposits (revealed using the von Kossa reaction). Under these conditions, both $CD105^{POS}$ and $CD105^{NEG}$ populations efficiently differentiated along the osteoblastic lineage (Figure 4-7A top panel). Additionally, when confluent cultures were grown in the presence of the PPARγ agonist IBMX for 14-21 days, both populations successfully differentiated along the adipogenic lineage containing clusters of

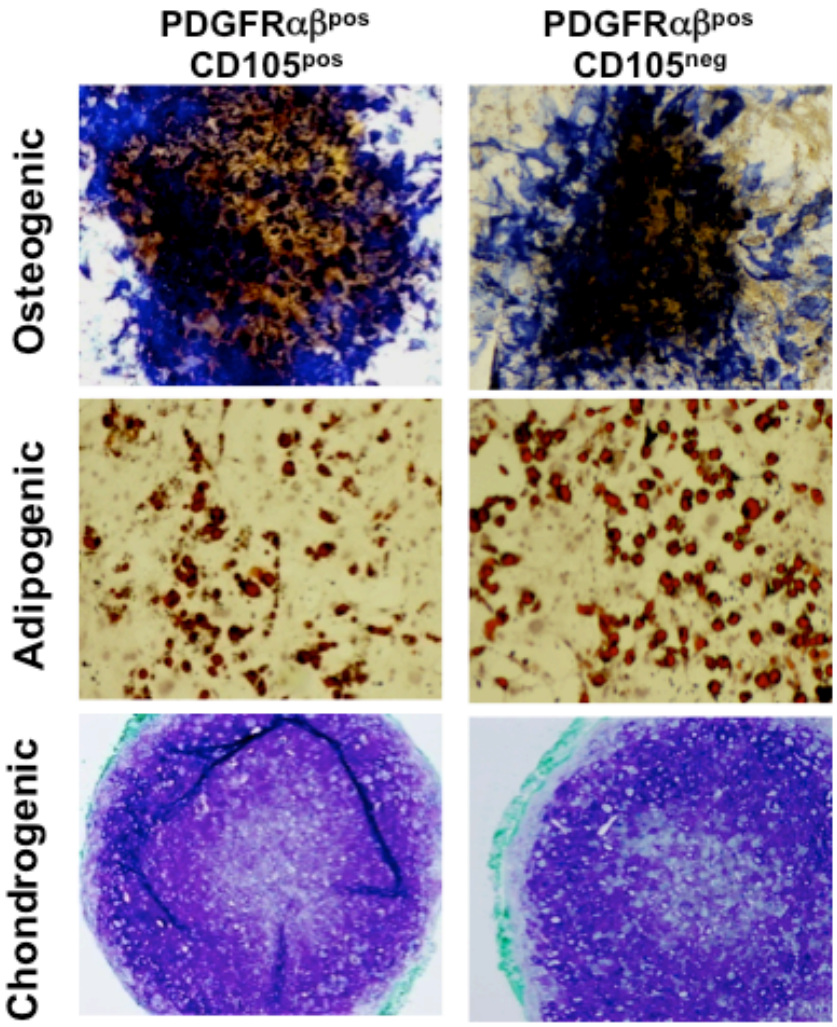

Figure 4-7: Lin^{NEG}PDGFRαβ^{POS}CD105^{POS} and 105^{NEG} populations contain MSC activity in vitro. *(A) In vitro multi-lineage differentiation of CD105^{POS} and 105^{NEG} populations. Osteogenic lineage differentiation was evaluated by alkaline phosphatase (blue) and Von Kossa (brown) staining. Adipogenic lineage differentiation assessed by Oil red O staining of lipid vacuoles. Chondrogenic lineage differentiation was assayed in micro-mass pellet cultures and stained with Toluidine blue.*

lipid-laden cells that stained with the neutral lipid stain Oil Red O (Figure 4-7 B middle panel). Chondrogenic differentiation was evaluated using standard micromass pellet culture assays. In these assays, both populations were able to generate chondrogenic pellets, revealed by the deposition of a sulphated proteoglycan-rich ECM stained with Toluidine Blue (Figure 4-7, bottom panels). These data provide evidence that both $CD105^{POS}$ and $CD105^{NEG}$ stromal cell subpopulations exhibit the capacity for multilineage differentiation to generate osteoblastic, adipose and chondrogenic progeny in vitro.

Although in vitro differentiation assays are readily used by many labs to assess multi-lineage differentiation potential, caution must be exercised in interpreting these assays since in vitro differentiation potential does not unambiguously predict their capacity for differentiation in vivo [126]. Therefore, we further tested the multipotency of each population using rigorous in vivo transplantation assays to determine the differentiation potential of the $CD105^{POS}$ and $CD105^{NEG}$ populations. For these assays, DBM cell suspensions were prepared from C57Bl/6 mice and fractionated by FACS on $CD105^{POS}$ expression. Following isolation, each population was expanded in culture to passage 3 or 4, at which time a portion of the cells were analyzed by flow cytometric analysis to validate the input pre-transplantation phenotype (see Figure 4-9 A). The remaining cells were loaded onto Gelfoam scaffolds at 5x10^5 cells/scaffold and implanted subcutaneously by blunt dissection into NOD-SCID mice as previously described [85, 88]. Initially,

Figure 4-8: $Lin^{NEG}PDGFR\alpha\beta^{POS}CD105^{POS}$ and 105^{NEG} populations generate ectopic bone and transfer the hematopoietic microenvironment in vivo. *In vivo ectopic bone tissue with associated hematopoietic bone marrow. Top panel represents empty scaffolds as controls (n=6), middle panels are representative bone formation from $CD105^{POS}$ population (n=8) and lower panel is from $CD105^{NEG}$ population (n=8) stained with H&E and Von Kossa (left to right).*

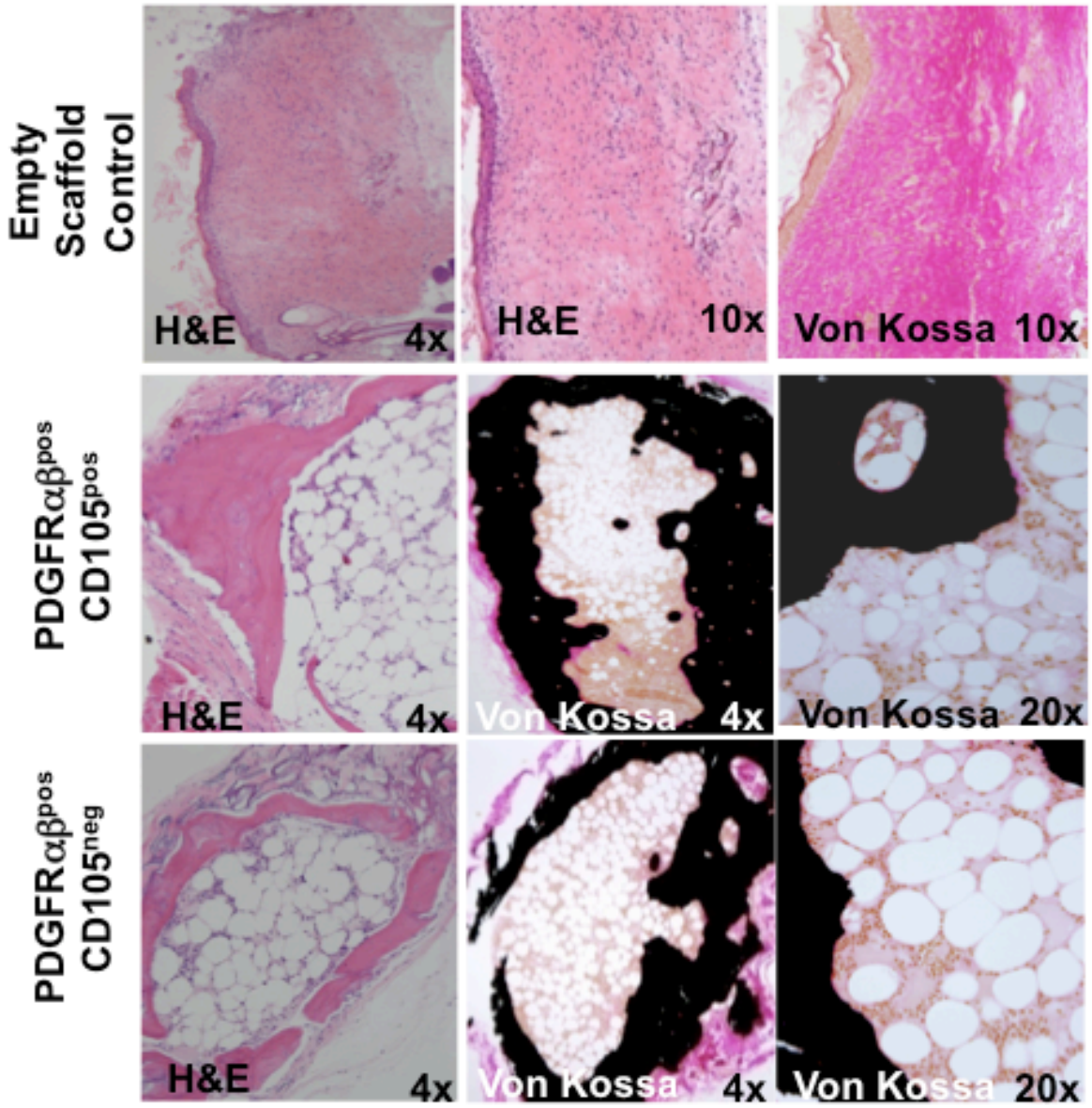
Empty Scaffold Control
H&E 4x
H&E 10x
Von Kossa 10x
PDGFRαβpos CD105pos
H&E 4x
Von Kossa 4x
Von Kossa 20x
PDGFRαβpos CD105neg
H&E 4x
Von Kossa 4x
Von Kossa 20x

scaffolds were recovered at 12 weeks post implant for histological evaluation. In all cases (8 out of 8), scaffolds contained an outer core of mineralized bone tissue surrounding an adipose rich BM tissue (Figure 4-8, middle and bottom panels) whereas only fibrous connective tissue was observed in mice transplanted with empty scaffolds as controls (n=6) (Figure 4-8, top panels). Thus both murine BM stromal stem/progenitor subpopulations also demonstrate the capacity to form histologically proven bone tissue and transfer the hematopoietic microenvironment in vivo.

While these data provide evidence that both $Lin^{NEG}PDGFR\alpha\beta^{POS}CD105^{POS}$ and 105^{NEG} stromal progenitor subpopulations demonstrate the capacity to generate an ectopic bone marrow organ it should be noted the transplants were performed using equivalent numbers of cells from each population and the formation of a bony ossicle was assessed at the one time point. This experimental design therefore does not preclude the possibility that the two populations may differ either in their potency or in the kinetics with which they each generate an ossicle. Furthermore this experimental approach also does not measure whether differences in the self-renewal potential of the two populations exist as would be demonstrated by secondary CFU-F formation and the generation of secondary bone-marrow ossicle upon secondary transplantation.

To begin to address such questions a series of studies were designed using the heterotypic bone ossicle forming assay in which fewer input cells were transplanted and the transplants were of shorter duration. For these studies, BMSC subpopulations were isolated from UBC-GFP mice (n=6 per group) in order to track

the fate and contribution to bone formation and hematopoietic supporting stroma by transplanted donor derived cells. Furthermore, the use of labeled cells facilitated analysis of the phenotype of the transplanted cells and the potential to re-isolate donor cells following transplantation by means of FACS. Previous experiments suggested that the $CD105^{POS}$ cells exhibited a greater proliferative advantage in culture (Figure 4-4) and generate significantly more CFU-F colonies (Figure 4-2 C) as well as generate qualitatively more larger colonies than $CD105^{NEG}$ cells further supporting evidence of a greater proliferative advantage in vitro (Figure 4-9 A i-iii).

To address the issues of potency and kinetics, $CD105^{POS}GFP^{POS}$ and $CD105^{NEG}GFP^{POS}$ cells were isolated from UBC-GFP mice as previously described and a some of the cells were plated for CFU-F assays to again confirm the clonogenic potential (Figure 4-9 Ai-iii) and the majority of isolated cells were expanded in culture to passage 3. At which time, cells were collected and a portion of the cells from each population were analyzed by FACS to confirm the pre-transplantation immunophenotype (Figure 4-9 B) and the remaining cells were loaded onto Gelfoam scaffolds and transplanted subcutaneous as previously described.

At 12 weeks post-transplant, mice were sacrificed and subjected to MicroCT analysis to identify bone containing ossicles macroscopically (Figure 4-9 C). Scaffolds were then recovered and processed for histology following decalcification. H&E staining of scaffolds further demonstrated ectopic bone formation and GFP immunohistochemistry was used to confirm the contribution from donor-derived cells. In these experiments, both populations demonstrated contribution to

osteoblast bone lining cells, mature osteocytes embedded in bone matrix, immature adipocytes containing multiple lipid droplets and immature, unilocular adipocytes (Figure 4-9 D). Furthermore, some scaffolds were crushed, enzymatically digested and the cells recovered by this process subjected to flow cytometric analysis. In these studies, scaffolds recovered from $CD105^{POS}GFP^{POS}$donor cells demonstrated a bimodal expression for CD105 similar to the distribution seen in freshly prepared tissue (Figure 4-9 Ai), with 58.6% of the cells retaining CD105 expression and 40.5% of the GFP^{POS} cells expressing low to negative levels of CD105 expression (Figure 4-9 E i&ii). However, $CD105^{NEG}$ donor cells remained negative for CD105 expression (4-9 E iv&v). Interestingly, when cells recovered from these scaffolds were plated at equivalent numbers in culture for secondary CFU-F assays we were only able to find colonies from scaffolds derived from the $CD105^{POS}$ donor cells (Figure 4-9 Eiii), where as the $CD105^{NEG}$ donor cells grew scattered throughout the well without any evidence of colony formation (Figure 4-9 E vi). We were not able to accurately enumerate the colonies in this experiment due to overgrowth of host GFP-Neg fibroblasts in the tissue surrounding the implants.

Nevertheless, these data represent important evidence suggesting that following transplantation in vivo, $CD105^{POS}$ cells generate both $CD105^{POS}$ cells and $CD105^{NEG}$ subpopulations but under identical transplant conditions, $CD105^{NEG}$ cells only give rise to $CD105^{NEG}$ cells. These results imply that $CD105^{POS}$ and $CD105^{NEG}$ are not independent self-maintaining populations but represent a hierarchy of BMSCs.

To address the issue of potency and kinetics, BMSCs fractionated as above on the basis of CD105 expression were again loaded onto scaffolds and transplanted subcutaneously at a dose of 1x10^5 cells per scaffold and transplanted for a total of 6 weeks (n=4). Histological analysis of these scaffolds demonstrated that although both populations generated bone tissue, only the $CD105^{POS}$ cells were able to generate adipose derived marrow (Figure 4-10 A), whereas the $CD105^{NEG}$ cells contributed mostly to bone formation (Figure 4-10 B) with only 1 of 4 scaffolds demonstrated a small area of marrow adipocytes. Because these transplantation assays were done with fewer input cells and for a shorter duration of time, these results suggest a potential difference in the potency of stem/progenitor cells within the two populations in vivo and in their differentiation kinetics.

Together, these transplantation studies demonstrate that although both populations contain clonogenic progenitors that are able to form ectopic bone at 5x10^5 cells per graph during a 12 week time point, the $CD105^{POS}$ population exhibits greater proliferative potential in vitro and in vivo and suggest that this population as a whole is more enriched in primitive stromal stem cells as demonstrated by their ability to generate both bone and adipose rich bone marrow from fewer cells in a shorter period of time in vivo. Our preliminary data also suggest that the capacity to form secondary CFU-F (as a measure of self-renewal capacity) following ectopic transplantation is restricted to the $CD105^{POS}$ subpopulation. Additionally, because $CD105^{POS}$ cells give rise to $CD105^{NEG}$ cells in vivo in the heterotypic bone forming model, we reasoned that within the $CD105^{POS}$ population exists a hierarchically more primitive stromal stem cell, which sits atop of

Figure 4-9: $Lin^{NEG}PDGFR\alpha\beta^{POS}CD105^{POS}$ population contains stromal stem/progenitors with secondary CFU-F generating potential. *(A) Representative FACS plot (i) and CFU-F images (ii-iii) from each population following prospective isolation. $CD105^{POS}$ (ii) population contains founder CFU-F with greater proliferative advantage compared to $CD105^{NEG}$ (iiii). Arrows highlighting qualitative difference in colony size. (B) Pre-transplantation immunophenotype of passage 3 culture expanded $CD105^{POS}$ and $CD105^{NEG}$ populations. (C) Micro CT imaging of subcutaneous scaffolds at 12 weeks post-transplant. Arrows indicate ectopic bone. (D) GFP immunohistochemistry of recovered scaffolds demonstrating donor derived bone and adipogenic marrow stoma. (E) Ectopic scaffolds were recovered, digested and analyzed by flow cytometric analysis and CFU-F assay. (Ei & iv) GFP expression of donor cells recovered from scaffolds. (E ii & v) Flow cytometric analysis of GFP+ donor cells following 12 weeks post-transplantation demonstrating $CD105^{POS}$ donor cells generate $CD105^{LOW/NEG}$ cells in vivo. (E iii & vi) GFP^{POS} cells plated from scaffolds demonstrating secondary CFU-F potential by $GFP^{POS}CD105^{POS}$ donor cells.*

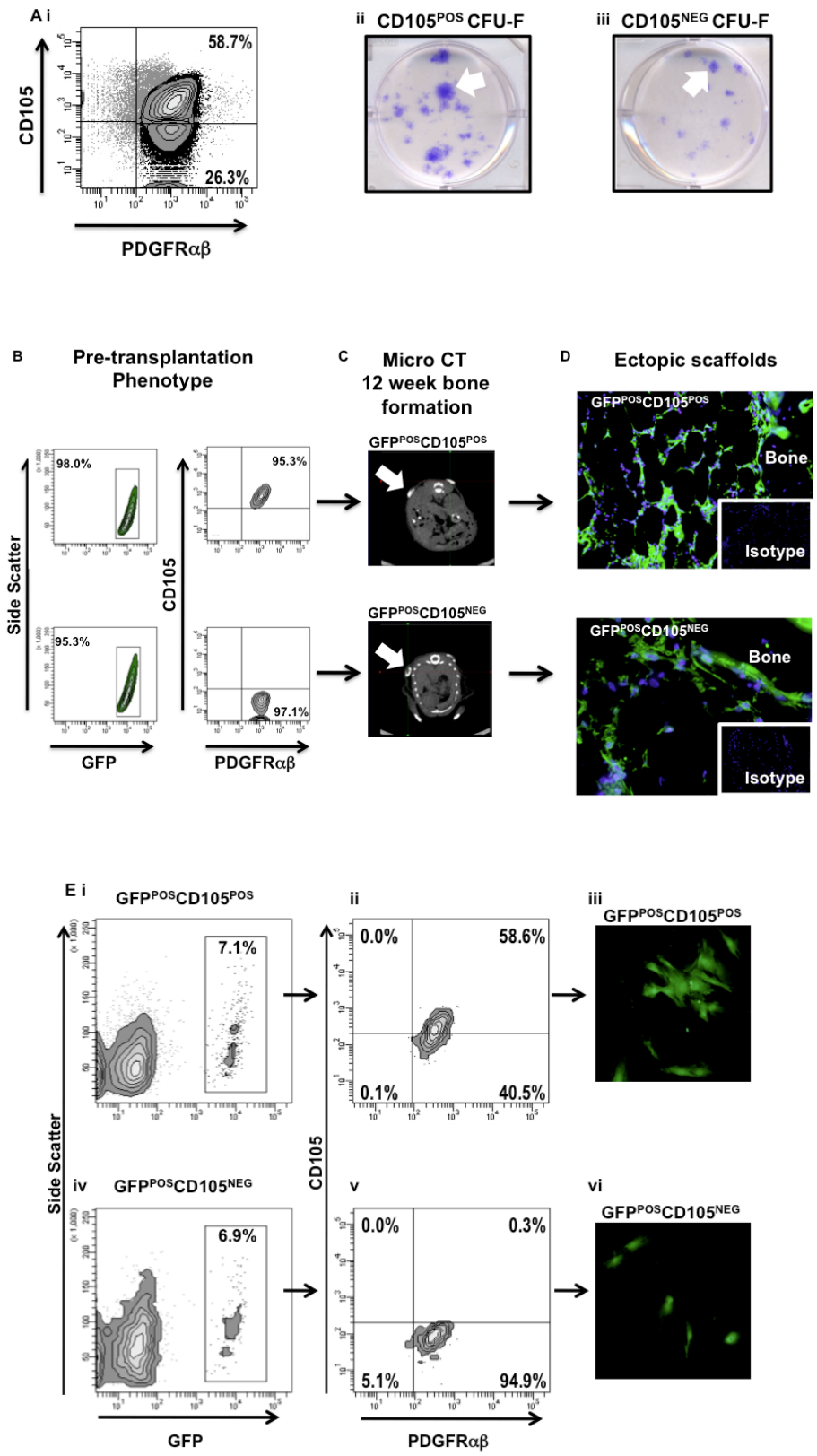
A i
58.7%
26.3%
CD105
PDGFRαβ
ii CD105POS CFU-F
iii CD105NEG CFU-F
B
Pre-transplantation Phenotype
98.0%
95.3%
95.3%
97.1%
Side Scatter
CD105
GFP
PDGFRαβ
C
Micro CT 12 week bone formation
GFPPOSCD105POS
GFPPOSCD105NEG
D
Ectopic scaffolds
GFPPOSCD105POS
Bone
Isotype
GFPPOSCD105NEG
Bone
Isotype
E i
GFPPOSCD105POS
7.1%
ii
0.0%
58.6%
0.1%
40.5%
iii
GFPPOSCD105POS
iv
GFPPOSCD105NEG
6.9%
v
0.0%
0.3%
5.1%
94.9%
vi
GFPPOSCD105NEG
Side Scatter
CD105
GFP
PDGFRαβ

a stromal cell hierarchy.

Although this proposed hierarchical model in the adult BM is largely speculative at this time, it is supported by studies from the Weissman lab using fetal bone-derived stromal cells [123]. This study described the ability of fetal bone derived stromal cells fractionated on CD105 and Thy1 expression to establish a stem/progenitor cell hierarchy in which $CD105^{POS}Thy1^{NEG}$ cells generated bone and HSC supporting BM in a kidney capsule ectopic transplant model while the $CD105^{POS}THY1^{POS}$ and $CD105^{NEG}$ populations generated bone tissue only. Furthermore, the authors provide evidence that the $CD105^{POS}THY1^{NEG}$ population follows the process of endochondral ossification, while the $CD105^{POS}THY1^{POS}$ population, expresses 5 fold higher levels of osteocalcin and appears to form bone without the cartilage intermediate [123].

Global transcriptional analysis of BM stromal stem/progenitor populations

After having established the existence of phenotypically distinct subpopulations that contain functional clonogenic osteoprogenitor cells, we next sought to determine if transcriptional profiling would provide additional evidence as to their biology and/or potentially point to a stromal stem/progenitor cell hierarchy. For these experiments, the $Lin^{NEG}PDGFR\alpha/\beta^{POS}CD105^{POS}$ and $Lin^{NEG}PDGFR\alpha/\beta^{POS}CD105^{NEG}$ stromal cell populations and hematopoietic lineage positive cells were prospectively isolated from three independent experiments.

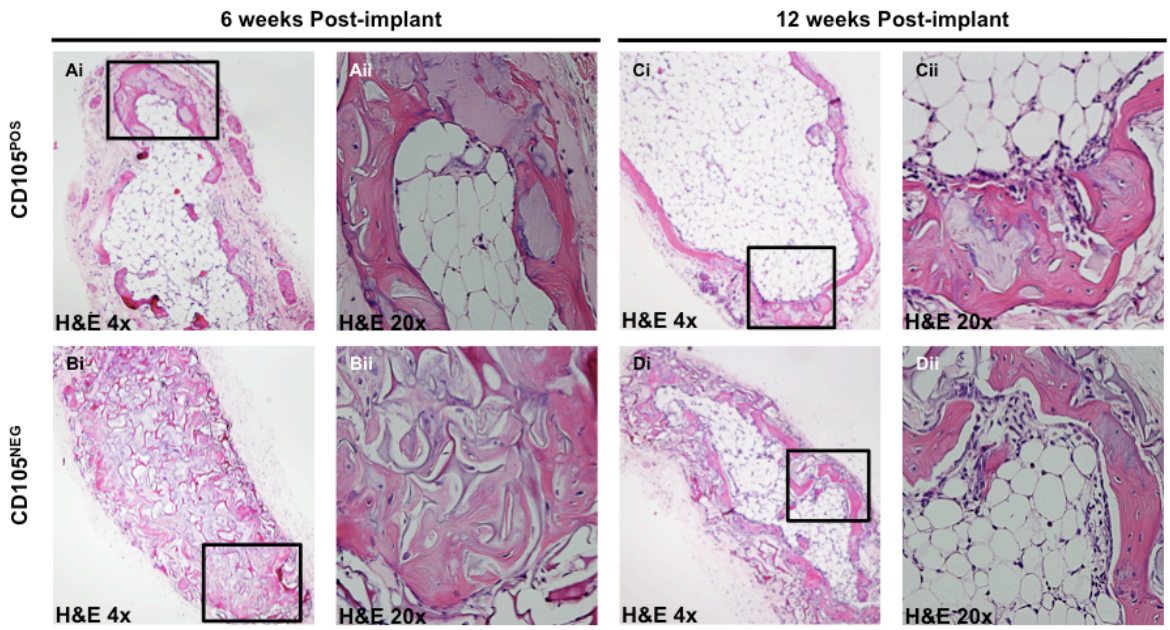

Figure 4-10: Time dependent developmental potential of ectopic bone and bone marrow formation by subpopulations of BMSCs. *The development of bone and bone-bone marrow tissue in ectopic sites is dependent on time and number of cells. (A & B) Representative images of scaffolds stained with H&E following 6 weeks post-transplant. (Ai-ii) CD105^{POS} scaffolds demonstrate the formation of bone and adipose rich bone marrow by 6 weeks, whereas CD105^{NEG} scaffolds contain only bone. By 12 weeks (C&D), both populations form bone and adipose rich bone marrow tissue. Boxes indicate regions imaged at 20x magnification.*

Endothelial cells were removed from the isolation strategy based on the $CD105^{bright}PDGFR\alpha\beta^{NEG}$ immunophenotype previously identified (see Figures 3-7 & 3-8). Total RNA was extracted from each population and subjected to gene expression profiling using the Illumina Sentrix Beadchip Array Mouse WG-6.v2 arrays. To ensure the purity of each population following isolation, post sort analysis was performed for each group and demonstrated purities for $CD105^{POS}$ at 97.4$\pm$1.9% and $CD105^{NEG}$ at 94.1$\pm$2.5%.

Following hybridization and detection, we compared the genes in common to both stromal cell populations that were expressed at least two fold greater with a p-value <0.01 to the genes expressed in hematopoietic lineage positive cells. From this analysis, we identified 1,798 annotated genes that were differentially expressed between stromal cells and all hematopoietic cells. As expected, the stromal cell populations demonstrated a clear mesenchymal signature in gene ontology analysis by DAVID (Table 4-1). A number of surface markers, extracellular matrix molecules and signaling pathways characteristic of mesenchymal cells were highly over-represented within these two populations consistent with known stromal cell biology (Table 4-2). Of interest, GO functional annotation analysis yielded an over representation of genes involved in signaling pathways (493 genes), secreted molecules (226 genes), ECM proteins (86 genes), cell adhesion molecules (108 genes), skeletal system development (74 genes), blood vessel development (62 genes), mesenchymal cell development (12 genes), and growth factors (26 genes).

Enrichment score 37.71	P Value
extracellular matrix	1.60E-46
Enrichment score 12.5	
cell adhesion	7.40E-15
biological adhesion	7.80E-15
Enrichment score 11.04	
collagen	6.40E-24
collagen fibril organization	1.00E-09
fibrillar collagen	2.60E-09
Enrichment score 9.25	
blood vessel development	5.70E-14
vasculature development	9.20E-14
angiogenesis	9.60E-10
blood vessel morphogenesis	1.70E-09
Enrichment score 9.08	
skeletal system development	7.20E-19
cartilage development	9.50E-13
bone development	3.50E-07
ossification	1.30E-06
osteoblast differentiation	1.30E-03

Enrichment Score: 5.01	
mesenchymal cell differentiation	3.10E-08
mesenchyme development	3.70E-08
mesenchymal cell development	7.80E-06
neural crest cell development	3.40E-04
neural crest cell differentiation	3.40E-04
neural crest cell migration	2.30E-02
Enrichment Score: 4.77	
TGF-beta receptor/activin receptor, type I/II	9.80E-13
TGF-beta signaling pathway	1.40E-12
growth factor receptor	9.40E-10

Table 4-1: Genes expressed in $Lin^{NEG}PDGFR\alpha\beta^{POS}CD105^{POS}$ and 105^{NEG} populations as compared to all hematopoietic cells by microarray and gene ontology analysis

GO Term	Count	p-value	Enrichment Score
Signal	493	2.70E-29	15.07
Secreted	226	7.40E-11	15.07
Extracellular matrix	86	4.30E-16	13.66
Cell Adhesion	108	4.10E-11	9.68
Skeletal System Development	74	3.00E-14	8.82
Blood Vessel Development	62	1.20E-11	8.81
Mesenchymal Cell Development	12	6.10E-03	2.88
Positive Regulation of Mesenchymal Cell Proliferation	9	9.30E-04	2.83
Skeletal System Morphogenesis	32	4.00E-06	2.73
PDGFR Signaling Pathway	8	6.00E-03	2.69
Collagen	9	5.40E-04	2.94
Vascular Endothelial Growth Factor Receptor Signaling Pathway	8	1.90E-04	2.07
Alkaline Phosphatase	10	10 7.9E-4	1.63
Growth Factor	26	1.50E-03	1.59
Chemokine Signaling	29	2.00E-02	1.31
Cytokine Signaling	27	3.70E-02	1.31

Table 4-2: Gene Ontology functional annotation of over-represented gene list in stromal cells as compared to hematopoietic cells by DAVID

Additionally, PDGFRα and β was highly expressed within the stromal cell fraction consistent with the immunophenotype used for their isolation and 8 genes were over-represented in the PDGFR signaling pathway. Other genes over-represented at the RNA level and validated at the protein level with monoclonal antibodies by FACS include VCAM1 and CD51 (Integrin αv) (Figure 4-11 A&B).

We then compared the gene expression profiles between the $CD105^{POS}$ and $CD105^{NEG}$ populations and looked for genes that differed by greater than 2 fold in either group with a p-value<0.01. This approach generated a relatively short list of genes that began to delineate potential different biological roles for each population in vivo. Of interest, gene ontology analysis of genes over-represented in the $CD105^{POS}$ population suggests this population is more closely involved with blood vessel development and vasculature stability and would be consistent with at least a proportion of the cells with this phenotype exhibiting a perivascular location (Table 4-3 & 4-4). This transcriptome analysis is also consistent the observations from the immunocytochemistry of sorted $Lin^{NEG}PDGFR\alpha/\beta^{POS}$ cells and the FACS analysis of both transgenic mouse lines suggesting that a fraction of the $CD105^{POS}$ cells express markers of more mature pericyte/mural cells (Figure 4-6). Of additional interest is the high level of expression of TGFβ receptor type II, which has been shown to form a complex with endoglin (CD105) in order to bind TGFβ 1 and act as a proliferation induced signal [127]. This may potentially also be a mechanism to augment TGFβ availability and its reported negative effects on endothelial cell proliferation.

A

Gene Symbol	$CD105^{POS}$ Ave. Signal	$CD105^{NEG}$ Ave. Signal
PDGFRα	1309.382	1397.341
PDGFRβ	137.6992	223.906
ENG (CD105)	79.7	5.4
Itgav (CD51)	462.3174	537.5847
Vcam1 (CD106)	6006.485	3614.295

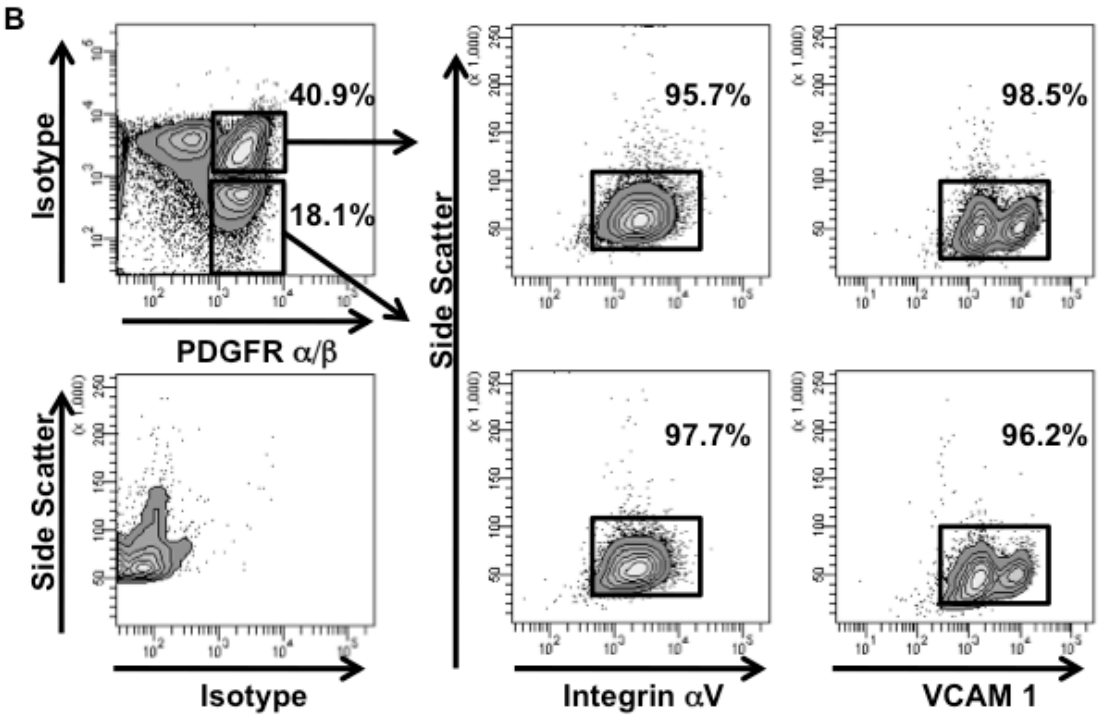

Figure 4-11: Microarray validation at the protein level with monoclonal antibodies. *(A) Gene list and average signal detection of RNA for cell surface markers identified by microarray analysis. (B) Validation of RNA targets at the protein level by flow cytometric analysis with monoclonal antibodies.*

The $CD105^{NEG}$ population, however, was enriched for a set of genes involved in skeletal development and bone mineralization. Some of the genes over-represented in the $CD105^{NEG}$ population include markers of immature osteogenic cells such Col1a1, osteonectin (SPARC), alkaline phosphatase 2, as well as markers of more mature osteoblasts including bone sialoprotein (IBSP), osteocalcin (BGLAP) and osteopontin (SPP1). Additionally, the $CD105^{NEG}$ population is enriched in cartilage related genes such Col2a1, cartilage oligomeric matrix protein (COMP) and chondrocadherin (CHAD) [128 & 129]. These noted differences in transcriptional profile together with our data demonstrating decreased proliferation in vitro, decreased bone forming potency in vivo and the lack of secondary CFU-F generating potential, all point to the $CD105^{NEG}$ population as being enriched in progenitor cells more committed to the osteogenic and chondrogenic lineages. As well, the higher expression of osteoblast specific genes for extracellular molecules suggest that this population is likely located adjacent to the endosteal region and trabecular bone regions within the marrow cavity providing cells and ECM proteins for the maintenance of general bone tissue turnover (Table 4-3 & 4-5).

	GO Term	P Value
$CD105^{POS}$ Population	Angiogenesis	1.30E-02
	blood vessel morphogenesis	2.80E-02
	vasodilation	3.50E-02
	cell adhesion	3.60E-02
	biological adhesion	3.60E-02
	blood vessel development	4.10E-02
	vasculature development	4.30E-02
	regulation of microtubule	4.70E-02
	regulation of tube size	6.20E-02
	regulation of blood vessel size	6.20E-02
	vascular process in circulatory system	6.40E-02
$CD105^{NEG}$ Population	biomineralization	3.30E-08
	biomineral formation	5 4.5E-7
	Bone matrix, Gla protein	1.50E-05
	osteocalcin	4.40E-04
	regulation of biomineral formation	3.80E-04
	regulation of ossification	4.20E-03
	ossification	9.40E-04
	Regulators of Bone Mineralization	1.50E-04
	bone development	1.30E-03
	skeletal system development	1.70E-03
	Integrin signalling pathway	1.70E-02

Table 4-3: Gene Ontology of genes enriched within $CD105^{POS}$ or $CD105^{NEG}$ populations.

Symbol	Gene Name	Genband ID	p value	Fold Change
ANGPTL1	Angiopoietin-like 1	NM_028333.2	1.81623E-05	2.958333333
DCN	Decorin	NM_007833.1	0.00604199	2.233201581
ENG	Endoglin (CD105)	NM_007932.1	4.84317E-09	9.784090909
SORT1	Sortilin 1	NM_019972.2	0.007979028	2.016632017
LRP5	Low density lipoprotein receptor protein 5	NM_008513.1	2.30866E-05	3.607929515
MEOX1	Mesenchyme hemeobox 1	NM_010791.3	0.002107609	2.215189873
GPX1	Glutathione peroxidase 1	NM_008160.5	6.90256E-06	2.711608338
CD248	Endosialin	NM_054042.2	8.87381E-05	8.819672131
THY1	Thymus cell antigen 1, theta	NM_009382.3	0.003093214	18.77852349
SMO	Smoothened homolog	NM_176996.3	0.000100612	2.486803519
IGSF10	Immunoglobulin superfamily, member 10	XM_913941.2	4.62296E-07	2.1046875
FBLN1	Fibulin 1	NM_010180.1	3.01266E-07	2.57518797
DLK1	Delta-like 1 homolog	NM_010052.4	0.049367371	6.642857143
TGFBRII	Transforming growth factor, beta receptor II	NM_009371.2	0.007696796	2.461538462
LAMA2	Laminin, alpha 2	NM_008481.2	0.001017185	5.918032787

Table 4-4: Lists of genes over-represented in the CD105^{POS} population.

Symbol	Gene Name	Genband ID	p value	Fold Change
IBSP	Integrin binding sialoprotein	NM_008318.1	3.07659E-05	2.67
BGLAP1	Bone gamma carboxyglutamate protein 1	NM_007541.2	0.000176856	5.67
BGLAP2	Bone gamma-carboxyglutamate protein 2	NM_001032298.2	0.000891292	6.55
COL1A1	Collagen Type I alpha	NM_007742.2	1.3889E-12	2.83
COL2A1	Collagen Type II alpha	NM_031163.2	0.000281482	5.22
GHR	Growth Hormone receptor	AK053579	5.8483E-05	2.38
FOXC1	Forkhead box C1	NM_008592.2	1.26119E-05	2.69
ACD	Adrenocortical dysplasia	NM_001012638.1	2.80899E-05	2.03
COMP	Cartilage oligomeric matrix protein	NM_016685.1	1.24222E-20	14.13
AKP2	Alkaline phosphatase 2	NM_007431.1	9.41673E-06	2.28
CHAD	Chondroadherin	NM_007689.4	0.005079723	18.05
SPARC	Secreted acidic cysteine rich glycoprotein	NM_009242.3	0.000236805	2.28
CFD	Complement factor D (adipsin)	NM_013459.1	0.00465436	3.42
ITGA10	Integrin, alpha 10	NM_001081053.1	0.002085691	2.31
SPP1	Secreted phosphoprotein 1	NM_009263.1	0.002306057	2.71
GNAQ	Guanine nucleotide binding protein, alpha q	AK085933	1.1452E-05	2.24

Table 4-5: Lists of genes over-represented in the CD105^{NEG} population.

4-4: SUMMARY

These studies describe the identification of two phenotypically distinct clonogenic stromal cell populations, based on the cell surface immuno-phenotype of $Lin^{NEG}PDGFR\alpha/\beta^{POS}CD105^{POS}$ and $Lin^{NEG}PDGFR\alpha/\beta^{POS}CD105^{POS}$. Interestingly, both populations contribute independently to CFU-F and stromal cell cultures in whole bone marrow samples. However, following serial passaging WBM adherent cultures eventually become homogeneous for CD105 expression. However, when each subpopulation is isolated by FACS and cultured separately, no interconversion between the two phenotypes in vitro is observed. Studies designed to rationalize the discrepancy between these two observations demonstrated that the $CD105^{POS}$ population as a whole exhibits a greater proliferative ability and thus out-competes the $CD105^{NEG}$ cells. Additionally, it has been previously reported that endoglin (CD105) is essential for proliferating endothelial cells. CD105 functions as a TGF-β co-receptor by forming a complex with TGF-β receptors type I, II and III. This complex binds TGF-β1 and abrogates the growth inhibitory effects of TGF-β1 [127].

Both populations contain stromal stem/progenitor elements that demonstrate tri-lineage differentiation capacity (osteogenic, adipogenic and chondrogenic) in vitro and in vivo as shown by the formation of histologically proven bone, BM adipocytes and hematopoiesis-supportive stroma. Interestingly, within the $Lin^{NEG}PDGFR\alpha/\beta^{POS}CD105^{POS}$ fraction, we identified a subpopulation, which co-expresses several markers of mature pericyte/mural cells and is enriched in genes related to blood vessel development and structure suggesting a perivascular nature

and function in situ. In contrast, transcriptome analysis of the $CD105^{NEG}$ population revealed a gene expression profile consistent with cells more committed to the osteo-chondro lineages suggesting this population represents a source of more immediate progenitors in vivo**.**

Together, these data suggest the identification of a stromal stem/progenitor cell hierarchy previously unrecognized within adult mouse BM. Based on these data, we propose a speculative model for a stromal stem/progenitor cell hierarchy in vivo within adult murine BM (Figure 4-12). Although we are not at this time able to conclusively prove the validity of this model, our functional assays and transcriptional profiling nevertheless suggest that these two populations are enriched in progenitor cells with over-lapping and distinct functions in vivo. However, because only a rare percentage of the $CD105^{POS}$ cells express either NG2 (4.2%) or αSMA (7.1%), this suggests that the majority of $CD105^{POS}$ cells are not mature perictyes, which raises an interesting question. Could the $CD105^{POS}$ population contain a stromal cell hierarchy with a primitive stromal stem cell "MSC" population residing within the $CD105^{POS}$ fraction, which gives rise to additional subpopulations of cells expressing CD105 and/or lacking CD105 expression? If so, perhaps a greater biological difference exist between the $CD105^{POS}$ and $CD105^{NEG}$ stromal cell fractions in vivo that we are unable to determine with the current protocols.

One potential way to prove the existence of this proposed hierarchy would be to utilize candidate genes identified in our microarray analysis as a means to identify those genes with tightly restricted patterns of expression in either the $CD105^{POS}$ or $CD105^{NEG}$ populations and to utilize the promoters for these genes in lineage tracing

studies to follow the fate of each population under homeostasis and in injury models of bone tissue. These types of studies would also prove useful in identifying the original identity and localization in situ of the cells so often identified in vitro as CFU-F and MSC.

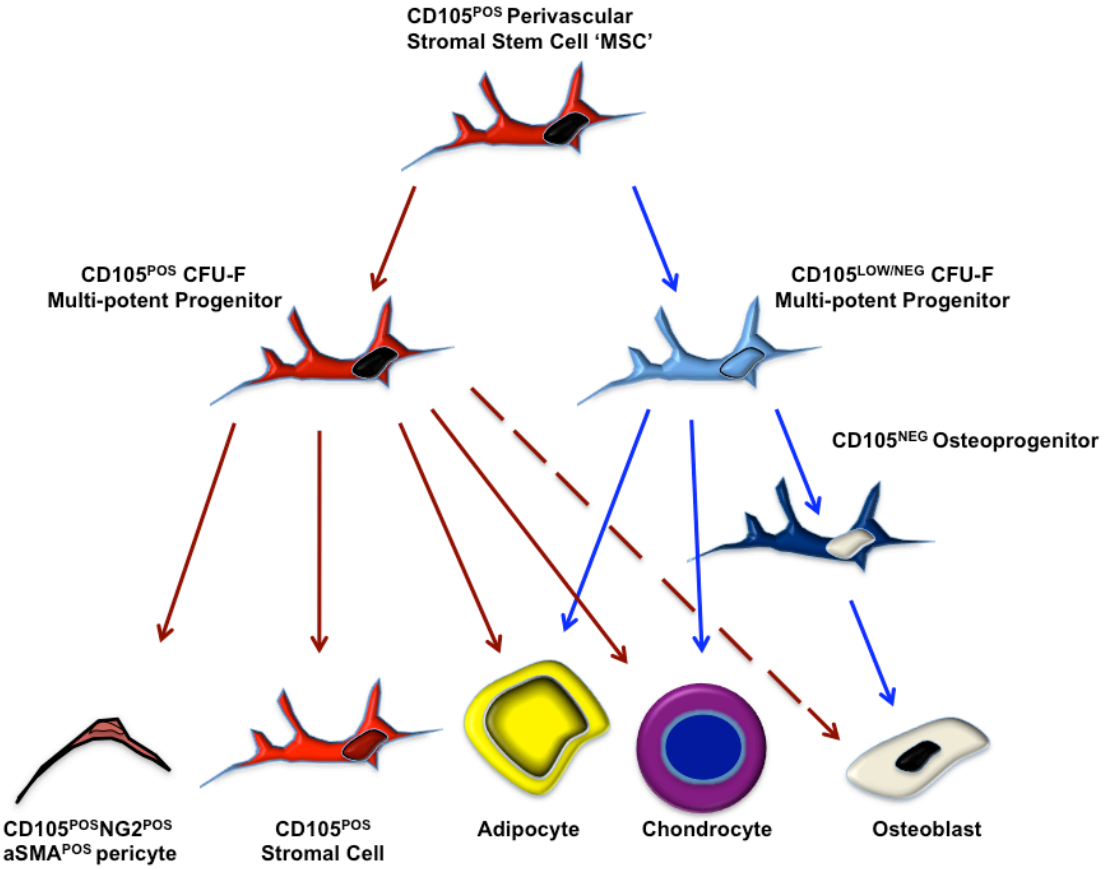

Figure 4-12: A speculative model for a stromal cell hierarchy. *A rare subpopulation within the CD105 fraction gives rise to CD105^{POS} and CD105^{NEG} multi-potent clonogenic progenitors, which generate CFU-F and adherent marrow cultures. In vivo, the CD105^{NEG} population is located a further distance away from the vasculature along the endosteum and provides committed osteoprogenitors for the maintenance of bone specific ECM components. The CD105^{POS} progenitors primarily give rise to the reticular stromal network, adipocytes and mature pericytes.*

CHAPTER 5:

FUNCTIONAL ASSESSMENT OF AN IN VITRO MODEL OF THE HEMATOPOIEITC MICROENVIRONMENT

5-1: PREFACE

In Chapter 5, I evaluate the ability of each primary BM stromal subpopulation, described and characterized in the previous chapter, to recapitulate the functional properties of the hematopoietic microenvironment in vitro by determining their capacity, using co-culture assays, to maintain and/or expand long-term repopulating mouse HSCs. For these studies, a CD45.1/CD45.2 congenic transplant model was utilized to investigate the potential of ex vivo co-cultured mouse HSCs to provide long-term multi-lineage blood repopulation in lethally irradiated host. I began these studies by first, successfully employing the FACS-based methodology described by Kiel, et al. [20] to isolate HSCs from adult mouse bone marrow and demonstrated their potency in the F1 chimeric transplant model used for these studies. By using this well-validated transplant model along with rigorous long-term primary and secondary blood reconstitution assays, a quantitative assessment was conducted to determine the capacity of different stromal cell subpopulations to support the maintenance and/or numerical expansion of competitive long-term repopulating HSCs down to the single cell level.

5-2: INTRODUCTION

Adult stem cells are responsible for the overall tissue demands of the organism both during homeostasis and during time of stress and this is particularly true for highly regenerative tissues such as the intestine, skin and bone marrow [130, 131]. Within the bone marrow of adult mammals, HSCs act through a cellular hierarchy and give rise to all of the mature cells within the hematopoietic system. HSCs are functionally characterized by their ability to undergo extensive self-renewal in vivo for the life of an organism and provide serial long-term reconstitution of the entire hematopoietic system when transplanted into lethally irradiated mice providing evidence of extensive differentiation potential [3, 15]. On a daily basis, the hematopoietic system must be prepared to meet the demands of the body included during normal homeostasis as well as disease and/or stress induced by infection and acute blood loss. Consequently, the hematopoietic system is poised to rapidly respond to these external demands and therefore is tightly controlled by the bone marrow microenvironment.

The balance between self-renewal (generation of self) and differentiation (production of daughter cells with progressively less self-renewal potential and more mature in function) [41] is a highly coordinated and regulated process, governed by both intrinsic (cell-autonomous) and extrinsic (non-autonomous) mechanisms [7] and a detailed understanding of these mechanisms stands at the forefront of

considerable interest in HSC biology for the purposes of regenerative medicine and gene therapy.

The advances made by identifying and isolating nearly homogeneous populations of HSCs has yielded significant amounts of information regarding cell intrinsic regulatory mechanisms controlling stem cell behavior. However because of many technical challenges in dealing with bone-bone marrow tissue, the role of regulatory molecules governing cell extrinsic behavior has been much slower to progress and as a consequence there currently remains a lack of complete understanding of this process. The persistence of HSCs throughout adult life is contingent upon the permissive microenvironment in which HSCs reside in vivo, originally proposed in the niche hypothesis [16]. In the adult mouse, the bone marrow is the primary site of hematopoiesis during homeostasis and several reports have documented the role of the bone marrow microenvironment in regulating HSC behavior as described in Chapter 2 of this dissertation. From these studies, several key molecules have been discovered which play essential roles in governing HSCs under normal growth conditions. Additionally, there is convincing evidence that the hematopoietic microenvironment may also contribute to abnormal conditions such as aplastic anemia and cancer and these observations have further driven interest in the microenvironment for the purpose of therapeutic targeting under disease conditions [132].

One approach taken by many investigators to identify extrinsic regulators of HSCs has been through the use of mouse genetics. Several mouse models have been generated and have led to the identification of many genetically necessary cell-

extrinsic factors for maintaining HSCs in vivo [15, 44]. Such molecules include SCF, Angiopoietin 1, CXCL12 (SCF-1), osteopontin, and Ca^{2+} ion. However, while the application of mouse genetics as applied to gain- and loss-of-function studies has resulted in significant discoveries of these genetically determined factors, there still remains a paucity of information and limitations as applied to this approach in identifying the specific cells types responsible for generating these regulatory molecules in vivo. This disparity can be partially attributed to several distinguishing complications in working with bone marrow tissue. To name a few, there is currently a lack of cell surface markers suitable for identifying subpopulations of candidate niche cells in vivo, few cell specific promoters which could potentially be used to drive Cre-recombinase in deleting specific molecules in specific subpopulations of stromal cells and the outstanding difficulty of imaging live animals through thick cortical bone tissue.

A second approach taken by many investigators has been to apply the long-term bone marrow culture system first reported by Dexter and colleagues [60, 61] as a means to interrogate the heterogeneous microenvironment in vitro. As reviewed in the previous chapters, the bone marrow microenvironment is comprised of a diverse population of hematopoietic macrophage and non-hematopoietic stromal cells. Together these cell types comprise a complex three-dimensional scaffold upon which cells of hematopoietic origin migrate and receive various cues governing their behavior. Interestingly, long-term marrow cultures are largely comprised of adherent cells, which mimic the hematopoietic microenvironment in vivo and this culture system has yielded significant discoveries regarding extracellular regulatory

molecules in addition to the ones identified through a genetic based approach. However, although diverse in cell types, this current culture system does not allow a prospective analysis of the exact cells responsible for forming these adherent layers with HSC supporting behavior. Lastly, as demonstrated by Dexter and others, this culture system primarily supports the proliferation of hematopoietic progenitors with a progressive loss in HSC function [61].

Some of the hematopoietic cytokines which have been elucidated by these combined approaches and well-studied in vitro include Il-3, Il-6, SCF, TPO, Flt3-L, Il-11 [133]. Resulting from these discoveries, many labs have attempted to study the role of these factors, alone or in various combinations, by in vitro based suspension culture approaches. Although some combinations have been reported to support the maintenance of HSCs [62], under these suspension culture conditions, HSC function is often rapidly lost and little ex vivo expansion of functional HSCs is observed. These studies indicate the need for additional cellular and/or molecular components more closely representative of the microenvironment in vivo. Since the initial studies conducted by Dexter and colleagues [61] demonstrating the necessary role of the adherent bone marrow stroma in maintaining primitive mouse hematopoietic progenitor cells, a great amount of interest has been placed on identifying the key cellular components within this heterogeneous layer, which provides the greatest supportive capacity.

Because long-term marrow cultures are performed in the context of a heterogeneous mixture of adherent cells, this approach does not lend itself to a prospective analysis of the cells responsible for providing either positive or negative

HSC regulatory functions. One popular method employed to overcome this limitation has been to generate cloned stromal cell lines and test their ability to support hematopoietic stem and progenitor cells in vitro. And while some success has been garnered using cell lines derived from fetal tissue, such as the fetal liver line AFT024, little evidence exists of cells with a similar capacity within the adult BM [63]. This raises the question of whether or not the correct cells responsible for supporting HSCs in vitro have ever been isolated.

Additional complications arising from these studies include the use of high concentrations of horse serum and a number of the reported studies use heterogeneous populations of hematopoietc cells enriched for stem/progenitor cells, but have not been demonstrated at a signle cell resolution to determine the proportion of cells that contain true LT-HSC repopulating ability. Taken together, it is not clear what combined negative effects these external factors may be contributing to the attrition of functional HSCs and the observed lack of HSC expansion. A key question still needing to be addressed is the nature and identity of the adult BM stromal cell(s) responsible for supporting the maintenance or expansion of HSCs both in vivo and in vitro. However, there has been an emergence of experimental evidence beginning to point to the stromal stem/progenitor cell as a key cellular constituent of the vascular niche. Interestingly, several lines of emerging data are resulting in a [134] unified notion that two stem cells not only occupy the same microenvironment, but also suggest that one stem/progenitor population, the MSC, is directly involved in the extrinsic regulation of the other, the HSC. And although, previous studies indicate the existence of two anatomically distinct niches [15, 44],

what most of these models leave out are the stromal cell reticulum, which spans the entire width and length of long bones. It appears for our own studies and those of others that non-hematopoietic stromal elements may provide the critical link in defining a unified HSC niche.

In the following chapter, we provide direct and indirect evidence that the dual properties of stromal stem/progenitor cells (MSC; osteoprogenitors) in generating bone and bone marrow tissue also coincides with their role as cellular constituents of the bone marrow microenvironmental 'niche'. Having previously identified distinct subpopulations of BMSCs each with stromal stem/progenitor activity in vivo, we also demonstrate their ability to support the maintenance of HSCs in vitro by co-culture assays and in vivo transplantation studies. Furthermore, data from our transcriptome analysis of freshly isolated BMSC populations and analysis of a specific genetic mouse model suggests a direct role of these populations in establishing and maintaining the hematopoietic stem cell niche in vivo by governing HSC behavior. We therefore, hypothesized that the cellular constituents of the vascular niche in vivo would provide a discovery platform from which to identify cells with HSC maintenance capabilities in vitro and would additionally provide an experimental tool from which to identify novel HSC regulatory molecules in future studies.

5-3: RESULTS

DISTINCT POPULATIONS OF BMSCs EXPRESS HIGH LEVELS HSC REGULATORY MOLECULES IN VIVO

Having identified perivascular cells that are $Lin^{NEG}PDGFR\alpha/\beta^{POS}CD105^{POS}$ and direct osteo-progenitor cells ($CD105^{NEG}$) each with the capacity to transfer the hematopoietic microenvironment in vivo using an ectopic transplantation model, we postulated that at least a portion of the cells within these two populations represent the cellular elements of the vascular/perivascular HSC niche. This notion was further supported by our transcriptome analysis of prospectively isolated $Lin^{NEG}PDGFR\alpha/\beta^{POS}CD105^{POS}$ and $CD105^{NEG}$ populations. Based on these microarray studies, both populations were shown to express significant levels of a number secreted molecules known genetically to be involved in regulating HSCs in vivo, consistent with their proposed role as niche cells (Table 5-1). Additionally, both populations have high levels of transcripts for extracellular matrix components and adhesion molecules (Table 4-1, Chapter 4) that have also been implied as having established roles in regulating hematopoiesis within the context of the hematopoietic microenvironment [131, 135].

Furthermore in collaboration with Dr. Sean Morrison's lab, we have demonstrated that both stromal cell populations, $Lin^{NEG}PDGFR\alpha/\beta^{POS}CD105^{POS}$ and $CD105^{NEG}$, represent the major cell source for stem cell factor (SCF) in vivo and their selective depletion leads to a 50% reduction in functional HSCs in the adult BM

[136, and personal communication]. Taken together, these data demonstrate a role for the $Lin^{NEG}PDGFR\alpha/\beta^{POS}CD105^{POS}$ and $CD105^{NEG}$ populations in establishing and maintaining the vascular/perivascular niche in vivo, unifying the dual role of the stromal stem/progenitor population as both osteoprogenitors and HSC niche constituents. Based on these observations, we reasoned that both populations would recapitulate, in vitro, the supportive microenvironment function of maintaining HSCs and provide a platform from which to identify additional HSC regulatory molecules that would permit the ex vivo expansion of functional HSCs.

Gene Symbol	Average Signal	
	$CD105^{POS}$	$CD105^{NEG}$
Angpt1	694.5193	564.8462
Angpt2	492.4574	575.6781
Angpt4	123.3827	105.1272
Angptl1	85.18382	28.81895
Angptl2	505.7258	454.7759
Angptl4	732.7595	762.4637
Cxcl12	11180.25	13085.08
Il7	1035.723	974.8479
Stem Cell Factor	1705.002	1429.119
Vegfa	600.0796	820.4082
Vegfb	86.10397	152.9635
Vegfc	1279.06	1031.092

Table 5-1: Hematopoietic stem cell regulatory molecules expressed in vivo by $Lin^{NEG}PDGFR\alpha\beta^{POS}CD105^{POS}$ and $Lin^{NEG}PDGFR\alpha\beta^{POS}CD105^{NEG}$ populations.

ESTABLISHING THE TRANSPLANT MODEL

HSCs have been isolated to near homogeneity using a combination of cell surface markers referred to as the LSKSLAM immunophenotype (LSKCD48$^-$ CD150$^+$), based on the lack of expression of mature hematopoietic markers (Lin$^-$), expression of Sca1 and c-kit (SK), lack of expression of CD48 (CD48$^-$) and homogeneous expression of CD150 (CD150$^+$) [20]. Although rigorously demonstrated by other labs, our lab had not previously used this specific immunophenotype to isolate HSCs so a formal limit dilution analysis of their repopulating ability was still lacking. Additionally, we used CD45.2 (C57Bl/6)/ CD45.1 (B6.SJL/Ptprc^aPep^3/BoyJ) F1 chimeric mice as a recipient source for these transplantation studies so it was essential to determine the repopulating ability of SLAM HSCs in these mice and to determine the reproducibility and reliability of detection of low numbers of input competitor cells, test cells and support cells for the analysis of the co-culture studies. Furthermore, this analysis would provide the foundation for determining the number of input cells to be used in our co-culture system.

To generate F1 chimeric mice, we crossed C57Bl/6 mice, with the CD45.2 allele (Ly5.2) expressed in all hematopoietic cells, to B6.SJL/Ptprc^aPep^3/BoyJ mice which express the CD45.1 allele (Ly5.1) in all hematopoietic cells (Figure 5-1). The resulting F1 progeny contain both CD45.1 and CD45.2 alleles in all hematopoietic cells representing a double positive population by flow cytometric analysis with a combination of CD45.2 and CD45.1 monoclonal antibodies

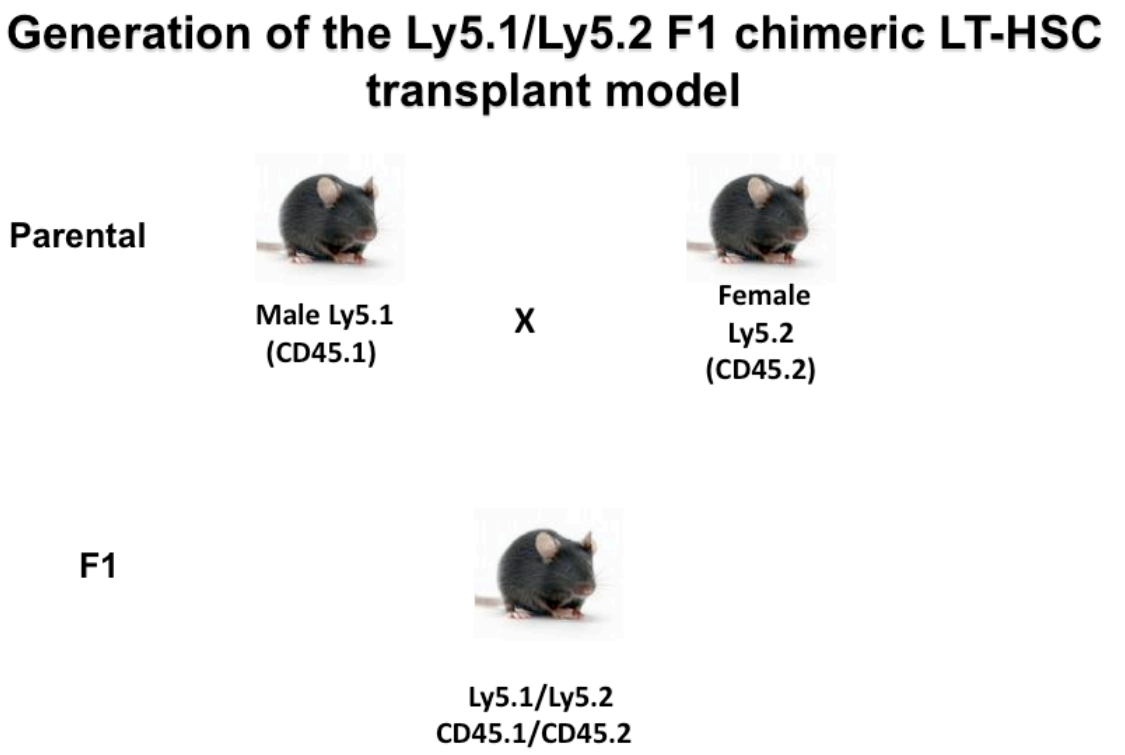

Figure 5-1: Generation of LT-HSC reconstituting transplantation model. *Adult male CD45.2 (C57Bl/6) mice were mated to adult female CD45.1 (B6.SJL/Ptprc^aPep^3/BoyJ) mice and the resulting F1 progeny are used as recipients for all reconstituting transplantation studies.*

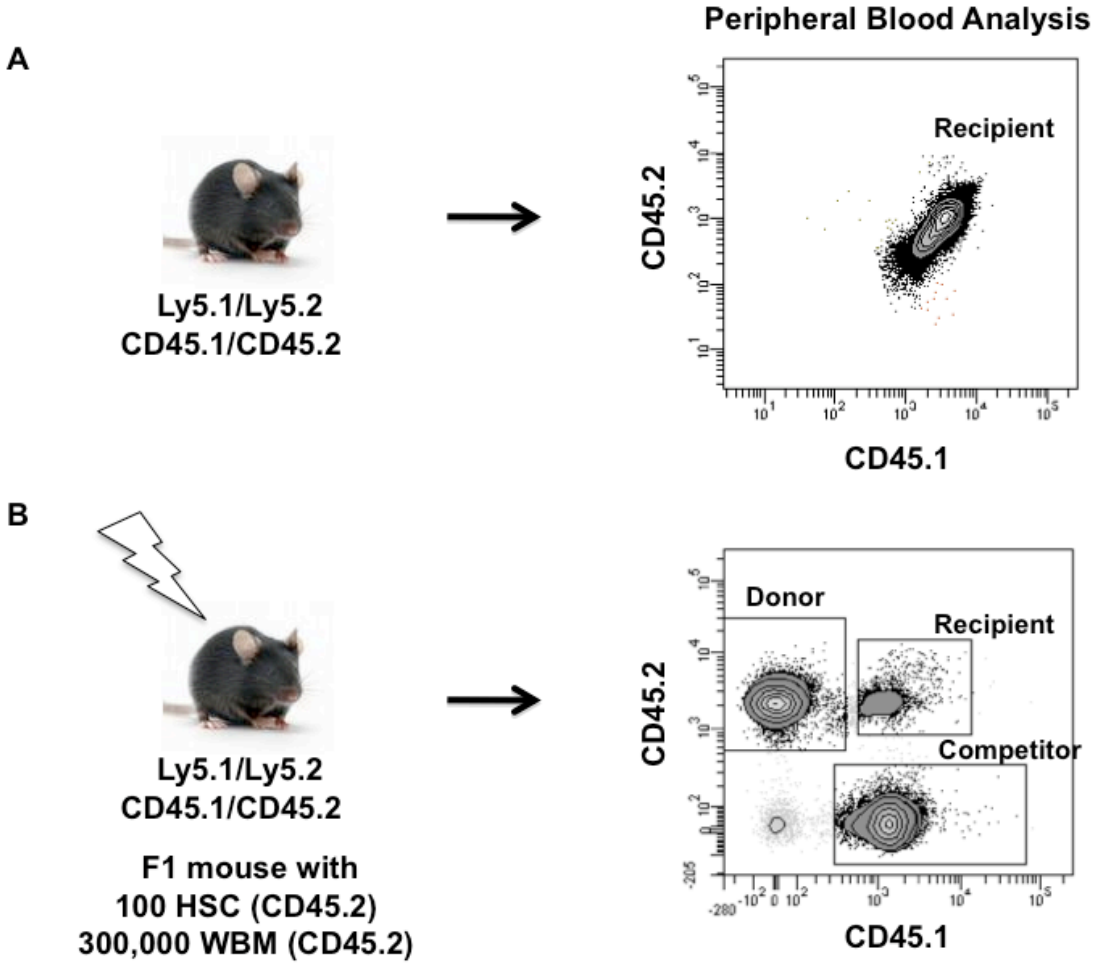

Figure 5-2: Schematic of F1 Peripheral Blood analysis in WT and following lethal irradiation and competitive transplantation. *(A) Peripheral blood analysis of control F1 chimeric mouse using CD45.1 and CD45.2 monoclonal antibodies. (B) Peripheral blood analysis of an F1 mouse under competitive repopulating assay conditions. Following lethal irradiation F1 mouse transplanted with 100 HSCs isolated from CD45.2 mice along with 300,000 whole bone marrow cells isolated from CD45.1 mice.*

(Figure 5-2 A). Additionally, this model allows for the monitoring of transplanted hematopoietic cells in a direct competitive reconstitution assay, whereby donor cells can be competed against an HSC population of know reconstituting ability and also allow the determination of reconstitution provided by the recipient (support cells) (Figure 5-2 B).

To begin these studies, SLAM HSCs (Figure 5-3) were double sorted to ensure their purity from CD45.2 mice at 8-10 weeks of age and visually confirmed microscopically in terasaki wells to contain the appropriate number(s) of input cells (Figure 3-4 A). Next, we transplanted 3, 10, 30 or 100 SLAMHSCs into lethally irradiated F1 mice, 8-12 weeks of age along with 300,000 whole bone marrow (WBM) cells isolated from CD45.1 mice at 8-10 weeks of age. Hematopoietic reconstitution was measured by determining the percentage of donor type (test) cells in the peripheral blood at 6, 12 and 20 weeks and within the bone marrow at 20 weeks.

In these experiments, mice receiving 3 SLAM HSCs demonstrated on average a 4.25% chimerism of CD45.2 donor HSCs (Figure 5-4 B) in the peripheral blood with 25% demonstrating long-term multi-lineage reconstitution. However, all mice transplanted with 10 (100%), 30 (100%) or 100 (100%) cells demonstrated multi-lineage reconstitution with 64-90% of the hematopoietic cells being donor derived out to 20 weeks post-transplant (Figure 5-4 B). Since 10 SLAM HSCs reproducibly provided significant levels of donor-derived multi-lineage reconstitution at 20 weeks post-transplant (Figure 5-5 A-C, D & E), we reasoned that 10 input

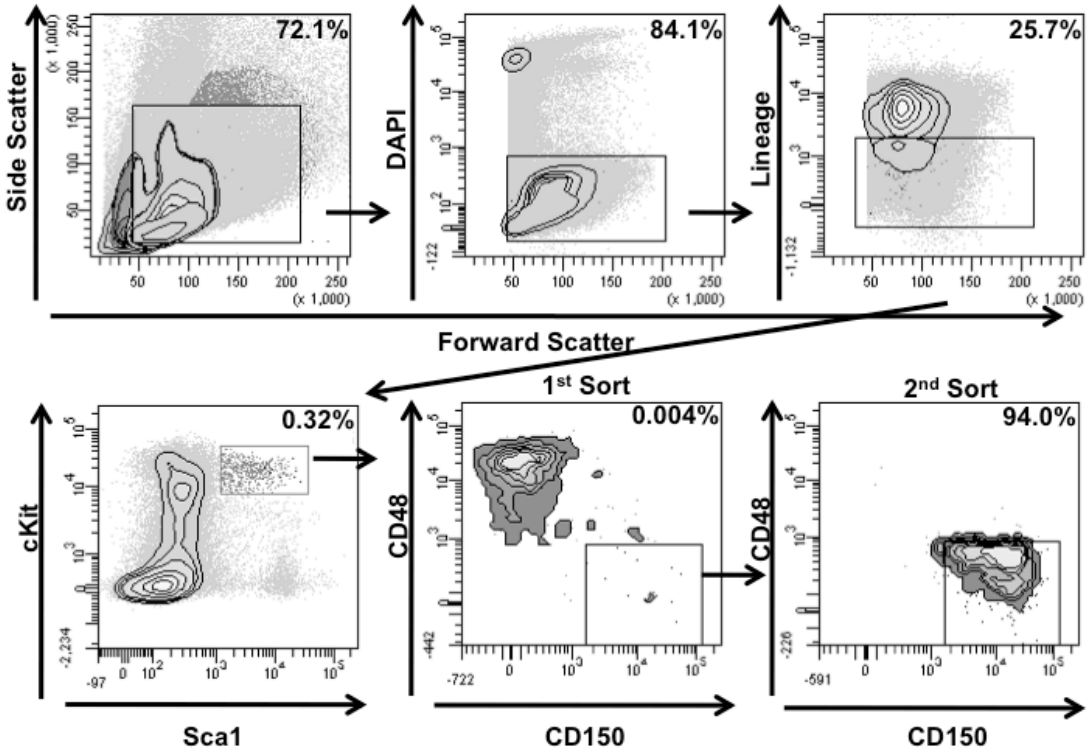

Figure 5-3:Gating strategy for the prospective isolation of SLAM HSCs. *HSC sort gates are set to first determine the appropriate scatter profile and to select for single cells by a doublet exclusion gate. Next, viable cells are gated on to remove dead cells from the analysis. All viable single cells are the subjected to a hematopoietic lineage positive gate to remove mature hematopoietic cells and a stem and progenitor gate is used to enrich for HSC by gating on all c-kit & Sca1 double positive cells. The final gates are set to enrich for a well-validated HSC population based on lack of expression for CD48 and positive expression of CD150. Finally the LSKCD48-CD150+ cells are resorted to ensure a pure population for LT-HSC transplantations.*

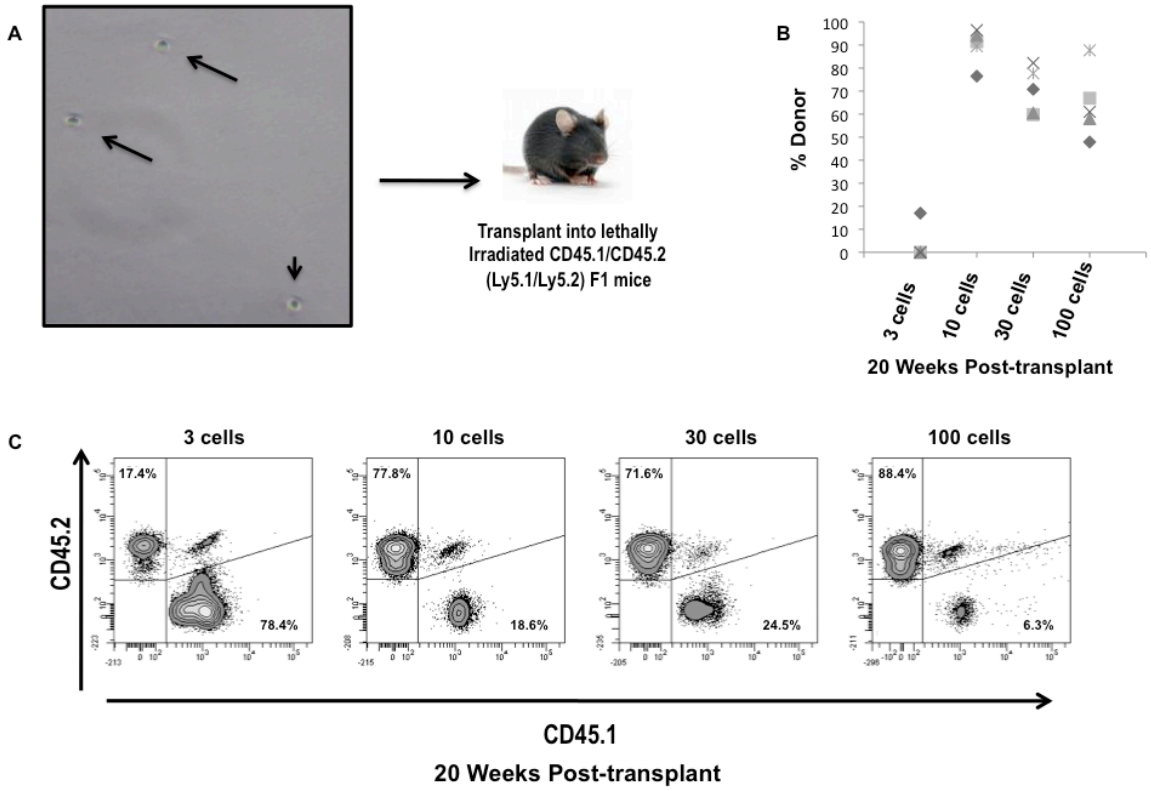

Figure 5-4: LSKSLAM cells are highly enriched for LT-HSCs. (*A) Microscopic validation and enumeration of cells for transplantation. (B) Percentage of donor derived CD45.2 cells in peripheral blood at 20 weeks post-transplantation. (C) Representative FACS plots of peripheral blood analysis at 20 weeks post-transplant demonstrating high levels of donor derived multi-lineage reconstitution (D) with 10, 30 & 100 freshly isolated HSCs at 20 weeks post-transplantation (n=5 mice per group).*

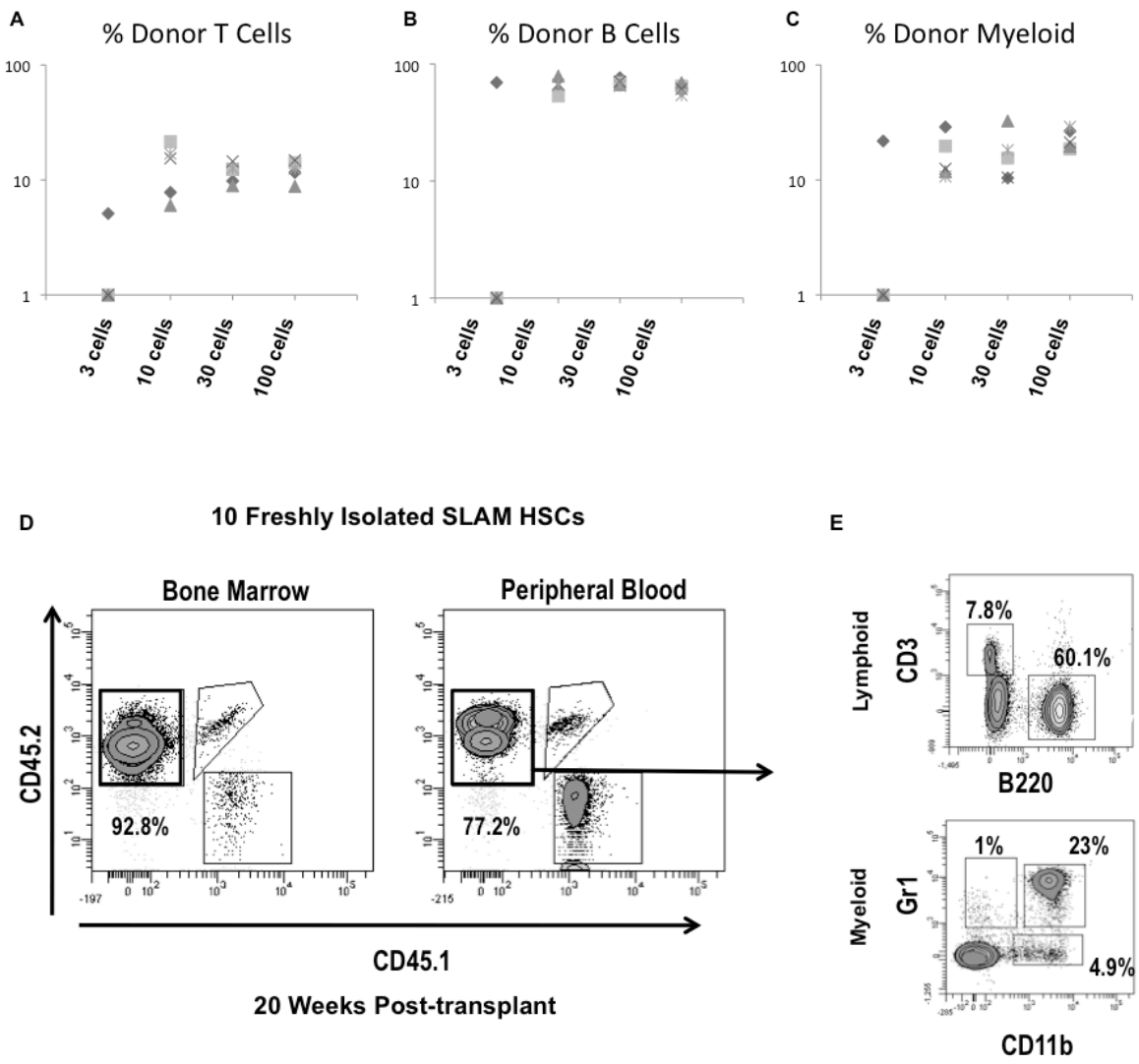

Figure 5-5: Donor derived multi-lineage blood reconstitution. *Multi-lineage blood reconstitution was evaluated by flow cytometric analysis and the percentage of donor derived T cells (A), B cells (B) and myeloid cells (C) for each mouse was plotted for the 20 week post-transplant time point. Representative FACS plots for peripheral blood and bone marrow analysis demonstrating donor derived hematopoietic cells (D) and multi-lineage reconstitution (E) from 10 freshly isolated CD45.2 HSCs.*

Cell Dose	# Mice reconstituted	% Blood reconsitution	% Donor CD45.2	% Donor T Cells	% Donor B Cells	% Donor Myeloid
3	1 of 5	20%	4.25±8.5%	1.3±3.9%	17.4±34.7%	5.45±10.9
10	5 of 5	100%	89.62±7.8%	13.5±6.5%	64.8±9.4%	16.72±7.7%
30	5 of 5	100%	70.2±10.03%	11.62±2.3%	51.6±7.1%	17.4±9.1%
100	5 of 5	100%	64.3±14.8	12.6±2.4%	61.6±5.8%	22.98±4.6%

Table 5-2: Global reconstitution of SLAM HSCs cells per input dose.

SLAM HSCs would be sufficient as the input dose for our initial series of co-culture studies.

EVALUATION OF LT-HSC SUPPORTING ACTIVITY

We next set out to compare the ability of the $CD105^{POS}$ and $CD105^{NEG}$ populations to support long-term multi-lineage reconstituting HSCs in vitro by co-culture assays. For these experiments, $Lin^{NEG}PDGFR\alpha/\beta^{POS}CD105^{POS}$ and $Lin^{NEG}PDGFR\alpha/\beta^{POS}CD105^{NEG}$ BM stromal stem/progenitor populations were isolated from F1 chimeric mice and allowed to reach confluence in 48 well plates coated with fibronectin. Approximately 5-7 days after isolation and plating in normal growth media, SLAM HSCs were double sorted from B6.SJL/Ptprc^aPep^3/BoyJ (CD45.1) mice (Figure 5-6 A) and 10 HSCs were visually counted (Figure 5-6 B) and added to each well containing a confluent layer of BM stromal stem/progenitor cells (Figure 5-6 C) in Stem Span serum free expansion media supplemented with a combination of the following cytokines each at $1/10^{th}$ the optimal concentration: IL-6 (10ng/ml), SCF, TPO and Flt3L (each at 5ng/ml). As a control, 10 HSCs were added to wells coated with fibronectin, which did not contain any stromal layers in the presence of the 0.1X concentration of cytokines (Figure 5-6 C, top panel). Previous studies in our lab had determined that at a 0.1x cytokine concentration HSCs do not proliferate and most die. Therefore, this concentration would allow us to examine the direct contribution to HSC survival and expansion provided by the stromal layers.

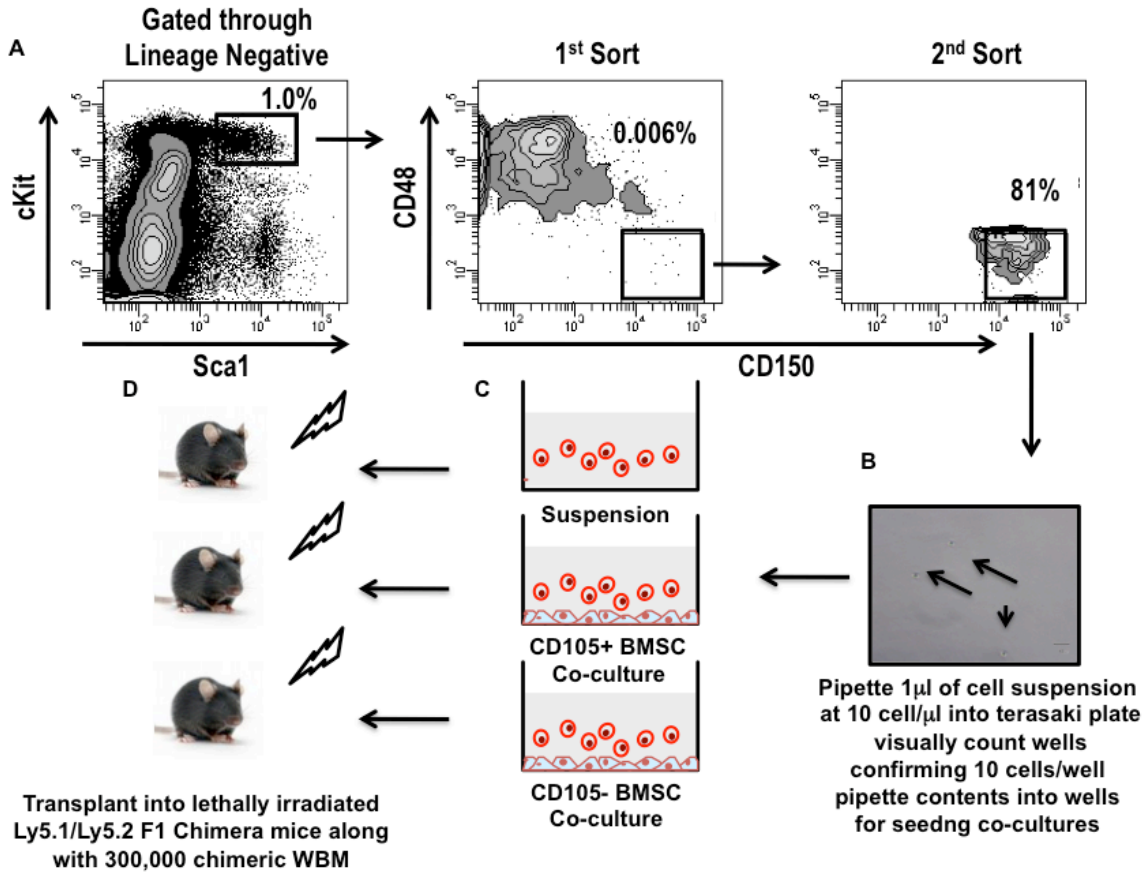

Figure 5-6: Schematic of SLAM HSC isolation and co-cultures. *(A) Representative FACS plots showing the gating strategy to double sort SLAM HSCs. (B) Microscopic image of a single terasaki well confirming an accurate count of HSCs. (C & D) Schematic drawing of co-culture conditions and images depicting the mouse model used as transplant recipients.*

The co-cultures were left undisturbed and maintained at 5%CO_2, 5%O_2 at 37°C for a total of 10 days. 10 days after the initial seeding of wells with SLAM HSCs, we observed a significant increase in hematopoiesis in the wells containing either $CD105^{POS}$ (Figure 5-7, middle panel) or $CD105^{NEG}$ (Figure 5-7, right panel) stromal layers, however we could not detect any increase in hematopoietic cells in the control stromal-free wells under these culture conditions (Figure 5-7, left panel). Following the 10 days in culture, the entire contents of each well was collected with trypsin and placed into separate tubes on ice in PBS. Additionally, 300,000 WBM cells from F1 mice were added to each co-culture cell suspension. The entire contents of each tube was then transplanted into the retro-orbital sinus of lethally irradiated 8-12 week C57Bl/6-B6.SJL/Ptprc^aPep^3/BoyJ (CD45.1/CD45.2) F1 chimeric mice.

Peripheral blood analysis from two independent experiments was evaluated for donor-derived reconstitution at 6, 12 and 16-18 weeks. Additionally, bone marrow was collected at the time of sacrifice and 1 million WBM cells were serially transplanted into lethally irradiated F1 secondary recipient mice from each experiment that contained multi-lineage reconstitution in the primary transplant recipients in order to assess in vivo self-renewal potential. In this experimental setting, all mice transplanted with the progeny of 10 HSCs from either $CD105^{POS}$ (100%) or $CD105^{NEG}$ (100%) stromal cell co-cultures demonstrated robust multi-lineage reconstitution in primary (Figure 5-8) and secondary recipients (Figure 5-9).

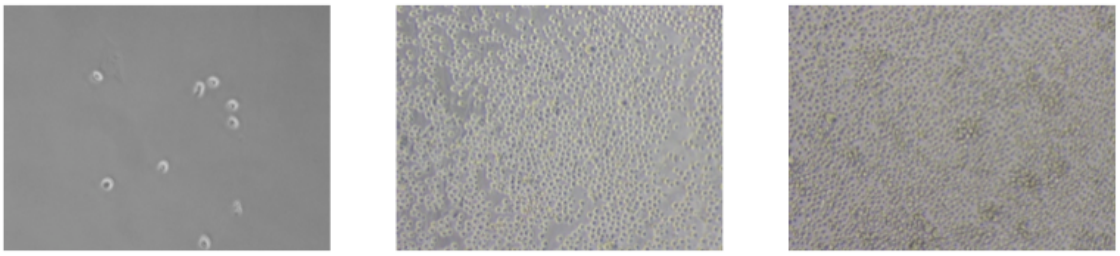

Figure 5-7: Robust hematopoiesis in adult BM stromal-HSC cocultures.

Representative images of robust hematopoietic activity from 10 input HSCs at day 10 of cocultures with CD105^{POS} and CD105^{NEG} adherent stromal layers. HSCs cultured in suspension without stromal layers do not expand and most undergo rapid attrition and cell death.

However, we could not detect any donor-derived reconstitution from suspension cultures (Figure 5-8 A&B). On average, the progeny of 10 HSCs co-cultured with $CD105^{POS}$ BMSC gave rise to 65±23.6% donor derived CD45.1 cells in the peripheral blood while the progeny of 10 HSCs co-cultured on $CD105^{NEG}$ BMSCs provided 49.3±19.5% donor derived CD45.1 cells in primary transplant recipients (Figure 5-8 A&B). Although the $CD105^{NEG}$ population demonstrated slightly lower levels of blood reconstitution, the difference was not statistically significant. Successfully reconstituted primary recipients from $CD105^{POS}$ and $CD105^{NEG}$ BMSC co-cultures were able to reconstitute secondary recipients with 100% efficiency generating, 56.5±29.4% and 40.15±24.1% donor derived CD45.1, respectively (Figure 5-9 A&B). Furthermore, transplanted HSCs derived from $CD105^{POS}$ or $CD105^{NEG}$ co-cultures (10 input HSCs) were able to out-compete the 300,000 WBM cells (approximately 18 HSCs) demonstrating that both BM stromal cell populations maintain functional HSCs ex vivo.

Figure 5-8: Maintenance of transplantable LT-HSCs is dependent on CD105^{POS} and CD105^{NEG} BMSCs. *(A) Long-term multilineage reconstitution from 10 SLAM HSCs co-cultured on CD105^{POS} and CD105^{NEG} BMSCs. (B) Representative FACS plots from peripheral blood analysis at 18 weeks pot-transplant.*

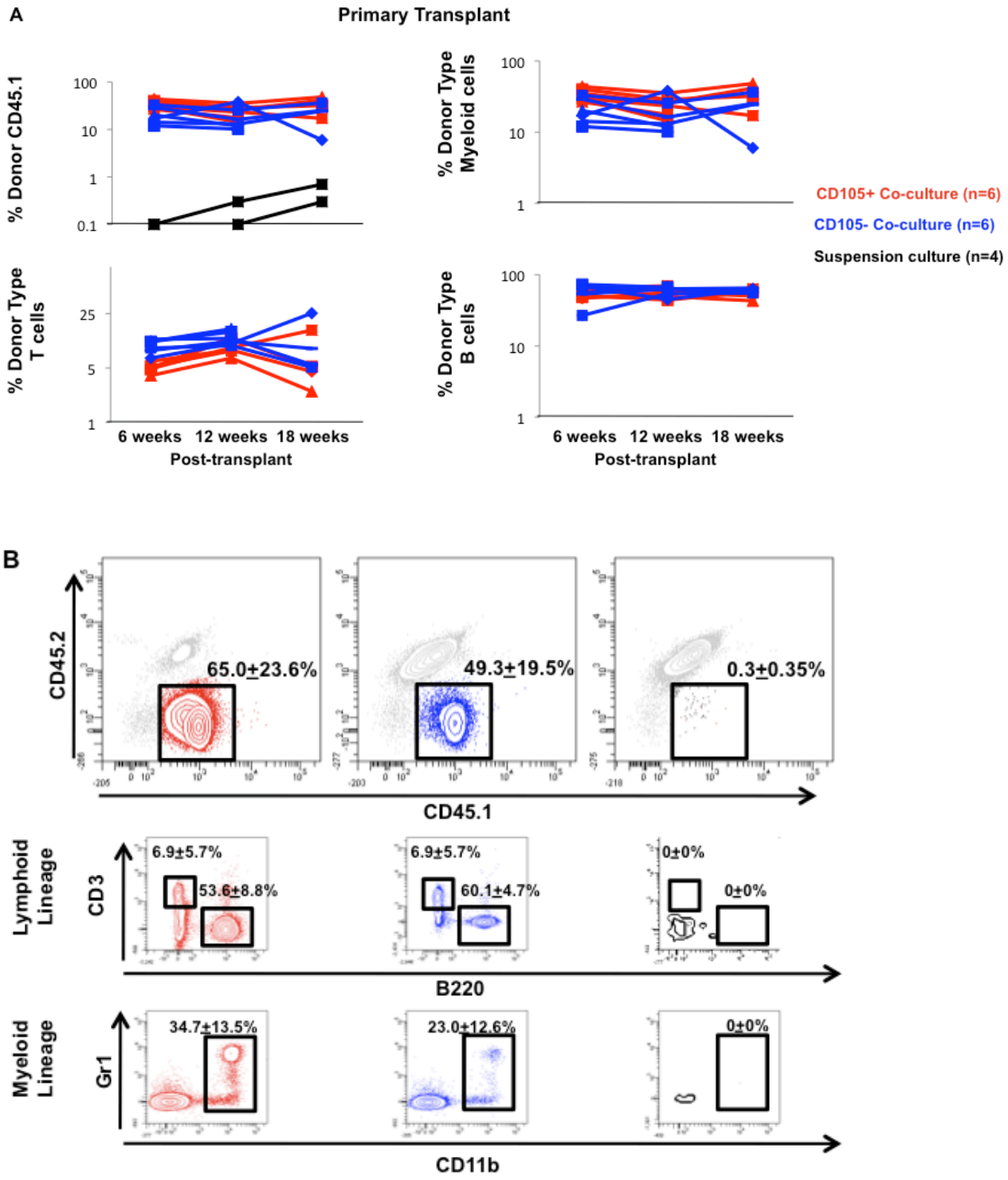
A
Primary Transplant
% Donor CD45.1
100
10
1
0.1
% Donor Type Myeloid cells
100
10
1
% Donor Type T cells
25
5
1
% Donor Type B cells
100
10
1
6 weeks 12 weeks 18 weeks
Post-transplant
6 weeks 12 weeks 18 weeks
Post-transplant
CD105+ Co-culture (n=6)
CD105- Co-culture (n=6)
Suspension culture (n=4)
B
CD45.2
65.0±23.6%
49.3±19.5%
0.3±0.35%
CD45.1
Lymphoid Lineage
CD3
6.9±5.7%
53.6±8.8%
6.9±5.7%
60.1±4.7%
0±0%
0±0%
B220
Myeloid Lineage
Gr1
34.7±13.5%
23.0±12.6%
0±0%
CD11b

Figure 5-9: SLAM HSCs co-cultured on CD105^{POS} and CD105^{NEG} BMSCs demonstrate robust ability to undergo self-renewal in vivo. *(A) Long-term multilineage reconstitution in secondary recipients provided by 10 SLAM HSCs co-cultured on CD105^{POS} and CD105^{NEG} BMSCs. (B) Representative FACS plots from peripheral blood analysis at 18 weeks pot-transplant.*

A

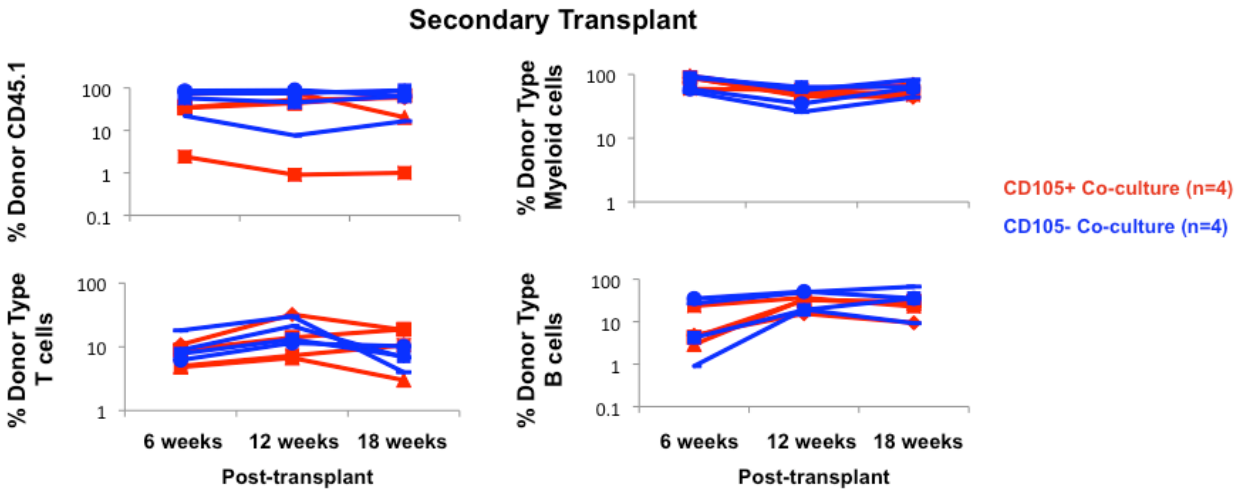
Secondary Transplant
% Donor CD45.1
% Donor Type Myeloid cells
% Donor Type T cells
% Donor Type B cells
100
10
1
0.1
6 weeks
12 weeks
18 weeks
Post-transplant
CD105+ Co-culture (n=4)
CD105- Co-culture (n=4)

B

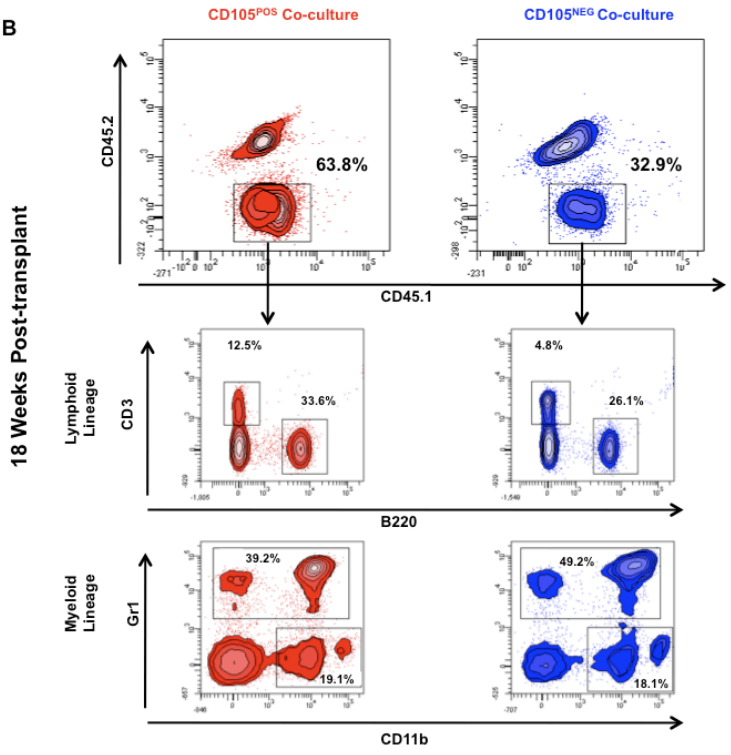
CD105POS Co-culture
CD105NEG Co-culture
18 Weeks Post-transplant
CD45.2
CD45.1
63.8%
32.9%
Lymphoid Lineage
CD3
B220
12.5%
33.6%
4.8%
26.1%
Myeloid Lineage
Gr1
CD11b
39.2%
19.1%
49.2%
18.1%

PRIMARY CD105^{POS} BMSCs SUPPORT HSC EXPANSION EX VIVO

In order to begin addressing the question of whether or not either population supported the expansion of HSCs ex vivo, we conducted a series of additional transplantation experiments using either limiting numbers of the progeny cells derived from the HSC co-cultures or by initiating the co-cultures with a ***single*** SLAM HSC. We first conducted a preliminary experiment to evaluate the potential numerical expansion of co-cultured HSCs based on a limit dilution analysis of 10 input HSCs. For this experiment, 10 freshly isolated HSCs from CD45.1 mice were placed into co-cultures for 10 days under the identical conditions detailed above and transplantation assays were based on a limiting dilution of the cultured progeny. Following the 10 day co-culture period, lethally irradiated F1 mice were transplanted with either the total progeny from 10 input B6.SJL/Ptprc^aPep^3/BoyJ (CD45.1) HSCs, 1/2 the input progeny (5 cell equivalents), 1/3 the input progeny (3 cell equivalents) or 1/10th the input progeny (1 cell equivalent). Additionally, freshly isolated SLAM HSCs were double sorted from C57BL/6 (CD45.2) mice and 10 (CD45.2) HSCs along with 300,000 WBM cells from F1 mice were added to each co-culture cell suspension dilution. Based on the design of our transplant model, we were able to track in vivo the respective multilineage differentiation potential of each population (Figure 5-2 B) and to determine the ability of cultured HSCs to compete against prospectively isolated HSCs in vivo.

In this experimental design, the product of 10 HSCs from CD105^{POS} co-cultures outcompeted the 10 freshly isolated HSCs by more than 5/1-10/1 ratios providing on average 74.4% of the total hematopoietic content as compared to 6.3%

Figure 5-10: Competitive repopulation between co-cultured HSCs and freshly isolated HSCs. (*A) FACS plots demonstrating a competitive advantage of CD105^{POS} BMSC co-cultured HSCs over freshly isolated HSCs, while CD105^{NEG} BMSC co-cultured HSCs demonstrate equal potency to freshly isolated HSC in head-to-head competitive transplant setting. (B) Total blood reconstitution from mice transplanted with various cell equivalent doses of co-cultured progeny at 6, 12 and 20 weeks post-transplant. (C) 1 SLAM HSC equivalent from CD105^{POS} BMSC co-culture demonstrates long-term multi-lineage blood reconstitution.*

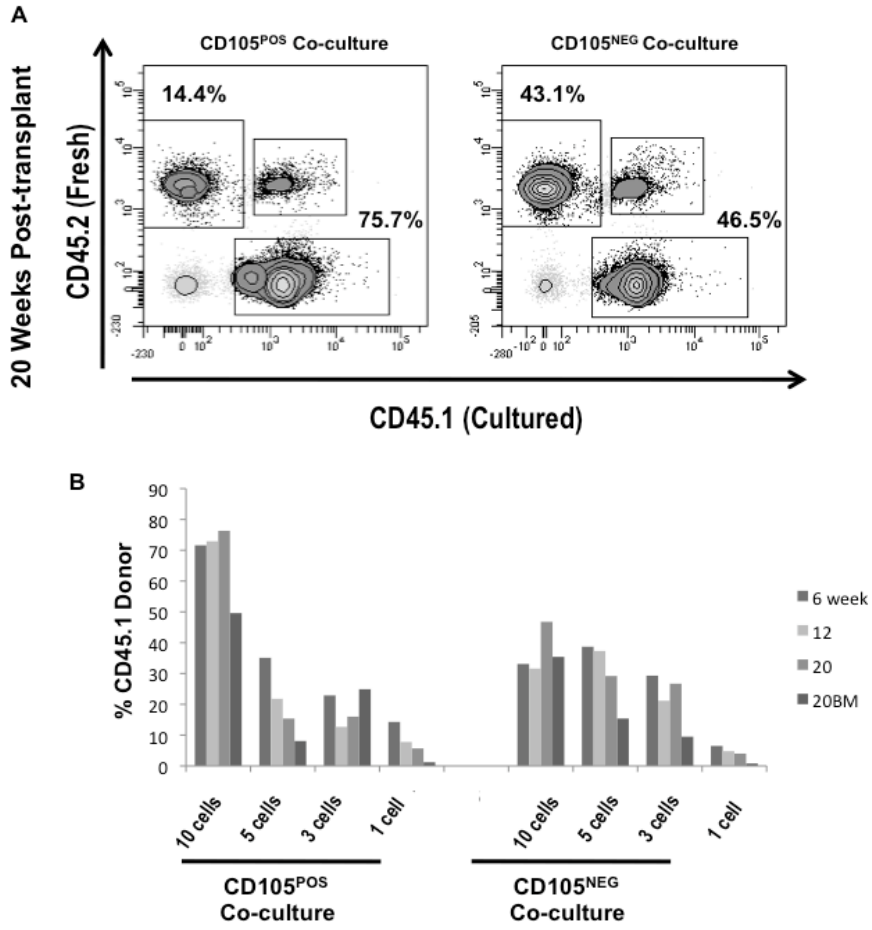
A
CD105POS Co-culture
CD105NEG Co-culture
14.4%
75.7%
43.1%
46.5%
20 Weeks Post-transplant
CD45.2 (Fresh)
CD45.1 (Cultured)
B
% CD45.1 Donor
6 week
12
20
20BM
10 cells
5 cells
3 cells
1 cell
CD105POS Co-culture
CD105NEG Co-culture
C
20 weeks post-transplant analysis from mice transplanted with 1 cell equivalent
CD105POS Co-culture
CD105NEG Co-culture
5.7%
4%
19.3%
55.6%
19.7%
55.3%
5.0%
2.6%
0.1%
0.8%
CD45.2
CD45.1
CD3
B220
Gr1
CD11b

blood reconstitution derived from the freshly isolated CD45.2 HSCs (Figure 5-10 A, left panel). However, blood reconstitution levels were nearly identical between the progeny of 10 $CD105^{NEG}$ co-cultured HSCs (41.9%) as compared to 10 freshly isolated HSCs (32.8%) in the same mouse (Figure 5-10 A, right panel). In the mice transplanted with the product 5, 3 or 1 cell equivalents we did not observe a significant difference in total blood reconstitution (Figure 5-10 B), however, we did observe a significant difference in the level of multilineage reconstitution between the two groups at each of these cell doses. Specifically, with each cell dilution from $CD105^{NEG}$ co-culture we observed a significant decrease in cells of the myeloid lineage and at the 1 cell equivalent dose the CD45.1 donor cells were completely of the lymphoid lineage (Figure 5-10 C) suggesting that as HSCs divide in co-cultures with $CD105^{NEG}$ BMSCs the cells become biased towards the lymphoid lineage.

However, mice transplanted with each dilution of the progeny from the $CD105^{POS}$ co-culture all demonstrated multi-lineage engraftment out to 20 weeks post-transplant including those transplanted at the 1 cell equivalent dose (Figure 5-10 C). Perhaps more importantly, multiple mice demonstrated long-term multi-lineage engraftment at 20 weeks at the 1 cell equivalent dose from the $CD105^{POS}$ co-culture as compared to only 1 mouse surviving from the $CD105^{NEG}$ co-culture at 1 cell equivalent dose. Collectively, these data suggest that the 10 input HSCs (CD45.1) from the $CD105^{POS}$ co-cultures under went expansion ex vivo, while HSCs from the $CD105^{NEG}$ co-culture did not expand but rather some were maintained as functional stem cells in culture. Although, mice transplanted with limiting numbers of $CD105^{POS}$ co-cultured HSCs did provide long-term reconstitution,

the lower numbers of input co-cultured progeny failed to outcompete the 10 freshly isolated C57Bl/6 (CD45.2) HSCs (Figure 5-10 C) suggesting that the level of expansion was not at a 10 cell equivalent dose.

To better address the prospect of HSC expansion, we set up a series of experiments to ask the question if a single co-cultured HSC could reconstitute lethally irradiated mice in a competitive transplantation assay. For these studies, a single double sorted B6.SJL/Ptprc^aPep^3/BoyJ (CD45.1) HSC was placed into culture wells containing confluent layers of either $Lin^{NEG}PDGFRa/b^{POS}CD105^{POS}$ or $CD105^{NEG}$ BMSC population (Figure 5-11). Following 10 days of culture, each well was transplanted into lethally irradiated F1 Chimeric mice that initially contained a single HSC. As shown in 5-12 A, co-cultures from the $CD105^{POS}$ group contained more hematopoietic progeny and when transplanted these cultures demonstrated significantly greater ability to provide long-term multi-lineage blood reconstitution in 7 of 8 mice with an average level of CD45.1 reconstitution of 50.6$\pm$26.9% (Figure 5-12 B &C, Figure 5-13 A-C). The $CD105^{NEG}$ co-cultures generated on average 23.3$\pm$26.1% donor derived engraftment with only 4 of 8 mice surviving and showing donor derived reconstitution (Figure 5-12 B & C, Figure 5-13 A-C).

In this same set of transplantation studies, we also transplanted the progeny of a single co-cultured HSC into 10 mice to assess the level of HSC expansion from the single initiating HSC. Of note, 5 out of the 10 mice transplanted with the progeny of a single HSC co-cultured with $CD105^{POS}$ BMSCs demonstrated long-term observable levels of blood reconstitution (Table 5-3). However, levels of multi-lineage repopulation were not equally distributed across mice and consisted of a

larger proportion of lymphoid reconstitution with some mice containing only low levels of myeloid reconstitution. These data suggest that HSCs can expand at a clonal level in vitro when cultured on $CD105^{POS}$ BSMCs. In agreement with our previous transplantation studies, none (0 of 10) of the mice from the single HSC $CD105^{NEG}$ co-culture showed any level of reconstitution (Table 5-3). Although, these results indicate a significant difference in the ability of the $CD105^{POS}$ BSMC population to maintain and expand transplantable HSCs at a clonal level compared to the $CD105^{NEG}$ population, more work is needed to formally quantitate this difference at the clonal level in primary and secondary recipients. By transplanting multiple mice with a variety of cell doses from clonally derived co-cultured HSCs one could determine by Poisson statistics the level of functional LT-HSC expansion.

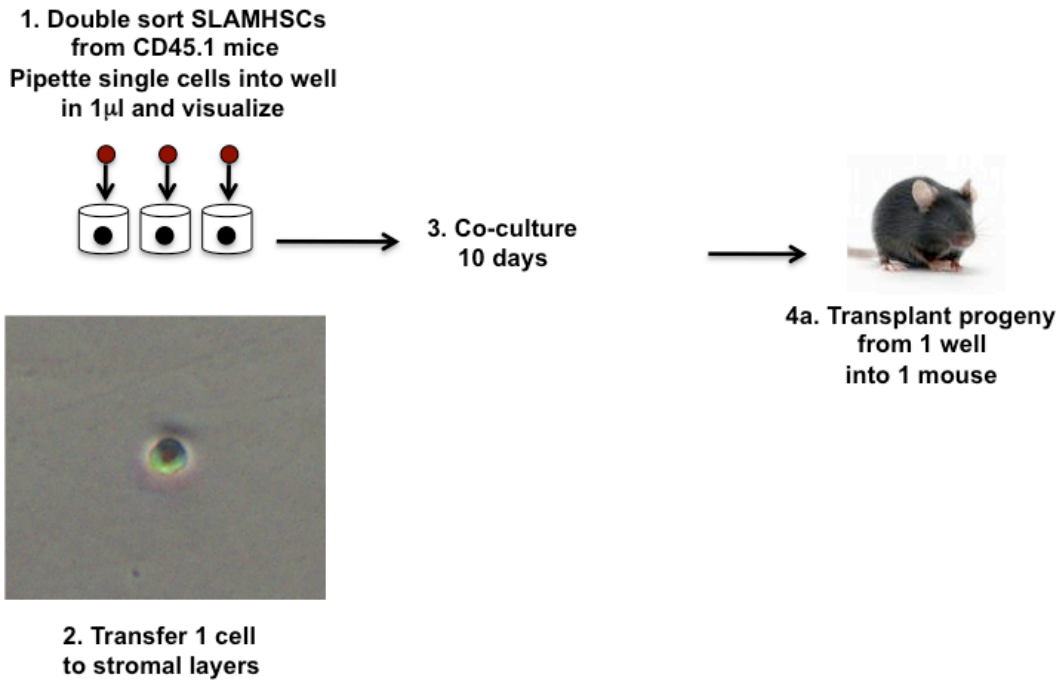

Figure 5-11: Schematic of single HSC co-culture assays. *SLAM HSCs were double sorted as shown previously and microscopically counted. Wells containing a single HSC were transferred to BMSCs co-cultures for 10 days and transplanted into a single lethally irradiate mouse or a single well was split into 10 mice.*

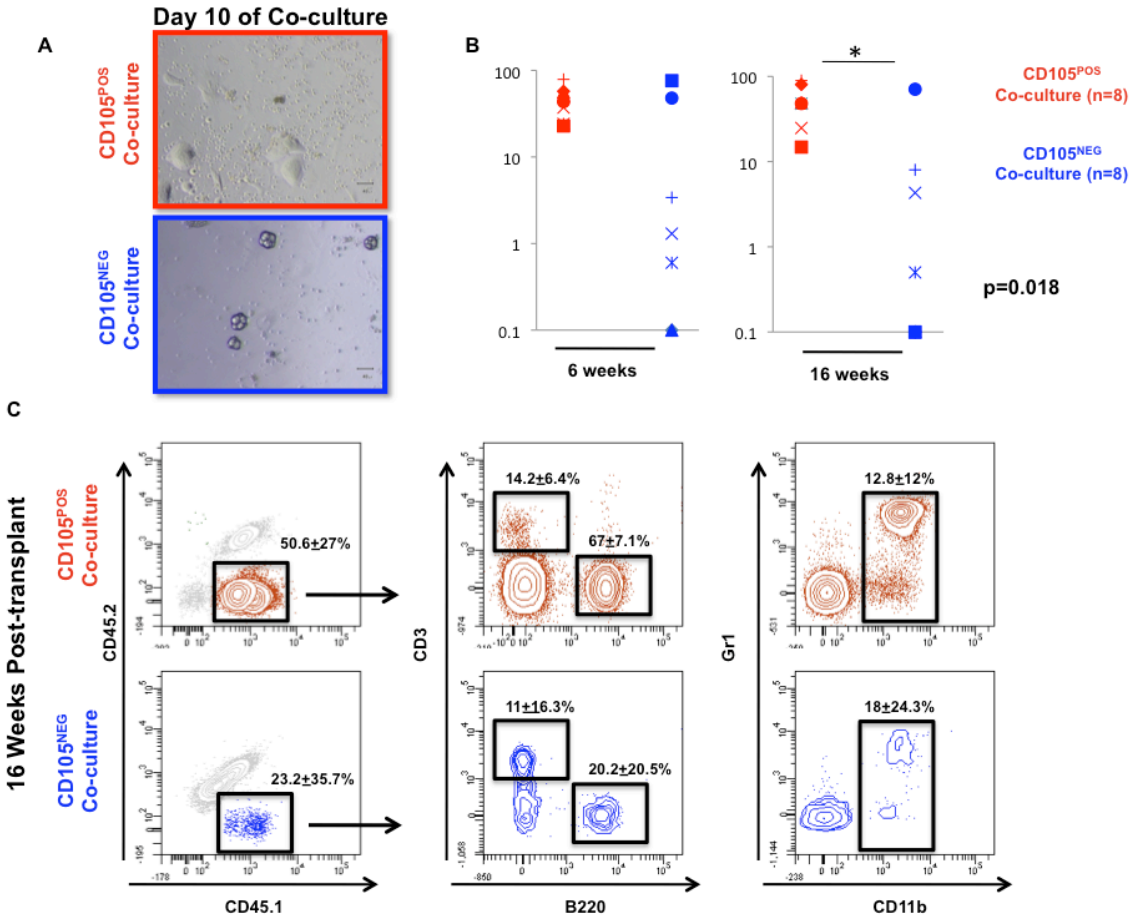

Figure 5-12: CD105^{POS} BMSCs support the expansion of single SLAM HSCs in long-term competitive transplantation assays. *(A) Images of co-cultures derived from a single HSC at the time of transplantation. (B) Donor derived blood reconstitution at 6 and 16 weeks post-transplant from a single co-cultured HSC. (C) Representative FACS plots of peripheral blood analysis demonstrating multi-lineage reconstitution by single co-cultured HSC.*

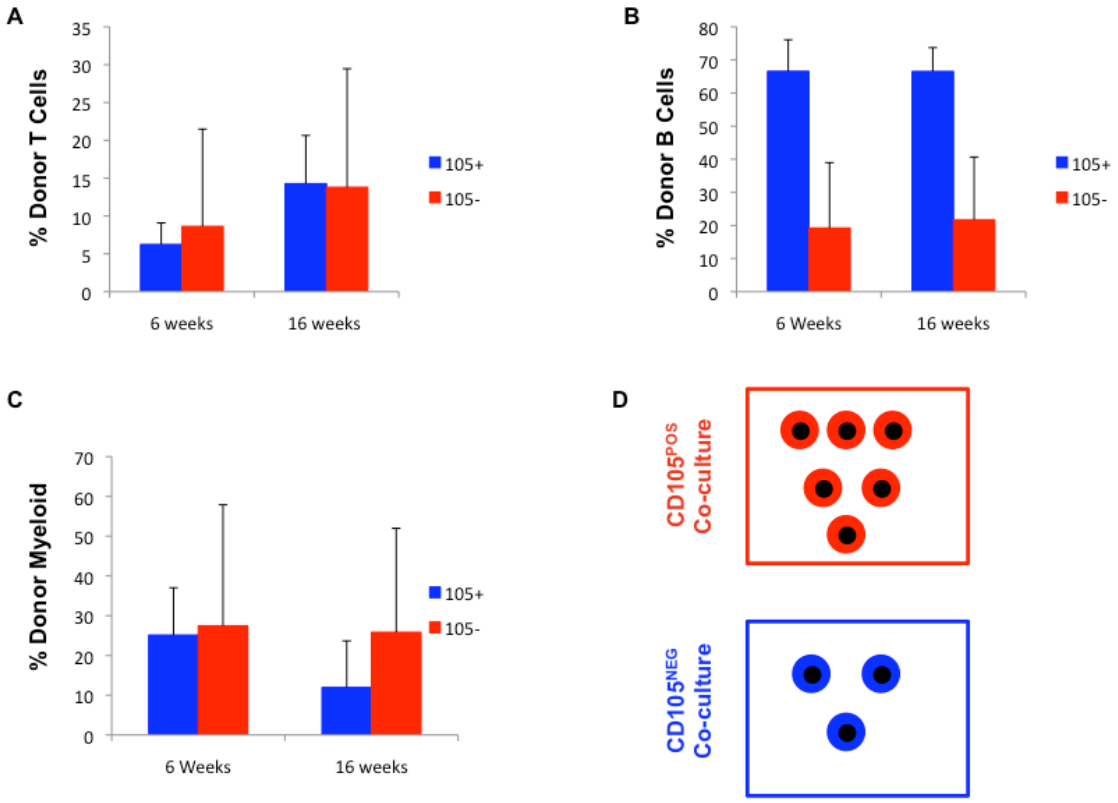

Figure 5-13: Long-term multi-lineage repopulation derived from clonal HSC co-cultures with BMSC subpopulations. *Peripheral blood reconstitution from donor derived T cells (A), B cells (B) and myeloid cells (C). Data represent mean ± Std. Dev. (D) Schematic diagram demonstrating increased ex vivo expansion of clonal HSCs in CD105^{POS} BMSC co-cultures.*

BMSC Population	# mice engrafted	% of mice engrafted	% Donor CD45.1	% Donor T cell	% Donor B cell	% Donor Myeloid
$CD105^{POS}$	5 of 10	50%	1.4 ±0.7%	8.14±9.7%	78.5±21.2%	1.18±0.9%
$CD105^{NEG}$	0 of 10	0				

Table 5-3: Reconstitution by clonally expanded HSC in to multiple mice.

5-4: SUMMARY

Taken together, these co-culture transplantation studies provide evidence for different roles in the $CD105^{POS}$ and $CD105^{NEG}$ BMSC populations in vitro. While both populations demonstrate the ability to support the maintenance of HSCs at a 10 cell input dose, only the $CD105^{POS}$ population was able to demonstrate any observable level of expansion of repopulating HSCs. These findings provide insight into potential different functional roles in vivo as well. It is possible that HSCs migrate away from the vascular niche and lose contact with the $CD105^{POS}$ perivascular niche cells, where they either enter into cell cycle and/or begin to differentiate along the long cellular processes of the intravascular $CD105^{POS/NEG}$ stromal reticulum, in accord with the model proposed by Nagasawa et al [25]. There is experimental evidence for this model in regards to B cell development [137]. Additionally, it is possible that HSCs closely associated with the $CD105^{NEG}$ osteo-progenitor cells along the endosteal region are exposed to qualitatively different growth factors that maintain HSCs in a more quiescent/dormant state [29 & 67-71]. Invoking such a model also implies perhaps a direct role for the involvement of the sinusoidal endothelial cells not only in governing HSC behavior, but perhaps more importantly a role in governing the behavior of the perivascular niche cells, which may support self-renewal divisions of HSCs localized to the vascular niche.

CHAPTER 6:

DISCUSSION

AND FUTURE DIRECTIONS

In this dissertation, I have made progress towards addressing two key outstanding questions in the field of bone marrow stromal cell biology. First, I have presented experimental evidence of a robust reproducible methodology that simultaneously yields the non-hematopoietic clonogenic stromal population as well as the vascular fraction from adult murine bone marrow. This methodology has in turn enabled studies that have led to the in vivo identification and prospective isolation of distinct populations of BMSCs that each fulfill the criteria for defining 'stromal/mesenchymal stem cells' based on the gold standard assay of in vivo heterotypic bone formation. Additional data provide evidence in support of the hypothesis that the two stromal cell subpopulations represent a stromal cell hierarchy in vivo. Furthermore, these studies have also provided evidence in support of the existence of a perivascular/reticular niche for HSCs, a transcriptional profile consistent with the role of these stromal cells as candidate HSC niche cells in vivo and in addition have resulted in the identification of a subpopulation of BMSCs that support transplantable HSCs in vitro.

The bone marrow has garnered considerable interest of many investigators from the perspective of basic science as well as regenerative medicine and stem cell based therapies. This interest can largely be derived from the observation that the bone marrow represents a rarely unique organ in that it is the residence of two widely studied adult stem cell populations, one is of hematopoietic origin (hematopoietic stem cells) and has been demonstrated at the single cell level to generate the entire hematopoietic system [20]. The other stem/progenitor population

is of a non-hematopoietic stromal origin, commonly referred to as stromal or mesenchymal stem cells (MSC) and by virtue of function as an osteoprogenitor has the proposed role of contributing bone physiology [120, 134]. The unique feature of the bone marrow's system of dual stem cell components, which interact on a functional level, raises many promising opportunities for discoveries in the regulation of HSCs and bone biology in both normal and disease conditions [7,91, 132].

HSCs represent one of the most well characterized adult mammalian stem cell populations studied to date [1] while the canonical properties of MSCs, in contrast, have proven to be much more elusive. Progress in exploring the identity and physiological role of MSCs in the mouse model has been considerably hampered by the paucity of knowledge regarding cell surface markers suitable for both in situ identification and prospective isolation of these stromal stem/progenitors [27] and arguably, also by the inadequate methodologies that have been used to obtain MSC from bone marrow. This is in dramatic contrast to progress in the identification and purification of murine HSC using monoclonal antibodies to cell surface markers where it is now routinely possible to isolate HSC at near unity as demonstrated by complete regeneration of the entire hematopoietic system following transplantation of a single prospectively isolated HSC [20]. However, the derivation of MSC from the BM of mice continues to represent a particular challenge to those investigators who seek to exploit the power of mouse genetic models to answer questions regarding the basic biology of MSC or who wish to conduct preclinical studies in the mouse as a means to test newly developed MSC-based cellular therapies.

A large focus of this dissertation was centered around addressing one of the major factors contributing to the difficulty in establishing homogeneous cultures of murine BM stromal cells, namely the low incidence of CFU-F in the BM which varies between 0.3 – 2 CFU-F/ million BM cells (C57Bl/6) up to approximately 3 CFU-F per million (BALB/c) across various mouse strains [97, 102, 109]. In accord with these data, in the current study C57Bl/6 BM prepared by standard flushing methods used in a majority of laboratories and assayed under the conditions described in these previous reports contains 0.22-2.33 CFU-F per million cells. However, when BM cells were isolated using the alternate protocol described in this dissertation, the frequency of CFU-F was increased to approximately 380 CFU-F per million mononuclear cells based on limit dilution analysis.

This dramatic improvement in the incidence and recovery of CFU-F was a consequence of several methodological improvements, the first and most significant being the means by which BM cell suspensions were prepared prior to CFU-F assay. We demonstrate that the generation of plugs of marrow with a preserved microvasculature followed by sequential enzymatic disaggregation of the plugs, consistently yielded CFU-F numbers at least 2 orders of magnitude greater than those obtained by the standard flushing technique. It will be noted that this approach is somewhat analogous to that used to isolate MSC from adipose tissue in which enzymatic digestion of the stromal vascular fraction is required to release MSC from their association with blood vessels [142]. The importance of the means by which BM is rendered into a single cell suspension on the recovery of CFU-F was also recognized by Friedenstein and colleagues [109] who reported enhanced CFE when

BM was prepared by mechanical dissociation followed by trypsin digestion of remaining clumps.

Also contributing to the improved recovery of CFU-F in presented here is the establishment of the assays at low oxygen tension. CFU-F cultures initiated at 5% O_2 demonstrated a 30-fold increase in CFE compared to those established under normoxia, findings in keeping with previous studies [144]. Aside from their perivascular location, [22, 23, 115] little is currently known about the molecular composition of the niche occupied by CFU-F in the BM in vivo, but these findings would suggest that stromal progenitors, like hematopoietic stem cells, [145] occupy a hypoxic microenvironment. It should also be noted that the high plating efficiency of CFU-F demonstrated in these studies is occurring in the absence of exogenous mitogenic growth factors such as FGF2 or feeder cells as shown in previous reports [97, 108, 109] to be necessary for optimal CFE of CFU-F from mouse BM. Our data in no way exclude a role for accessory cells and their products in promoting the growth of CFU-F and it will be of interest to determine if the CFE reported here can be further improved following addition of feeder cells and/or growth factors and moreover, to define the requirements of CFU-F isolated using the new methodology for growth in serum-free conditions.

Growth of the DBM cells at high cell density resulted in adherent cell layers containing both stromal cells and vascular endothelial cells, in addition to hematopoietic cells, thereby demonstrating the ability of this new methodology to facilitate isolation of the BM stromal-vascular fraction. From these primary cultures we successfully isolated by FACS, vascular endothelial cells and were able to

serially passage these cells in vitro as a largely homogeneously pure population. To our knowledge, this represents the first report demonstrating successful isolation and propagation of vascular endothelial cells from mouse BM and we anticipate this finding will significantly advance studies of these relatively poorly characterized cells.

In the same primary cultures, $Lin^{NEG}/PDGFR\alpha/\beta^{POS}$ cells were shown to comprise approximately 30% of adherent cells and upon FACS, generated cultures of polygonal fibroblast like cells which expressed a range of cell surface markers previously ascribed [27, 103, 104, 110] to murine BM-derived MSC, demonstrated robust multi-lineage differentiation in vitro and gave rise to bone ossicles containing bone marrow following ectopic transplantation. From the femora and tibiae of 5 mice prepared using the new methodology, we typically isolate by FACS between 1 – 2 million stromal cells at P0 and up to 20 million by P3 over a 3 week time period. This compares with less than 1 million cells generated using the standard flush methodology at P3, which often times are still contaminated with hematopoietic cells. Such cultures were difficult to passage beyond P3 in contrast to those cultures initiated from DBM, likely a consequence of senescence due to exhaustion of the proliferative capacity of the markedly lower numbers of CFU-F recovered in flushed BM.

Further to these differences in cell generative potential, flow cytometric analysis of $Lin^{NEG}/PDGFR\alpha/\beta^{POS}$ cells prepared from flushed and DBM-derived cultures also revealed phenotypic differences. MSC derived from flushed BM exhibited high levels of Sca-1 and abundant expression of Thy-1 on the majority of cells as described previously whereas DBM-derived cells demonstrated 10-fold

lower levels of Sca-1 and low level Thy-1 on only 25% of the population. In addition, CD105 demonstrated bimodal expression on DBM MSC with distinct $CD105^{POS}$ and $CD105^{LOW/-}$ populations in contrast to the flushed BM MSC in which only the $CD105^{POS}$ population was evident. Although the significance of this observation was initially unclear, it was noteworthy that in freshly prepared DBM, the $Lin^{NEG}/PDGFR\alpha/\beta^{POS}$ population also exhibits the same bimodal expression of CD105 (see Figure 3-9). Our initial interpretation of this finding was that while DBM allows isolation of both subpopulations of BMSCs, BM prepared by the standard flushing technique may bias toward the $CD105^{POS}$ subpopulation perhaps as a consequence of their selective survival during BM isolation or preferential outgrowth in vitro, both of which became a question we sought to address. Further studies to explore the disparity in cell populations elicited by the two BM cell isolation methodologies were addressed in Chapter 4 of this Dissertation.

An important advance described in the current studies was the successful *prospective* isolation of CFU-F from BM of adult wild-type mice. Previous reports used either murine fetal bone [123] or were reliant on transgenic mice strains expressing specific reporters [23, 24]. Initially, by focusing on the $Lin^{NEG}/PDGFR\alpha/\beta^{POS}$ stromal cell population as a whole, we were able to show that all of the CFU-F activity in both C57Bl/6 and BALB/c mice was derived using this immunophenotype and the increased frequency of this population in BALB/c mice correlating with a significant increase in CFU-F incidence in this strain, in agreement with previous studies [102]. These data highlight the utility of this methodology and suggest its broad applicability to the isolation and quantitation of stromal progenitors

across different strains of inbred mice. Finally, in accord with our hypothesis that the low yield of MSC achieved by flushing of BM reflects the loss of these cells associated with the marrow vasculature, whole mount staining of BM plugs demonstrated Lin^{NEG}/PDGFRα/β^{POS} cells both in perivascular locations and as a network of stromal cells in inter-sinusoidal regions of the BM (see Figures 3-10, 3-11 & 3-12).

The notion that a single stromal stem/progenitor population is responsible for CFU-F activity within the bone marrow is a widely disseminated concept within the field of MSC biology. However, in this dissertation we provide direct evidence challenging this notion. With the development of the novel isolation and imagining strategies described in this dissertation and the identification of cell surface markers useful for in situ localization, we choose to further elucidate the physiological relevance of the bimodal distribution with respect to CD105 expression within primary adherent cultures as well as within freshly prepared DBM cell suspensions. To this end, we provided evidence that two phenotypically distinct populations within the adult murine BM both contribute to CFU-F activity as well as to the initiation of long-term MSC cultures (Figure 4-1 & 4-2).

Although these two populations contributed to the generation of adherent stromal cell cultures at clonal and non-clonal plating densities at nearly equal frequency, the Lin^{NEG}PDGFR$\alpha\beta^{POS}$$CD105^{POS}$ population represented a significantly greater number of total cells in freshly prepared tissue and in whole bone marrow cultures upon serially passaging. Additionally, the $CD105^{POS}$ population contains a significantly greater number of CFU-F when prospectively isolated from fresh BM

tissue. The question then becomes, why? Is there a functional and/or physiological difference in the activity of these two populations that might explain the difference in frequency?

To address these questions, we used a series of in vitro and vivo assays coupled with transcriptional profiling of prospectively isolated subpopulations to explore differences between the properties of these two stromal cell subpopulations. With the development of an isolation strategy to prospectively isolate BMSC subpopulations, we were in a unique position to address fundamental questions in the MSC field. In particularly, where are MSC located in vivo and what are their physiological functions. Unfortunately, the large body of data in the MSC field, especially regarding murine MSC, is based on what amounts to a retrospective analysis and characterization of 'MSC' performed following extensive serial propagation in vitro [27, 103, 104, 110]. Because, culture conditions are substantially different from the native in vivo environment, it is likely that these analyses will be significantly biased as a consequence of studying the properties of stromal stem/progenitor populations maintained under non-physiological conditions ex vivo. By defining a composite cell surface immunophenotype that demonstrates fidelity in vitro (Figure 3-9) and in vivo (Figure 4-1 & 4-2), these studies have provided evidence that the non-hematopoietic stromal elements in bone marrow are not entirely representative of the homogeneous populations most often studied and characterized in long-term cultures.

In addition to the isolation of distinct clonogenic (CFU-F) populations, we describe the existence of two BMSC populations that contribute independently to the

generation of ectopic bone complete with BM adipocytes and hematopoietic-supportive stroma defining each population as having with stem/progenitor activity. Additionally, our transplantation data suggests that there is a difference in both the potency and kinetics ascribed to heterotopic bone ossicle formation by each of these populations. The stromal cell subpopulation identified as the $Lin^{NEG}PDGFR\alpha/\beta^{POS}CD105^{POS}$ fraction is able to generate bone-bone marrow tissue at a faster rate in vivo with fewer cells than that determined within the $Lin^{NEG}PDGFR\alpha/\beta^{POS}CD105^{NEG}$ fraction. Additionally we demonstrate that when recovered from ectopic bone tissue, the $Lin^{NEG}PDGFR\alpha/\beta^{POS}CD105^{POS}$ fraction also gives rise to cells identified as $CD105^{LOW/NEG}$ suggesting that $CD105^{NEG}$ cells are a derivative of $Lin^{NEG}PDGFR\alpha/\beta^{POS}CD105^{POS}$ cells. Furthermore, we provide evidence that mature pericytes/mural cells are also a subpopulation of the larger $CD105^{POS}$ population. Does this data point to a potential model of a stromal stem progenitor hierarchy?

Evidence in support of this notion was derived from transcriptional profiling of prospectively isolated $Lin^{NEG}PDGFR\alpha/\beta^{POS}CD105^{POS}$ and $Lin^{NEG}PDGFR\alpha/\beta^{POS}CD105^{NEG}$ populations. Our microarray data demonstrates that the $CD105^{NEG}$ population contains a list of over-represented genes classically identified in skeletal development and bone mineral biogenesis, including markers such as Col1a1, osteonectin and alkaline phosphatase which are thought to be contained in immature osteogenic populations. The $CD105^{NEG}$ fraction also expressed genes at the RNA level consistent with cells of a more mature osteoblast nature, including bone sialoprotein, osteocalcin and osteopontin [22, 121].

Additionally, the $CD105^{NEG}$ population is also enriched in cartilage related genes such Col2a1, cartilage oligomeric matrix protein and chondrocadherin (CHAD) [128, 129]. Together, these data suggest that the $CD105^{NEG}$ population represents cells more committed to the osteogenic and chondrogenic lineages and thus are positioned further downstream of a stromal stem cell that may also give rise to cells of more mature pericyte function as well.

Emerging evidence from lineage tracing studies suggest that there are perivascular cells within adult mouse bone marrow developmentally derived from two distinct embryological origins, the mesoderm [121] and neural crest [122]. However, these authors do not address whether or not the labeled cells seen in these models are the same cells routinely used and characterized as MSC from adult BM tissue. So the question from these studies remains open as to whether or not adult BM stem/progenitor stromal populations are derived from different development lineages. Our data suggests that the population often characterized in the literature as being $CD105^{POS}$ in culture is of the same mesodermally derived source as the $CD105^{NEG}$ progenitor population. From these findings, we speculate that the $CD105^{POS}$ population contains a rare population of immature stem/progenitor cells which gives rise to the cells of a mature pericyte function [125] as well as cells of the $CD105^{NEG}$ population which serve as more direct osteoprogenitor cells closely aligned with the endosteal region, growth plate and potentially bone trabeculae serving as the major reservoir of committed cells providing bone and cartilage specific ECM proteins potentially contributing to the overall maintenance of bone tissue turnover.

Together, these data suggest the identification of a stromal stem/progenitor cell hierarchy previously proposed [86], yet largely unrecognized within the BM stromal cell field. Based on these data, we propose a speculative model describing a stromal stem/progenitor cell hierarchy in vivo within adult murine BM (Figure 4-12). Although we are not at this time able to conclusively validate this model, our functional assays and transcriptional profiling data suggest that these two populations are enriched in clonogenic progenitor cells with over-lapping and distinct functions in vivo. Additionally, similar evidence has been provided in fetal derived bone tissue [123]. It will be of great interest to the field of MSC biology as well as studies focused on defining the formation and maintenance of HSC niches to determine how these two populations interact to form distinct microenvironments with perhaps different biological functions in vivo.

One potential way to provide additional experimental evidence for this proposed hierarchy would be to utilize genes identified in our microarray studies that are differentially expressed and conduct extensive lineage tracing studies to follow the fate of each population under homeostasis in the embryo and the adult as well as in injury models of bone tissue in the adult. If this model is correct and the $CD105^{NEG}$ population represents a more committed progenitor downstream of the $CD105^{POS}$ stem/progenitor population, then we would not expect to see any contribution to the $CD105^{POS}$ population from labeled cells derived from transgenic mice expressing Cre-recombinase under the control of promoters identified from our microarray studies of over-represented genes in the $CD105^{NEG}$ population similar to studies conducted using the Col1A1 promoter described by Maes et al. [121]. It

would be of great interest to use this strategy to identify the source of cells that not only form the bone marrow stromal tissue during development, but more importantly those cells that serve as the endogenous source of adult stromal stem cells. Are they truly perivascular cells as suggested and if so do they have their own unique microenvironment contributing to self-renewal? These types of studies would also prove useful in identifying the original identity and localization in situ of the cells so often identified in vitro as CFU-F and MSC.

Within the adult BM, functional HSC activity is maintained through interactions with stem cell niches. Two current models suggest the existence of distinct HSC niches, one proposed niche involves osteoblast cells closely associated with the internal surface of the bone, referred to as the endosteal niche [18, 19, 29, & 69]. While subsequent studies have identified a vascular/perivascular niche comprised of sinusoidal endothelial cells and perivascular stromal cells [20-26]. And with the use of mouse genetics several key regulatory molecules have been identified as being necessary to maintain functional HSCs in vivo [14-15 &44]. However, it is currently not known which cell types are the primary sources responsible for generating these regulatory molecules in vivo. Currently, it is the interest of many laboratories to dissect specific regulatory networks, which govern HSC behavior in an extrinsic mechanism and to identify the primary cells contributing to this direct extrinsic regulation. In Chapter 5 of this dissertation, we begin to elucidate to identity of stromal cell subpopulations, which are the major source of genetically necessary HSC regulatory molecules and contribute to the maintenance and expansion of HSCs ex vivo.

To this end, I describe a well-validated transplantation model to tract in vivo the blood reconstitution derived from co-cultured HSCs, which are directly competed against freshly isolated HSCs. From these studies, we demonstrate that two BMSC populations are able to maintain functional HSCs in culture; however only the $CD105^{POS}$ BMSC population demonstrated the ability to significantly outcompete freshly isolated HSCs. Furthermore, I developed a co-culture system that allows for the study of the expansion of functional clonally derived HSCs. In these experiments, $CD105^{POS}$ co-cultured HSCs (100%) demonstrated a significant increase in donor derived multi-lineage reconstitution, while only 4 of 8 mice (50%) from $CD105^{NEG}$ -single HSC co-cultures demonstrated blood reconstitution, suggesting a more limited expansion of functional stem cells. Taken together, these results demonstrate that the PDGFR$\alpha\beta CD105^{POS}$ stromal cell subpopulation is distinguished by a unique capacity to support the expansion of long-term reconstituting HSCs in vitro.

In this experimental setting, it is possible to determine the fate of individual stem cells in a well-validated transplant model. Furthermore, single cell qPCR and microarray analysis could be applied to gain a better understanding of the extrinsic regulation governing these differences in HSC behavior. When done in combination with lineage tracing studies of the candidate niche cells, it could, for the first time, be a method to identify different microenvironments in vivo with different functional roles. Although, the evidence provided in this dissertation makes significant advances to the field of MCS and HCS niche biology, there is still much more work that needs to be done in order to better address each of these

outstanding questions that have largely been unanswerable. With the development of this novel approach to the isolate phenotypically defined BMSC subpopulations comprising the stromal tissue of mouse BM, it is to be hoped that these studies will ultimately contribute to a greater understanding of the role of stromal cell subpopulations in regulation of hematopoiesis, and will complement efforts currently underway in other laboratories based on the use of transgenic mouse models.

The isolation and characterization distinct clonogenic BMSC populations with different functional roles in vitro and in vivo are the major findings of this dissertation. Taken together, we propose a model (Figure 6-1) in which a stromal cell hierarchy lays the foundation for creating distinct microenvironments in vivo with different functional roles in regulating HSCs. We propose that the $CD105^{POS}$ BMSC population contains a subpopulation of perivascular stromal stem cells closely associated with the abluminal surface of sinusoidal vessels comprising the vascular niche. Within this microenvironment, HSCs are able to undergo self-renewal to maintain the stem cell pool and contribute progenitor cells for the daily requirement of mature effector cells continuously released into the blood stream. Additionally, the $CD105^{POS}$ population generates mature pericyte cells associated with the smaller vessels and generates cells comprising the intersinusoidal reticular network. Whereas, in support of previous publications [29, 67-71] the $CD105^{NEG}$ osteo-progenitor cells associated with the endosteal region contributes to the regulation of quiescence/dormant HSCs as well as the differentiation of lymphoid progenitor cells generating mature B-cells [137]. In support of these proposed roles, our functional data and microarray analysis points to both populations as being cells comprising

the CXCL-12-GFP (CAR) cells [24, 25, 137] and those identified using Nestin-GFP [23] and SCF-GFP [136] mouse models.

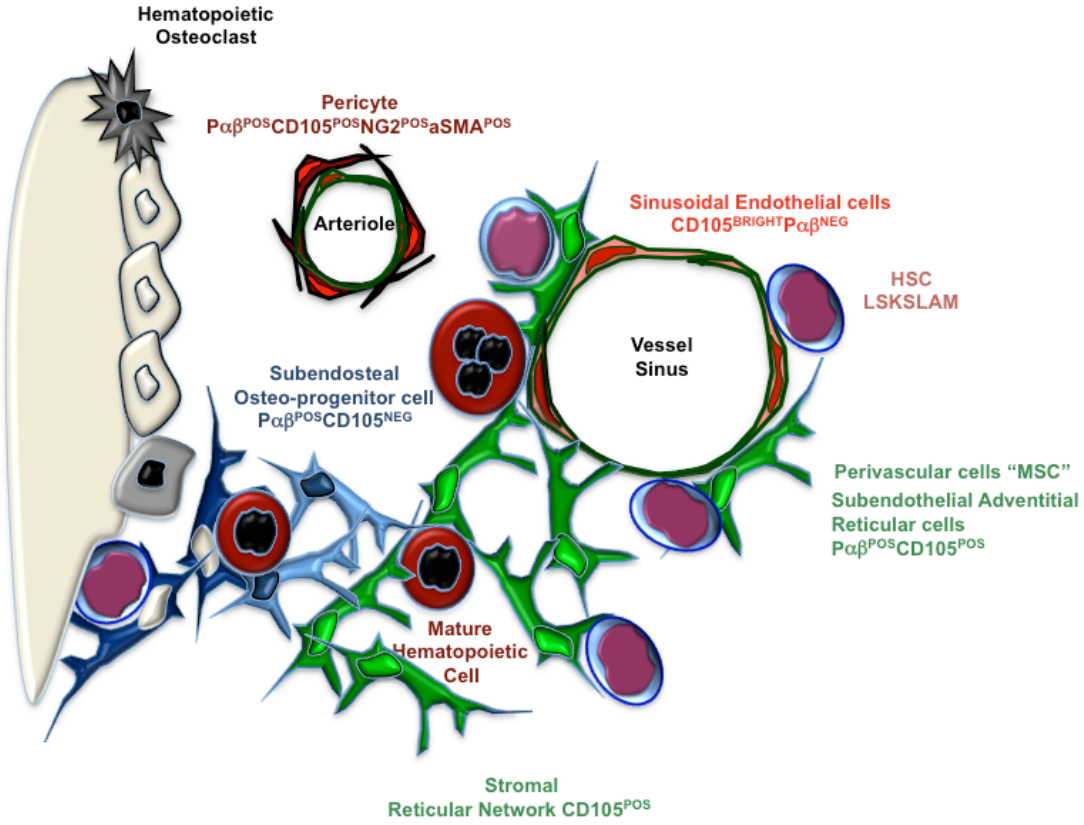

Figure 6-1:Schematic of the Bone Marrow Microenvironment. *Proposed model for a stromal cell hierarchy providing stromal progenitor cells responsible for generating both perivascular and endosteal niche cellular consitutents in vivo.*

CHAPTER 7:

MATERIALS AND METHODS

MATERIALS AND METHODS

Animals

8-12 week old C57BL/6, B6.SJL/Ptprc^aPep^3/BoyJ, BALB/c and NOD-SCID mice originally purchased from Jackson Laboratories and breed in our animal facility were used as the source of bone marrow tissue and transplant recipient animals. Additional mice used as a source of BM cells include; transgenic mice harboring the NG2-DsRed transgenic mice (Tg(Cspg4-Ds Red.T1)1Akikj) were purchased from Jackson Laboratories and αSMA-RFP mice were a generous gift from Dr. Frank Marini at MD Anderson Cancer Center and UBC-GFP mice originally purchased from Jackson Laboratories were a generous gift from Dr. Mikhail Kolonin at the University of Texas at Houston. For competitive transplantation assays, C57BL/6 and B6.SJL/Ptprc^aPep^3/BoyJ mice were crossed to generate F1 chimeras which were used as transplant recipients. Animals were caged under standard conditions and fed a laboratory diet and acidified water ad libitum. Care and use of the laboratory animals was according to animal protocols/guidelines established by the University of Texas Health Science Center at Houston Animal Welfare Committee.

Isolation of Murine Bone Marrow cells

Mice were sacrificed by CO_2 asphyxiation and cervical dislocation, femora and tibiae were excised, cleaned of attached muscle tissue and stored on ice in harvest medium (PBS supplemented with 2% v/v FBS). To prepare BM cells by flushing, a 23-gauge needle (BD Bioscience) was inserted into the growth plate of femora or

tibiae from which the epiphyses had been removed at the metaphysis below the marrow cavity and the bone marrow removed by flushing in 5 mls of PFE (PBS supplemented with 2% FCS and 2mM EDTA). The resulting suspension was then triturated several times to break up clumps, drawn through a 20-gauge needle and filtered through a 70μm cell strainer (BD Bioscience).

To isolate BM plugs, the ends of the tibiae and femora were removed as above and a 1ml syringe fitted with 23-gauge needle (BD Bioscience) containing ice-cold PFE was inserted into the growth plate and the BM plug gently expelled from the cut ends of the bones in 1 ml of PFE. BM plugs were transferred to 15 ml conical tubes (Falcon) containing a mixture of Collagenase Type I (3mg/mL; Worthington, Lakewood NJ) and Dispase (neutral protease, grade II; 4mg/mL; Roche) in PBS and incubated for 15 minutes at 37°C. Following a brief vortex for 10-20 sec on low setting, undigested BM was allowed to settle and BM cells in suspension transferred to a new tube containing 10mls of PFE and placed on ice. This fraction is referred to as fraction 1. To the undigested BM tissue remaining after the first incubation was added additional Collagenase/Dispase solution and the process repeated an additional two times yielding fractions 2 and 3, respectively. Each fraction was then either filtered separately through 70μm cell strainer (BD Bioscience) or the three fractions were pooled prior to filtration (referred to throughout text as DBM). The cells were washed twice by centrifugation in PFE prior to plating under various conditions, as described below.

CFU-F Assays

For assay of clonogenic fibroblast colony-forming cells (CFU-F), single cell suspensions of BM cells prepared by the standard flushing methodology or DBM were plated in triplicate over a range of plating densities in 6-well plates (BD Bioscience) in 2mls of complete growth medium comprising alpha-MEM (Invitrogen, Life Technologies, Carlsbad, CA) supplemented with 20% (v/v) lot-selected fetal bovine serum (Hyclone, Thermo Scientific, Rockford, IL), sodium pyruvate (1mM/ml, MP Biomedicals), gluta-MAX (2mM/ml), penicillin (100U/ml) and streptomycin (100μg/ml) (all from Gibco, Life Technologies). Cultures were incubated at 37°C in a humidified incubator at 5% CO_2 and 5% O_2 for 72 hours washed with medium and re-fed with complete growth medium for an additional 11 days. On day 14, wells were briefly rinsed with PBS and then stained with 0.1% Toluidine blue in 4% formalin (both from Sigma, St. Louis, MO) to allow enumeration of colonies. Only colonies containing >50 stromal cells were scored. Additionally for CFU-F assays from prospectively isolated BMSCs, clusters containing 10-50 cells were scored.

Establishment and Characterization of Primary cultures of DBM (P_0 culture)

DBM from digestions 1 – 3 was also plated at non-clonal densities (1 x10^6/ cm^2) to allow growth both of stromal cells and of vascular endothelial cells. Cells were plated on dishes or chamber slides (LabTek, Nunc, Rochester, NY) coated with fibronectin (Sigma) at 5μg/cm^2 in either alpha-MEM supplemented with 20% FBS or in EGM2-MV (Lonza, Switzerland). Cultures were placed in a 37°C humidified incubator at 5% CO_2 and 5% O_2, washed at 72 hours and maintained under these conditions with

media changes every 3 days until attaining confluence and were designated P_0 cultures.

Characterization of the Cellular Composition of P_0 cultures

A.) ***In-situ staining:*** P_0 cultures established in chamber slides slides were placed on ice for 30 minutes and washed x3 in ice-cold basal αMEM (Gibco). Cultures were first incubated with purified rat mAbs, washed and revealed with donkey anti-rat Cy3 (1:500) (Jackson ImmunoResearch, West Grove, PA). Following washing, Fc block was added for 20 minutes prior to the addition of flurochrome conjugated rat mAb (see table S1) for 30 minutes on ice. Following mAb staining, cells were fixed in 4% PFA (Electron Microscopy Sciences, Hatfield, PA) for 15 minutes at room temperature, washed 3 times in PBS and then coverslipped in Prolong Gold containing DAPI (Molecular Probes). Imaging was performed on an inverted fluorescence microscope (Olympus BX51) and captured with an Olympus DP71 camera.

B.) ***Flow cytometric analysis:*** P_0 cultures or cells at subsequent passages were detached at day 7 of culture by addition of 0.05% trypsin-EDTA (Gibco) washed in PFE and filtered through a 40μm cell strainer to obtain a single cell suspension. Cells were resuspended in 100μl of PFE and blocked in Fc block for 20 minutes on ice, followed by staining with flurochrome conjugated or isotype control antibodies on ice for 20 minutes. Prior to analysis, cells were resuspended in PFE containing 0.6 μg/ml DAPI (Invitrogen) and either analyzed on an LSR II (BD Bioscience) or subjected to FACS using a FACS Aria II (BD Bioscience, San Jose, CA) fitted with a

100μm nozzle and Blue Diode 488, HeNe 633 and UV 355 lasers to isolate stromal cells and/or vascular endothelial cells. For complete list of antibodies used for FACS, see table S1.

Prospective isolation of CFU-F from fresh BM

BM cells freshly prepared from DBM plugs as described above were labeled with the biotinylated hematopoietic lineage antibody cocktail (Table S1) on ice for 20 minutes, washed, filtered and then incubated with sheep anti-rat Dynal beads (Invitrogen) according to manufactures instructions. Following removal of bead bound lineage positive cells, the unbound fraction was incubated in Fc block for 20 minutes on ice and stained with monoclonal antibodies as described above.

Marrow Stromal Cell Differentiation Assays

(A.) ***in vitro:*** Purified bone marrow stromal cells isolated by FACS were expanded in culture in aMEM-20% FBS to passage 3 at which time cultures were used for in vitro differentiation assays as described elsewhere [102, 104, 138] Briefly, for osteogenic differentiation, cells were plated at a density of $4.2x10^3$ cells/cm^2 in αMEM supplemented with 20% FBS, 10^{-8} M dexamethasone, 5mM inorganic phosphate and 100uM ascorbate-2 phosphate (ASC-2P) (all from Sigma) and cultures for 14 days prior to Von Kossa and alkaline phosphatase staining (Vector Blue Alkaline Phosphatase substrate Kit; Vector Labs). For adipogenic differentiation cells were plated at a density of $2.1x10^4$ cells/cm^2 in αMEM supplemented with 20% FBS until the cells reached confluence at which time the medium was changed to DMEM supplemented with 10% FBS, 10% horse serum, 10^{-8} dexamethasone, 500

μM IBMX and 60 μM indomethacin and cultured for 21 days and adipose differentiation was evaluated following oil red O staining.

Chondrogenic differentiation was carried out according to previously established protocols [102, 139]. Briefly, 250,000 BM stromal cells were pelleted and cultured in chondrogenic serum-free media (Lonza) supplemented with 10ng/ml TGF-β3 (R&D Systems, Minneapolis, MN) in 15ml falcon conical tubes for 21 days. Pellet cultures were fixed overnight in Zn fixative (Shandon/Thermo, Waltham MA) at 4°C and processed for standard embedding in paraffin wax according to standard procedures. Morphological assessment of 5 μm sections was assessed by means of standard H&E staining and sulfated polysaccharides were revealed following staining with Toluidine Blue (0.1% w/v; Sigma) and with Alcian Blue 8GX (Sigma) followed by brief counterstaining using fast nuclear red (Vector Laboratories) according to standard procedures. Immunohistological staining for collagen type II was performed by incubating pellet sections with antibody 2B1.5 (Thermo-Scientific) or isotype control antibody followed by immunoperoxidase staining using the mouse ABC kit (Vector Laboratories) as previously described [140].

(B.) ***in vivo:*** To determine their capacity to form bone in vivo, $Lin^{neg}PDGFR\alpha/\beta^{pos}$ cells at P3 were collected by brief trypsinization and 1.5x10^6 cells were resuspended in 50μl αMEM-20% growth media, loaded onto Gel-foam sponges (Baxter, Deerfield, IL) and covered in a fibrin clot (Sigma) at 37°C. Scaffolds were then subcutaneously transplanted into 2-3 month old NOD-SCID mice as described [141]. At 12 weeks, mice were sacrificed, scaffolds were recovered, fixed overnight

in 10% buffered formalin at 4^0C and decalcified for 1 week in 10% EDTA, embedded in paraffin and stained with H&E or Masson's Trichrome according to standard procedures. Additional scaffolds were not decalcified and embedded in methyl methacrylate resin (Lawrence Bone Disease Program of Texas Bone Core, MD Anderson Cancer Center, Houston, TX) and sections stained using the von Kossa reaction and with Goldner's Trichrome.

Whole mount immunofluoroesence staining of bone marrow plugs

Intact bone marrow plugs prepared as above were fixed in freshly prepared 2% paraformaldehyde for 10 minutes at RT and then washed thrice in DPBS for 15 minutes. Using a scalpel, each plug was cut in two and each half transferred to a single well of a 96-well round bottom plate (BD Bioscience) for antibody staining. BM plugs were first incubated overnight at 4°C in blocking buffer comprising DPBS with 3% BSA (Sigma), 2% FCS, 2% horse serum and 2% normal donkey serum (Jackson ImmnoResearch). BM plugs were then incubated overnight with gentle rocking at 4°C with purified anti-PDGFRα and anti-PDGFRβ antibodies or isotype controls. BM plugs were then washed throughout the following day at 4°C and incubated overnight with donkey anti-rat Cy3 diluted 1:500 in blocking buffer. Next, the samples were washed throughout the day in DBPS supplemented with 2% normal rat serum (Jackson Immunoresearch) and then incubated overnight with MECA32-Alexa 488 and VE-Cadherin-Alexa 488 or with rat IgG1 and IgG2a-Alexa 488 isotype controls. After washing, the BM plugs were counterstained with DRAQ5 (1:1000; Biostatus Limited) for 30 minutes at RT, transferred onto cover slips and surrounded by several layers of 120μm SecureSeal imaging spacers (Grace Biolabs, Bend,

Oregon) to provide a depth of approximately 300-500μm and then immersed in prolong gold anti-fade mounting medium (Molecular Probes). After applying a coverslip, specimens were inverted and allowed to cure overnight in the dark at RT prior to confocal imaging.

Characterization of vascular endothelial cells

Purified $Lin^{neg}CD105^{bright}PDGFR\alpha/\beta^{neg}$ cells were cultured on fibronectin coated wells in EGM2-MV. At passage 3, cells were plated into (LabTek,) slides coated with fibronectin and cultures were analyzed for the presence of endothelial markers by in situ staining described above. Additionally, cells were plated at 70% confluence and the following day incubated with 10μg/ml DiI-Ac-LDL (Biomedical Technologies, Stoughton, MA) for 4 hours at 37°C. Cultures were washes x3 in PBS and imaged on an inverted microscope for the presence of Ac-LDL uptake.

Isolation of Hematopoietic stem cells

Bone marrow was rigorously flushed with a 25-gauge needle and 5mls of ice cold PBS-2% FBS, 2mM EDTA and filtered through 40 micron cell strainer (BD Bioscience). Cell suspensions were subjected to ammonium chloride potassium (BD Bioscience) for lysis of red blood cells, Fc blocked and stained with antibodies to mature hematopoietic lineage cells (LIN-), c-Kit, Sca1, CD150, CD48 (all from Biolegend). LSKCD48-CD150+ HSCs were double sorted on a FACS Aria (BD Bioscience).

Co-culture and Long-term competitive reconstitution assay

Fractionated stromal cell populations were plated in fibronectin coated 48 well plates at 5,000-10,000 cells/well in complete growth media until reaching confluence. At which time, LSKCD48-CD150+ HSCs were double sorted from 8-10 week old B6.SJL/Ptprc^aPep^3/BoyJ and resuspended at 10 cells/μl in Stem Span serum free expansion media (Stem Cell Technologies). To validate accurate cell numbers, 1μl of HSC cell suspension was added to a single micro-well in a terasaki plate and the entire well was imaged and counted. Wells containing 10 cells were then transferred to a single well of established stromal layers in 500μl of Stem Span supplemented with Flt3L (10ng/ml), IL-6 (2ng/ml), Kit-ligand (10ng/ml) and TPO (5ng/ml). Suspension cultures without stromal layers were used as controls. Cultures were placed at 5%CO_2, 5%O_2 37°C for 10 days. Following 10 day co-culture period, entire content of a single well was collected, resuspended in 100ml of PBS with a radio protective dose of 300,000 WBM cells from 8 week old F1 mice and 10 freshly prepared LSKCD48-CD150+ HSCs from C57BL/6 mice. The entire cell suspension was drawn into a 1ml insulin syringe and injected into the retro-orbital venous sinus of 8-12 week old F1 recipient mice that received 2 doses of 550 rad whole body radiation with 2 hours of rest between each dose. Mice were maintained on normal diets with acidified water at libitum. Peripheral blood was obtained at 6, 12 and 18 weeks in EDTA coated micro-tubes (BD Bioscience) and bone marrow was collected at 16-20 weeks depending on the experiment. Samples were subjected to ammonium chloride potassium (BD Bioscience) for lysis of red blood cells, Fc blocked and stained with antibodies to CD45.1, CD45.2, B220, Mac-1, CD3 and Gr1 (all from Biolegend). Following mAb staining cells were washed, filtered and

resuspended in PFE contain 0.6mg/ml of DAPI and analyzed on a LSRII. Additionally, 1x10^6 WBM cells collected at 18-20 weeks were transplanted in lethally irradiated F1 secondary recipients and analyzed as described above.

Illumina Gene expression Analysis

All analyses were performed using GenomeStudio software (Illumina, Inc.) by The Microarray Core Lab, University of Texas Medical School at Houston. Bone marrow samples prepared as described above were sorted from 8 week old BALB/c mice into four groups (Hematopoietic Lineage positive cells, $Lin^{NEG}PDGFR\alpha/\beta^{NEG}CD105^{BRIGHT}$, $Lin^{NEG}PDGFR\alpha/\beta^{POS}CD105^{POS}$ and $Lin^{NEG}PDGFR\alpha/\beta^{POS}CD105^{LOW/-}$) for a total of three independent experiments and total RNA was isolated using RNeasy RNA isolation kit (Qiagen). Each experimental sample was kept separate to represent 3 independent biological replicates. Total RNA amplification and microarray hybridization was performed as follows. We used 300 nanograms of total RNA for all amplifications. Amplification of purified total RNA samples was done according to the manufactors recommendations using the Illumina TotalPrep RNA Amplification Kit (Ambion, Cat# IL1791). Briefly, first strand cDNA synthesis was performed with RNA, T7 oligo(dT) primers and reverse transcriptase mix and incubated for 2 hours at 42 ºC. Additionally, second strand cDNA synthesis was performed by first preparing a master mix containing RNase H and DNA polymerase. The RNase H and DNA polymerase master mix was immediately added following the completion of the first strand reverse transcription reaction mix and was incubated for 2 hours at 16 ºC. cDNA filter cartridges (part of the amplification kit) were used to remove RNA, primers, enzymes and salts that

would inhibit in vitro transcription. The synthesis of biotinylated cRNA was performed by in vitro amplification for a 14-hour amplification step in the presence of a dNTP mix containing biotin-dUTP and T7 RNA polymerase. Following amplification, the concentration of purified cRNA was determined by a NanoDrop ND-1000 Spectrophotometer (NanoDrop Technologies, DE). Microarray hybridization on the Illumina Sentrix Beadchip Array Mouse WG-6.v2 arrays was performed as follows. 1.5 micrograms of amplified cRNA product was loaded onto the Illumina Mouse WG-6.v2 arrays and hybridization was performed for 17 hours at 58ºC in an Illumina Hybridization Oven (Illumina, Cat# 198361). Immediately following hybridization, the chips were washed and the detection of biotin-labeled cRNA on the arrays was done by incubation with straptavidin-Cy3. Next, Illumina bead arrays were allowed to dry and subsequently scanned with the Illumina BeadArray Reader (Illumina, CA). All sata analysis was performed with the GenomeStudio software (Illumina, CA). Additionally, GenomeStudio and Ingenuity Pathway Analysis (Ingenuity Systems, Inc.) softwares were used for clustering and pathway analysis, respectively.

Quality control and pre-processing

Raw signals of all the build-in controls were checked as quality control for the performance of the arrays. Sample-independent controls were used to check:

a. Hybridization (control molecules at low, medium and high concentrations);

b. Signal generation (background, noise, biotin labeling and hybridization at high and low stringency).

Housekeeping genes were used as sample-dependent controls. Background was subtracted and arrays were normalized using *quantile*. The reproducibility of biological or technical replicates was checked through comparisons among individual samples. Outliers were removed if necessary. The remaining samples were grouped and the average signal intensities of samples within the group were used for differential expression analysis.

Statistical Analysis

Statistical analysis was performed with SigmaStat version 3.5 with significance being assigned to $p < 0.05$.

Table 7-1: List of Antibodies

Antibody	Clone	Company	Dilution
CD31-FITC	MEC 13.3	BD Bioscience	1/100
MECA32-Alexa 488	MECA32	Biolegend	1/100
VE-Cadherin-Alexa 488	BV13	eBioscience	1/100
VEGFR2-purified	Avas 12a1	BD Bioscience	1/100
PDGFRb purified	APB5	Biolegend	1/100
PDGFRb-APC	APB5	Biolegend	1/100
PDGFRa-purified	APA5	eBioscience	1/100
PDGFRa-APC	APA5	eBioscience	1/100
CD105-purified	MJ7/18	Biolegend	1/100
CD105-PECy7	MJ7/18	Biolegend	1/100
Hematopoietic Lineage Cocktail			
CD45-Biotin	30-F11	Biolegend	1/100
CD11b-Biotin	M1/70	Biolegend	1/100
Gr1-Biotin	RB6-8C5	Biolegend	1/100
F4/80-Biotin	BM8	Biolegend	1/100
CD3-Biotin	17A2	Biolegend	1/100
B220-Biotin	RA3-6B2	Biolegend	1/100
CD19-Biotin	6D5	Biolegend	1/100
Ter119-Biotin	Ter1119	BD Bioscience	1/100
CD45-APCCy7	30-F11	Biolegend	1/100
CD11b-APCCy7	M1/70	Biolegend	1/100
F4/80-APCCy7	BM8	Biolegend	1/100
CD3-APCCy7	17A2	Biolegend	1/100
Gr1-APCCy7	RB6-8C5	Biolegend	1/100
B220-APCCy7	RA3-6B2	Biolegend	1/100
CD19-APCCy7	6D5	Biolegend	1/100
Ter119-APCCy7	Ter119	BD Bioscience	1/100
CD16/32	93	eBioscience	1/100
Polyclonal Abs			
eNOS	Rb Poly	BD Bioscience	1/100
GFP	Goat poly	Gentex	1/100
NG2	Rb poly	Millipore	1/100
Donkey anti-rat Cy3 Steptavidin-594		Jackson ImmunoResearch Invitrogen	1/500 1/500
Streptavidin-ACPCy7		eBioscience	1/100

Bibliography

1. Bryder, D., D.J. Rossi, and I.L. Weissman, *Hematopoietic stem cells: the paradigmatic tissue-specific stem cell.* Am J Pathol, 2006. 169(2): p. 338-46.
2. Jacobson LO, Simmons EL, Marks EK, Robson MJ, Bethard WF, Gaston EO. The role of the spleen in radiation injury and recovery. *J Lab Clin Med.* 1950. 35(5):746-70.
3. Weissman, IL, and Shizuru, JA. The origins of the identification and isolation of hematopoietic stem cells, and their capability to induce donor-specific transplantation tolerance and treat autoimmune diseases *Blood.* 2008. 112 (9): 3543-3553.
4. Lorenz E, D. Uphoff, T.R. Reid, E. Shelton. Modification of irradiation injury in mice and guinea pigs by bone marrow injections. *J Natl Cancer Inst* 1951.12:197-201.
5. Jacobson LO, E.L. Simmons, E. Marks, J.H. Eldredge. Recovery from radiation injury*. Science* 1951.113:510-511.
6. Weissman, I.L. Stem cells: units of development, units of regeneration, and units in evolution*. Cell*. 2000. 100(1): 157-68.
7. Adams, G.B. and D.T. Scadden. The hematopoietic stem cell in its place. *Nat Immunol*. 2006. 7(4): 333-7.
8. Mohty M, Bilger K, Jourdan E, Kuentz M, Michallet M, Bourhis JH, Milpied N, Sutton L, Jouet JP, Attal M, Bordigoni P, Cahn JY, Sadoun A, Ifrah N,

Guyotat D, Faucher C, Fegueux N, Reiffers J, Maraninchi D, Blaise D. Higher doses of CD34+ peripheral blood stem cells are associated with increased mortality from chronic graft-versus-host disease after allogeneic HLA-identical sibling transplantation. *Leukemia*. 2003. 17(5):869-75.

9. Gluckman E, Broxmeyer HE, Auerbach AD, Friedman HS, Douglas GW, Devergie A, Esperou H, Thierry D, Socie G, Lehn P, Cooper S, English D, Kurtzberg J, Bard J, and Boyse EA. Hematopoietic reconstitution in a patient with Fanconi's anemia by means of umbilical-cord blood from an HLA-identical sibling. *N. Engl J Med* 1989. 26;321(17):1174-8.

10. Broxmeyer HE, Cooper S, Hass DM, Hathaway JK, Stehman FB, Hangoc G. Experimental basis of cord blood transplantation. *Bone Marrow Transplantation.* 2009. 44: 627–633.

11. Broxmeyer HE. Cord blood hematopoietic stem cell transplantation. StemBook [Internet]. Cambridge [MA]: Harvard Stem Cell Institute, 2010.

12. Barker JN, Davies SM, DeFor T, Ramsay NK, Weisdorf DJ, Wagner JE. Survival after transplantation of unrelated donor umbilical cord blood is comparable to that of human leukocyte antigen-matched unrelated donor bone marrow: results of a matched-pair analysis. *Blood*. 2001. 15;97(10):2957-61.

13. Barker JN, Wagner JE. Umbilical cord blood transplantation: current practice and future innovations. *Crit Rev Oncol Hematol*. 2003. 48(1):35-43.

14. Morrison, S.J. and A.C. Spradling. Stem cells and niches: mechanisms that promote stem cell maintenance throughout life. *Cell*. 2008. 132(4): 598-611.

15. Kiel, M.J. and S.J. Morrison. Uncertainty in the niches that maintain haematopoietic stem cells. *Nat Rev Immunol,* 2008. 8(4):290-301.
16. Schofield, R. The relationship between the spleen colony-forming cell and the haemopoietic stem cell*. Blood Cells.* 1978. 4(1-2):7-25.
17. Li, L. and T. Xie. Stem cell niche: structure and function*. Annu Rev Cell Dev Biol*. 2005. 21:605-31.
18. Calvi LM, Adams GB, Weibrecht KW, Weber JM, Olson DP, Knight MC, Martin RP, Schipani E, Divieti P, Bringhurst FR, Milner LA, Kronenberg HM, Scadden DT. Osteoblastic cells regulate the haematopoietic stem cell niche. *Nature*. 2003. 425(6960): 841-6.
19. Zhang, J., Zhang J, Niu C, Ye L, Huang H, He X, Tong WG, Ross J, Haug J, Johnson T, Feng JQ, Harris S, Wiedemann LM, Mishina Y, Li L. Identification of the haematopoietic stem cell niche and control of the niche size*. Nature*. 2003. 425(6960):836-41.
20. Kiel MJ, Yilmaz OH, Iwashita T, Yilmaz OH, Terhorst C, Morrison SJ. SLAM family receptors distinguish hematopoietic stem and progenitor cells and reveal endothelial niches for stem cells. *Cell*. 2005. 121(7):1109-21.
21. Sugiyama T, Kohara H, Noda M, Nagasawa T. Maintenance of the hematopoietic stem cell pool by CXCL12-CXCR4 chemokine signaling in bone marrow stromal cell niches*. Immunity*. 2006. 25(6):977-88.
22. Sacchetti B, Funari A, Michienzi S, Di Cesare S, Piersanti S, Saggio I, Tagliafico E, Ferrari S, Robey PG, Riminucci M, Bianco P. Self-renewing

osteoprogenitors in bone marrow sinusoids can organize a hematopoietic microenvironment. *Cell.* 2007. 131(2):324-36.

23. Méndez-Ferrer S, Michurina TV, Ferraro F, Mazloom AR, Macarthur BD, Lira SA, Scadden DT, Ma'ayan A, Enikolopov GN, Frenette PS. Mesenchymal and haematopoietic stem cells form a unique bone marrow niche. *Nature*. 2010. 466(7308):829-34.
24. Omatsu Y, Sugiyama T, Kohara H, Kondoh G, Fujii N, Kohno K, Nagasawa T. The essential functions of adipo-osteogenic progenitors as the hematopoietic stem and progenitor cell niche. *Immunity*. 2010. 33(3):387-99.
25. Nagasawa T, Omatsu Y, Sugiyama T. Control of hematopoietic stem cells by the bone marrow stromal niche: the role of reticular cells. *Trends Immunol*. 2011. 32(7):315-20.
26. Bianco P, Sacchetti B, Riminucci M. Osteoprogenitors and the hematopoietic microenvironment. *Best Pract & Res Clinic Haematol*. 2011. 24:37-47.
27. Anjos-Afonso F, Bonnet D. Prospective identification and isolation of murine bone marrow derived multipotent mesenchymal progenitor cells. *Best Pract Res Clin Haematol*. 2011. 24(1):13-24.
28. Suire C, Brouard N, Hirschi K, Simmons PJ. Isolation of the Stromal-Vascular Fraction of Mouse Bone Marrow Markedly Enhances the Yield of Clonogenic Stromal Progenitors. *Blood*. Prepublished January 18, 2012; DOI 10.1182/blood-2011-08-372334.

29. Wilson A, Laurenti E, Oser G, van der Wath RC, Blanco-Bose W, Jaworski M, Offner S, Dunant CF, Eshkind L, Bockamp E, Lió P, Macdonald HR, Trumpp A. Hematopoietic stem cells reversibly switch from dormancy to self-renewal during homeostasis and repair. *Cell.* 2008. 135(6): 1118-29.
30. Till, J.E. and C.E. McCulloch. A direct measurement of the radiation sensitivity of normal mouse bone marrow cells*. Radiat Res*. 1961. 14:213-22.
31. Wu AM, Till JE, Siminovitch L, McCulloch EA. Cytological evidence for a relationship between normal hemotopoietic colony-forming cells and cells of the lymphoid system. *J Exp Med.* 1968. 127(3):455-64.
32. Siminovitch, L., E.A. McCulloch, and J.E. Till. The Distribution of Colony-Forming Cells among Spleen Colonies*. J Cell Physiol*. 1963. 62:327-36.
33. Becker AJ, McCulloch EA, Till JE. Cytological demonstration of the clonal nature of spleen colonies derived from transplanted mouse marrow cells. *Nature*. 1963. 197:452-4.
34. Magli MC, Iscove NN, Odartchenko N. Transient nature of early haematopoietic spleen colonies. *Nature.* 1982. 295(5849):527-9.
35. Purton LE, Scadden DT. Limiting factors in murine hematopoietic stem cell assays. Cell Stem Cell. 2007. 1(3):263-70.
36. Spangrude GJ, Heimfeld S, Weissman IL. Purification and characterization of mouse hematopoietic stem cells. *Science.* 1988. 241(4861):58-62.
37. Morrison SJ, Lagasse E, Weissman IL. Demonstration that Thy(lo) subsets of mouse bone marrow that express high levels of lineage markers are not significant hematopoietic progenitors. *Blood*. 1994. 83(12):3480-90.

38. Morrison SJ, Wandycz AM, Hemmati HD, Wright DE, Weissman IL. Identification of a lineage of multipotent hematopoietic progenitors. *Development*. 1997. 124(10): 1929-39.

39. Ikuta K, Weissman IL. Evidence that hematopoietic stem cells express mouse c-kit but do not depend on steel factor for their generation. *Proc Natl Acad Sci U S A*. 1992. 89(4):1502-6.

40. Shen FW, Tung JS, Boyse EA. Further definition of the Ly-5 system. *Immunogenetics.* 1986. 24(3):146-9.

41. Orkin, S.H. and L.I. Zon. Hematopoiesis: an evolving paradigm for stem cell biology. *Cell*. 2008. 132(4): 631-44.

42. Wagers, A.J., J.L. Christensen, and I.L. Weissman. Cell fate determination from stem cells. *Gene Ther*. 2002. 9(10): 606-12.

43. Morrison, SJ, Lagasse E, Weissman IL. Demonstration that Thy (lo) subsets of mouse bone marrow that express high levels of lineage markers are not significant hematopoietic progenitors*. Blood*. 1994. 83(12):3480-90.

44. Wilson A, Trumpp A. Bone-marrow haematopoietic-stem-cell niches. *Nat Rev Immunol.* 2006. 6(2):93-106.

45. Mikkola HK, and Orkin SH. The journey of developing hematopoietic stem cells. *Development*. 2006. 133(19):3733-44.

46. Cumano A, Godin I. Ontogeny of the hematopoietic system. *Annu Rev Immunol.* 2007. 25:745-85.

47. Moore MA, Metcalf D. Ontogeny of the haemopoietic system: yolk sac origin of in vivo and in vitro colony forming cells in the developing mouse embryo. *Br J Haematol*. 1970. 18(3): 279-96.

48. Goldie LC, Lucitti JL, Dickinson ME, Hirschi KK. Cell signaling directing the formation and function of hemogenic endothelium during murine embryogenesis. *Blood.* 112(8):3194-204.

49. Godin IE, Garcia-Porrero JA, Coutinho A, Dieterlen-Lièvre F, Marcos MA. Para-aortic splanchnopleura from early mouse embryos contains B1a cell progenitors*. Nature.* 1993. 364(6432): 67-70.

50. Cumano A, Dieterlen-Lievre F, Godin I. Lymphoid potential probed before circulation in mouse, is restricted to caudal intraembryonic splanchnopleura. *Cell.* 1996. 86(6):907-16.

51. Cumano A, Ferraz JC, Klaine M, Di Santo JP, Godin I. Intraembryonic, but not yolk sac hematopoietic precursors, isolated before circulation, provide long-term multilineage reconstitution. *Immunity.* 2001. 15(3): 477-85.

52. Dzierzak E, Speck NA. Of lineage and legacy: the development of mammalian hematopoietic stem cells. *Nat Immunol.* 2008. 9(2):129-36.

53. Christensen JL, Wright DE, Wagers AJ, Weissman IL. Circulation and chemotaxis of fetal hematopoietic stem cells*. PLoS Biol.* 2004. 2(3): E75.

54. Wright DE, Wagers AJ, Gulati AP, Johnson FL, Weissman IL. Physiological migration of hematopoietic stem and progenitor cells. *Science*. 2001. 294(5548):1933-6.

55. Weiss L. The hematopoietic microenvironment of the bone marrow: An ultrastructural study of the stroma in rats. *The Anatomical Record.* 1976. 186 (2):161–184.

56. Travlos GS. Normal Structure, Function, and Histology of the Bone Marrow. *Toxicol Pathol*. 2006. 34 (5): 548-565.

57. Knospe WH, Blom J, Crosby WH. Regeneration of locally irradiated bone marrow. I. Dose dependent, long-term changes in the rat, with particular emphasis upon vascular and stromal reaction. *Blood.* 1966. 28(3):398-415.

58. Knospe WH, Blom J, Crosby WH. Regeneration of locally irradiated bone marrow. II. Induction of regeneration in permanently aplastic medullary cavities. *Blood*. 1968. 31(3):400-5.

59. McCulloch EA, Siminovitch L, Till JE, Russell ES, Bernstein SE. The cellular basis of the genetically determined hemopoietic defect in anemic mice of genotype Sl-Sld. *Blood*. 1965. 26(4): 399-410.

60. Dexter TM, and Lajtha LG. Proliferation of haemopoietic stem cells in vitro. *Br J Haematol.* 1974. 28(4):525-30.

61. Dexter TM, Wright EG, Krizsa F, Lajtha LG. Regulation of haemopoietic stem cell proliferation in long term bone marrow cultures. *Biomedicine*. 1977. 27(9-10): 344-9.

62. Zhang CC and Lodish HF. Cytokines regulating hematopoietic stem cell function. *Curr Opin Hematol*. 2008. 15(4):307-11.

63. Moore KA, Ema H, Lemischka IR. In vitro maintenance of highly purified, transplantable hematopoietic stem cells. *Blood*.1997. 89(12):4337-47.

64. Gong, J.K. Endosteal marrow: a rich source of hematopoietic stem cells. *Science*.1978. 199(4336): 1443-5.

65. Nilsson, S.K., Johnston HM, Coverdale JA. Spatial localization of transplanted hemopoietic stem cells: inferences for the localization of stem cell niches. *Blood.* 2001. 97(8): 2293-9.

66. Taichman RS, Reilly MJ, Emerson SG. Human osteoblasts support human hematopoietic progenitor cells in vitro bone marrow cultures. *Blood*. 1996. 87(2):518-24.

67. Stier S, Ko Y, Forkert R, Lutz C, Neuhaus T, Grünewald E, Cheng T, Dombkowski D, Calvi LM, Rittling SR, Scadden DT. Osteopontin is a hematopoietic stem cell niche component that negatively regulates stem cell pool size. *J Exp Med.* 2005. 201(11): 1781-91.

68. Nilsson SK, Johnston HM, Whitty GA, Williams B, Webb RJ, Denhardt DT, Bertoncello I, Bendall LJ, Simmons PJ, Haylock DN. Osteopontin, a key component of the hematopoietic stem cell niche and regulator of primitive hematopoietic progenitor cells. *Blood.* 2005. 106(4):1232-9.

69. Arai F, Hirao A, Ohmura M, Sato H, Matsuoka S, Takubo K, Ito K, Koh GY, Suda T. Tie2/angiopoietin-1 signaling regulates hematopoietic stem cell quiescence in the bone marrow niche. *Cell.* 2004. 118(2):149-61.

70. Yoshihara H, Arai F, Hosokawa K, Hagiwara T, Takubo K, Nakamura Y, Gomei Y, Iwasaki H, Matsuoka S, Miyamoto K, Miyazaki H, Takahashi T, Suda T. Thrombopoietin/MPL signaling regulates hematopoietic stem cell

quiescence and interaction with the osteoblastic niche. *Cell Stem Cell*. 2007. 1(6):685-97.

71. Qian H, Buza-Vidas N, Hyland CD, Jensen CT, Antonchuk J, Månsson R, Thoren LA, Ekblom M, Alexander WS, Jacobsen SE. Critical role of thrombopoietin in maintaining adult quiescent hematopoietic stem cells. *Cell Stem Cell.* 2007. 1(6):671-84.
72. Petit I, Szyper-Kravitz M, Nagler A, Lahav M, Peled A, Habler L, Ponomaryov T, Taichman RS, Arenzana-Seisdedos F, Fujii N, Sandbank J, Zipori D, Lapidot T. G-CSF induces stem cell mobilization by decreasing bone marrow SDF-1 and up-regulating CXCR4. *Nat Immunol*. 2002. 3(7):687-94.
73. Mancini SJ, Mantei N, Dumortier A, Suter U, MacDonald HR, Radtke F. Jagged1-dependent Notch signaling is dispensable for hematopoietic stem cell self-renewal and differentiation. *Blood.* 2005. 105(6): 2340-2.
74. Kiel MJ, Radice GL, Morrison SJ. Lack of evidence that hematopoietic stem cells depend on N-cadherin-mediated adhesion to osteoblasts for their maintenance. *Cell Stem Cell.* 2007. 1(2):204-17.
75. Kiel MJ, Acar M, Radice GL, Morrison SJ. Hematopoietic Stem Cells Do Not Depend on N-Cadherin to Regulate Their Maintenance. *Cell Stem Cell*. 2009. 4(2): 170-9.
76. Yin T and Li L. The stem cell niches in bone. *J Clin Invest*. 2006. 116(5):1195-201.

77. de Bruijn MF, Ma X, Robin C, Ottersbach K, Sanchez MJ, Dzierzak E. Hematopoietic stem cells localize to the endothelial cell layer in the midgestation mouse aorta. *Immunity.* 2002. 16(5):673-83.

78. Eilken HM, Nishikawa S, Schroeder T. Continuous single-cell imaging of blood generation from haemogenic endothelium*. Nature*. 2009. 457(7231): 896-900.

79. Kopp HG, Avecilla ST, Hooper AT, Rafii S. The bone marrow vascular niche: home of HSC differentiation and mobilization. Physiology. 2005. 20: 349-56.

80. Butler JM, Nolan DJ, Vertes EL, Varnum-Finney B, Kobayashi H, Hooper AT, Seandel M, Shido K, White IA, Kobayashi M, Witte L, May C, Shawber C, Kimura Y, Kitajewski J, Rosenwaks Z, Bernstein ID, Rafii S. Endothelial cells are essential for the self-renewal and repopulation of Notch-dependent hematopoietic stem cells*. Cell Stem Cell*. 2010. 6(3):251-64.

81. Laterveer L, Lindley IJ, Hamilton MS, Willemze R, Fibbe WE. Interleukin-8 induces rapid mobilization of hematopoietic stem cells with radioprotective capacity and long-term myelolymphoid repopulating ability. *Blood.* 1995. 85(8):2269-75.

82. Hooper AT, Butler JM, Nolan DJ, Kranz A, Iida K, Kobayashi M, Kopp HG, Shido K, Petit I, Yanger K, James D, Witte L, Zhu Z, Wu Y, Pytowski B, Rosenwaks Z, Mittal V, Sato TN, Rafii S. Engraftment and reconstitution of hematopoiesis is dependent on VEGFR2-mediated regeneration of sinusoidal endothelial cells. *Cell Stem Cell.* 2009. 4(3): 263-74.

83. Lo Celso C, Fleming HE, Wu JW, Zhao CX, Miake-Lye S, Fujisaki J, Côté D, Rowe DW, Lin CP, Scadden DT. Live-animal tracking of individual haematopoietic stem/progenitor cells in their niche. *Nature*. 2009. 457(7225):92-6.

84. Xie Y, Yin T, Wiegraebe W, He XC, Miller D, Stark D, Perko K, Alexander R, Schwartz J, Grindley JC, Park J, Haug JS, Wunderlich JP, Li H, Zhang S, Johnson T, Feldman RA, Li L. Detection of functional haematopoietic stem cell niche using real-time imaging. *Nature*. 2009. 457(7225):97-101.

85. Krebsbach PH, Kuznetsov SA, Bianco P, Robey PG. Bone marrow stromal cells: characterization and clinical application. *Crit Rev Oral Biol Med.* 1999. 10(2):165-81.

86. Owen M, Friedenstein AJ. Stromal stem cells: marrow-derived osteogenic precursors. *Ciba Found Symp*. 1988;136:42-60. Review.

87. Müller I, Kordowich S, Holzwarth C, et al. Animal serum-free culture conditions for isolation and expansion of multipotent mesenchymal stromal cells from human BM. *Cytotherapy*. 2006. 8(5): 437-44.

88. Bianco P, Kuznetsov SA, Riminucci M, Gehron Robey P. Postnatal skeletal stem cells. *Methods Enzymol*. 2006. 419:117-48. Review.

89. Caplan AI. Mesenchymal stem cells. *J Orthop Res*. 1991. 9(5):641-50.

90. Pittenger MF, Mackay AM, Beck SC, Jaiswal RK, Douglas R, Mosca JD, Moorman MA, Simonetti DW, Craig S, Marshak DR. Multilineage potential of adult human mesenchymal stem cells. *Science*. 1999. 284(5411): 143-7.

91. Bianco P, Robey PG, Simmons PJ. Mesenchymal stem cells: revisiting history, concepts and assays. *Cell Stem Cell*. 2008. 2(4):313-9.

92. Tavassoli M, Crosby WH. Transplantation of marrow to extramedullary sites. *Science*. 1968. 61(3836):54-6.

93. Friedenstein AJ, Chailakhjan RK, Lalykina KS. The development of fibroblast colonies in monolayer cultures of guinea-pig bone marrow and spleen cells. *Cell Tissue Kinet*. 1970. 3(4):393-403.

94. Friedenstein AJ, Chailakhyan RK, Latsinik NV, Panasyuk AF, Keiliss-Borok IV. Stromal cells responsible for transferring the microenvironment of the hemopoietic tissues. Cloning in vitro and retransplantation in vivo. *Transplantation*. 1974. 17(4):331-40.

95. Kronenberg HM. The role of the perichondrium in fetal bone development. *Ann N Y Acad Sci.* 2007.1116: 59-64.

96. Bianco P and Robey PG. Marrow stromal stem cells. *Journ Clin Invest*. 2000. 105:1663-1668.

97. Kuznetsov S, Gehron Robey P. Species differences in growth requirements for bone marrow stromal fibroblast colony formation In vitro. *Calcif Tissue Int.* 1996. 59(4): 265-70.

98. Lennon DP, Caplan AI. Isolation of rat marrow-derived mesenchymal stem cells. *Exp Hematol*. 2006. 34(11): 1606-7.

99. Kadiyala S, Young RG, Thiede MA, Bruder SP. Culture expanded canine mesenchymal stem cells possess osteochondrogenic potential in vivo and in vitro. *Cell Transplant*. 1997. 6(2):125-34.

100. Izadpanah R, Joswig T, Tsien F, Dufour J, Kirijan JC, Bunnell BA. Characterization of multipotent mesenchymal stem cells from the bone marrow of rhesus macaques. *Stem Cells Dev*. 2005. 14(4): 440-51.

101. Jessop HL, Noble BS, Cryer A. The differentiation of a potential mesenchymal stem cell population within ovine bone marrow. *Biochem Soc Trans*. 1994. 22(3): 248S.

102. Phinney DG, Kopen G, Isaacson RL, Prockop DJ. Plastic adherent stromal cells from the bone marrow of commonly used strains of inbred mice: variations in yield, growth, and differentiation. *J Cell Biochem*. 1999. 72(4):570-85.

103. Sun S, Guo Z, Xiao X, Liu B, Liu X, Tang PH, Mao N. Isolation of mouse marrow mesenchymal progenitors by a novel and reliable method. *Stem Cells.* 2003. 21(5):527-35.

104. Peister A, Mellad JA, Larson BL, Hall BM, Gibson LF, Prockop DJ. Adult stem cells from bone marrow (MSCs) isolated from different strains of inbred mice vary in surface epitopes, rates of proliferation, and differentiation potential. *Blood*. 2004. 103(5):1662-8.

105. Tropel P, Noël D, Platet N, Legrand P, Benabid AL, Berger F. Isolation and characterisation of mesenchymal stem cells from adult mouse bone marrow. *Exp Cell Res*. 2004. 295(2): 395-406.

106. Metcalf D. Formation in agar of fibroblast-like colonies by cells from the mouse pleural cavity and other sources. *J Cell Physiol*. 1972. 80(3): 409-19.

107. Aguilar S, Nye E, Chan J, Loebinger M, Spencer-Dene B, Fisk N, Stamp G, Bonnet D, Janes SM. Murine but not human mesenchymal stem cells generate osteosarcoma-like lesions in the lung. *Stem Cells.* 2007. 25(6): 1586-94.

108. Kuznetsov S, Mankani M, Bianco P, Robey P. Enumeration of the colony-forming units-fibroblast from mouse and human bone marrow in normal and pathological conditions. *Stem Cell Res*. 2009: 2(1): 83-94.

109. Friedenstein AJ, Latzinik NW, Grosheva AG, Gorskaya UF. Marrow microenvironment transfer by heterotopic transplantation of freshly isolated and cultured cells in porous sponges. *Exp. Hematol.* 1982. 10(2):217-227.

110. Baddoo M, Hill K, Wilkinson R, Gaupp D, Hughes C, Kopen GC, Phinney DG. Characterization of mesenchymal stem cells isolated from murine bone marrow by negative selection. *J Cell Biochem*. 2003. 89(6): 1235-49.

111. Soleimani M, Nadri S. A protocol for isolation and culture of mesenchymal stem cells from mouse bone marrow. *Nat Protoc*. 2009. 4(1): 102-6.

112. Short BJ, Brouard N, Simmons PJ. Prospective isolation of mesenchymal stem cells from mouse compact bone. *Methods Mol Biol*. 2009. 482:259-68.

113. Morikawa S, Mabuchi Y, Kubota Y, Nagai Y, Niibe K, Hiratsu E, Suzuki S, Miyauchi-Hara C, Nagoshi N, Sunabori T, Shimmura S, Miyawaki A, Nakagawa T, Suda T, Okano H, Matsuzaki Y. Prospective identification, isolation, and systemic transplantation of multipotent mesenchymal stem cells in murine bone marrow. *J Exp Med*. 2009. 206(11): 2483-96.

114. Xu S, De Becker A, Van Camp B, Vanderkerken K, Van Riet I. An improved harvest and in vitro expansion protocol for murine bone marrow-derived mesenchymal stem cells. *J Biomed Biotechnol.* 2010. 2010:1-10.

115. Crisan M, Yap S, Casteilla L, Chen CW, Corselli M, Park TS, Andriolo G, Sun B, Zheng B, Zhang L, Norotte C, Teng PN, Traas J, Schugar R, Deasy BM, Badylak S, Buhring HJ, Giacobino JP, Lazzari L, Huard J, Péault B. A perivascular origin for mesenchymal stem cells in multiple human organs. *Cell Stem Cell*. 2008. 3(3): 301-13.

116. Westen H, Bainton DF. Association of alkaline-phosphatase-positive reticulum cells in bone marrow with granulocytic precursors. *J Exp Med.* 1979.150(4):919-37.

117. Caplan AI. Mesenchymal stem cells. *J Orthop Res.* 1991. 9(5):641-50.

118. Kronenberg, HM. Developmental regulation of the growth plate. *Nature.* 2003. 423(6937):332-6.

119. Kuznetsov SA, Krebsbach PH, Satomura K, Kerr J, Riminucci M, Benayahu D, Robey PG. Single-colony derived strains of human marrow stromal fibroblasts form bone after transplantation in vivo. *J Bone Miner Res*. 1997. 12(9): 1335-47.

120. Bianco P, Riminucci M, Kuznetsov S, Robey PG. Multipotential cells in the bone marrow stroma: regulation in the context of organ physiology. *Crit Rev Eukaryot Gene Expr*. 1999. 9(2):159-73.

121. Maes C, Kobayashi T, Selig MK, Torrekens S, Roth SI, Mackem S, Carmeliet G, Kronenberg HM. Osteoblast precursors, but not mature osteoblasts, move into developing and fractured bones along with invading blood vessels. *Dev Cell.* 2010. 19(2): 329-44.

122. Nagoshi N, Shibata S, Kubota Y, Nakamura M, Nagai Y, Satoh E, Morikawa S, Okada Y, Mabuchi Y, Katoh H, Okada S, Fukuda K, Suda T, Matsuzaki Y, Toyama Y, Okano H. Ontogeny and multipotency of neural crest-derived stem cells in mouse bone marrow, dorsal root ganglia, and whisker pad. *Cell Stem Cell.* 2008. 2(4): 392-403.

123. Chan CK, Chen CC, Luppen CA, Kim JB, DeBoer AT, Wei K, Helms JA, Kuo CJ, Kraft DL, Weissman IL. Endochondral ossification is required for haematopoietic stem-cell niche formation. *Nature.* 2009. 457(7228): 490-4.

124. Zhu, X., Bergles, D., Nishiyama, A. NG2 cells generate both oligodendrocytes and gray matter astrocytes. *Devel*. 2008. 135:145-157.

125. Armulik A, Genove G, Betsholtz C. Pericytes: Development, Physiological and Pathological Perspectives, Problem and Promises. *Devel. Cell*. 2011. 21:193-215.

126. Gronthos S, Gronthos S, Zannettino AC, Hay SJ, Shi S, Graves SE, Kortesidis A, Simmons PJ. Molecular and cellular characterisation of highly purified stromal stem cells derived from human bone marrow. *J. Cell Sci. 2*003. 116(Pt 9):1827-35.

127. Lebrin F, Goumans MJ, Jonker L, Carvalho RL, Valdimarsdottir G, Thorikay M, Mummery C, Arthur HM, ten Dijke P. Endoglin promotes endothelial cell

proliferation and TGF-beta/ALK1 signal transduction. *EMBO J.* 2004. 23(20):4018-28.

128. Franzen A, Heinegard D, Solursh M. Evidence for sequential appearance of cartilage matrix proteins in developing mouse limbs and in cultures of mouse mesenchymal cells. *Differentiation.* 1987. 36(3):199-210.

129. Neame PJ, Tapp H, Azizan A. Noncollagenous, nonproteoglycan macromolecules of cartilage. *Cell Mol Life Sci*. 1999. 55(10):1327-40.

130. Morrison SJ, Shah NM, Anderson DJ. Regulatory mechanisms in stem cell biology. *Cell.* 1997. 88(3):287-98.

131. Jones DL, Wagers AJ. No place like home: anatomy and function of the stem cell niche. *Nat Rev Mol Cell Biol.* 2008. 9(1):11-21.

132. Lane SW, Scadden DT, Gilliland DG. The leukemic stem cell niche: current concepts and therapeutic opportunities. *Blood*. 2009. 114(6):1150-7.

133. Miller CL, Eaves CJ. Expansion in vitro of adult murine hematopoietic stem cells with transplantable lympho-myeloid reconstituting ability. *Proc Natl. Acad. Sci.,* USA .1997. 94:13648-13653.

134. Bianco P. Minireview: The stem cell next door: skeletal and hematopoietic stem cell "niches" in bone. *Endocrinology*. 2011.152(8):2957-62.

135. Simmons, PJ, Levesque, JP, Zannettino, AC. Adhesion molecules in haemopoiesis. *Baillieres Clin Haematol.* 1997. 10(3):485-505.

136. Ding, L, Morrison, SJ. Endothelial and perivascular stromal cells promote murine hematopoietic stem cell maintenance in the bone marrow by secreting

stem cell factor (SCF). Abstract 2359. Presented at International Society for Stem Cell Research. June 17, 2011. Toronto, Ontario Canada.

137. Tokoyoda K, Egawa T, Sugiyama T, Choi BI, Nagasawa T. Cellular niches controlling B lymphocyte behavior within bone marrow during development. *Immunity.* 2004. 20:707-718.

138. Gronthos S, Graves SE, Ohta S, Simmons PJ. The STRO-1+ fraction of adult human bone marrow contains the osteogenic precursors. *Blood.* 1994. 84(12):4164-73**.**

139. Mackay AM, Beck SC, Murphy JM, Barry FP, Chichester CO, Pittenger MF. Chondrogenic differentiation of cultured human mesenchymal stem cells from marrow. *Tissue Eng*. 1998. 4(4): 415-28.

140. Tanaka M, Jokubaitis V, Wood C, Wang Y, Brouard N, Pera M, Hearn M, Simmons P, Nakayama N. BMP inhibition stimulates WNT-dependent generation of chondrogenic mesoderm from embryonic stem cells. *Stem Cell Res*. 2009. 3(2-3): 126-41.

141. Schneider A, Taboas JM, McCauley LK, Krebsbach PH. Skeletal homeostasis in tissue-engineered bone. *J Orthop Res*. 2003. 21(5):859-64.

142. Brake DK, Smith CW. Flow cytometry on the stromal-vascular fraction of white adipose tissue. *Methods Mol Biol*. 2008. 456:221-9.

143. Lennon DP, Edmison JM, Caplan AI. Cultivation of rat marrow-derived mesenchymal stem cells in reduced oxygen tension: effects on in vitro and in vivo osteochondrogenesis. *J Cell Physiol*. 2001. 187(3):345-55.

144. Kubota Y, Takubo K, Suda T. Bone marrow long label-retaining cells reside in the sinusoidal hypoxic niche. *Biochem Biophys Res Commun.* 2008. 366(2):335-9.

Vita

Colby G. Suire was born in Abbeville, Louisiana on March 15, 1974, the son of Martha Simon Suire and William Suire, III. He completed his primary education at Fort Walton Beach High School, Fort Walton Beach, Florida. In Decemebr of 2005, he received his Bachelor of Science with a major in Biological Science from Louisiana State University. In May 2006, he matriculated into the Doctor of Philosophy program at the University of Texas Health Science Center in Houston. In January 2012, he completed his doctoral training in the laboratory of Dr. Paul J. Simmons at the Center for Stem Cell and Regenerative Research.